Università degli Studi di Messina

Dipartimento di Scienze Chimiche, Biologiche,

Farmaceutiche ed Ambientali

Dottorato di Ricerca in "Scienze Chimiche"

Doctor of Philosophy in "Chemical Sciences"

Development of sample-tailored gas chromatography strategies involving one, two and three analytical dimensions

---

PhD Thesis of:

Mariarosa Maimone

Supervisor:

Prof. **Peter Q. Tranchida**

Coordinator:

Prof. **Sebastiano Campagna**

SSD CHIM/10

XXIX Ciclo 2014-2016

TABLE OF CONTENTS

Chapter 1

General introduction and scope

The scope of modern gas chromatography (GC) analysis is to qualitatively and quantitatively characterize the profiles of complex samples, such as foods, fragrances, petrochemicals, etc. If the objective is connected to sensory analyis, then the purpose is to recognize and prioritise target organoleptically-interesting molecules, and distinguish them from other volatiles that may not have relevance to the overall odour of a sample.

The research work carried out during the three years of the PhD course in Chemistry Sciences can be placed within such contexts. In such a broad field of science separation, I have dealt with a number of innovative techniques, such as preparative (heart-cutting) multidimensional chromatography for the isolation and identification of highly-pure compounds; use of flow-modulated comprehensive two-dimensional gas chromatography (FM GC×GC) with different detectors as a powerful tool for the characterization of complex samples.

Finally, during the last year of PhD course, I approached sensorial analysis, exploring the use of gas chromatography-olfactometry (GC-O) for the determination of odour-active compounds in food samples.

With regard to preparative chromatography, a lab-constructed system composed of one liquid and three GC systems was used for the isolation of the most important sesquiterpenes belonging to sandalwood essential oil [1].

With regard to FM GC×GC, the studies are related to fragrances [2], bio-diesel [3], and an essential oil [4].

Finally, GC-O was exploited for the determination of the odour-active compounds belonging to *Heracleum transcaucasicum* [5].

As can be derived from the brief description, during the three-year research period one-, two-, and three-dimensional GC methods have been developed with fine tuning for various analytical scopes.

References

[1] S. Pantò, D. Sciarrone, M. Maimone, C. Ragonese, S. Giofrè, P. Donato, S. Farnetti, L. Mondello, J. Chromatogr. A, 1417 (2015) 96.

[2] P.Q. Tranchida, M. Maimone, F. A. Franchina, T. Rodrigues Bjerk, C. Alcaraz Zini, G. Purcaro, L. Mondello, J. Chromatogr. A, 1439 (2016) 144.

[3] F.A. Franchina, M. Maimone, D. Sciarrone, G. Purcaro, P. Q. Tranchida, L. Mondello, J. Chromatogr. A, 1402 (2015) 102.

[4] F.A. Franchina, M. Maimone, P. Q. Tranchida, L. Mondello, J. Chromatogr. A, 1441 (2016) 134.

[5] M. Maimone, A. Manukyan, P.Q. Tranchida, M. Steinhaus, Eur. Food Res. Technol. (2016) doi:10.1007/s00217-016-2815-9.

Chapter 2

Use of multiple dimensions in analytical separations

2.1 Theoretical considerations on resolution

At present, 1D (monodimensional) chromatography is the most commonly applied method for the separation of real-world samples. However, in the last three decades it has become increasingly clear that the baseline separation of all the constituents of a sample, or of specific target analytes from the rest of the matrix, is often an unreasonable challenge when using a single chromatography column.

The two fundamental aspects which govern all chromatography processes are:

(1) peak capacity (n_c) and
(2) stationary-phase selectivity.

The former parameter is related to the column characteristics (*i.e.*, length, internal diameter, particle diameter, stationary-phase thickness, intensity of analyte-stationary phase interactions, etc.), and to the experimental conditions (*i.e.*, mobile phase flow and type, temperature, outlet pressure, etc.). The other feature is related to the chemical composition of the stationary phase, and hence to the specific type of analyte-stationary phase interactions (*i.e.*, dispersion, dipole-dipole, H- bonding, electrostatic, size exclusion, etc.). Selectivity is also dependent on analyte solubility in the mobile phase, whenever this type of interaction occurs.

An experienced chromatographer, with knowledge of basic theory, will easily get the best out of a column or, in other words, will maximize the number of peaks that can be stacked side by side (with a specific resolution value) in a one-dimensional separation. However, it has been emphasized that such an analytical capability will fall far short of the peak capacity requirements for many applications. In fundamental work, Giddings demonstrated from a theoretical viewpoint that "no more than 37% of the peak capacity can be used to generate peak resolution" and that "many of the peaks observed under these circumstances represent the grouping of two or more close-lying components.", to conclude that "s" (the number of single component peaks) can never exceed

18% of n_c [1]. Although such a value does not take stationary-phase selectivity into account, it provides an excellent indication of the separation power of a one-dimensional chromatography system.

Equation 2.0 is well-known to be the master equation for resolution (considering two compounds), and it indicates that resolution (*Rs*) is affected by three parameters: efficiency (*N*, plate number), selectivity (α, separation factor) and retention (*k*, retention factor):

$$Rs = \frac{\sqrt{N}}{4}\left(\frac{\alpha-1}{\alpha}\right)\left(\frac{k2}{k2+1}\right) \qquad \text{Eq. 2.0}$$

The different degrees of influence, of *N*, α and *k* on R_S, can be observed in an excellent example shown in Figure 2.0 where the separation of two analytes (k_1 = 4.8; k_2 = 5.0; α = 1.05) on a GC column (N = 20,000), under fixed conditions, is considered. If we direct our attention to the three variables contained in Equation 2.0, and to the effects of their variation on resolution (visualized in Figure 2.1), we can draw the following conclusions:

k) If the column phase ratio is reduced (or a lower temperature applied) leading to an increase in the retention factors, then the benefits gained are very limited in terms of resolution. An increase in *k* has a substantial effect on R_S only for analytes with low *k* values (≤ 3).

α) If a more selective stationary phase is employed, thus increasing the separation factor, the resolution will benefit greatly. From Equation 2.0 it can be concluded that at lower values, an increase in α will lead to a considerable improvement in resolution, *viz.*, up to an α value of *circa* 3. At higher separation factor values, the function tends to level off. Of the three variables, selectivity has the greatest effect on resolution and, thus, it is fundamental to select the most suitable stationary phase for a given separation. However, it must also be noted that Equation 2.0 is valid only for a single pair of analytes and not for a complex mixture of compounds; in the latter case, a stationary phase change will often lead to a resolution improvement for some analytes, and a poorer result for others. The choice of the most selective stationary phase has the best effects only when a low-complexity sample is subjected to separation.

N) If the column length is extended by four times, leading to an increase in *N* by the same factor, then resolution is only doubled. It follows that an evident

improvement in peak resolution can only be achieved by extending the column length considerably. Such a modification is usually not desirable and certainly not a practical solution in view of the greatly increased analysis time. However, enhancing the plate number is without doubt the best choice whenever a medium or highly-complex mixture is subjected to chromatography. In fact, an increase in N will lead to the same percentage increase in resolution for all the constituents of a sample.

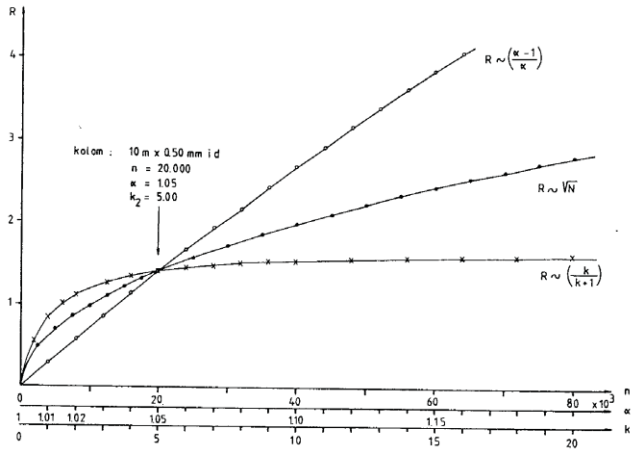

Figure 2.0. Resolution: influence of N, α and k [2].

Using longer columns makes it possible to increase the separation efficiency of one-dimensional GC analysis, but unfortunately, this will increase the analysis time in proportion with the third power of separation efficiency. As a result, the separation efficiency of 1D GC can only be increased at the expense of prohibitively-long analysis times. Thus, the most effective way of enhancing the separation efficiency (and the selectivity) of a chromatography system, with equivalent detection conditions, is by using a multidimensional chromatographic system, that is an additional separation dimension.

The main driving force behind the interest in multidimensional separations [1, 3-10], including GC×GC, has been the unrelenting need to resolve (identifiably and quantifiably separate) more components in complex mixtures.

2.2 Concept of multidimensionality

An enormous variety of combinations of different separation mechanisms can be used to create multidimensional separation systems. A significant number of such combinations have already been implemented successfully, and the

experimental results nicely illustrate the high separation power that is typically associated with these techniques. The basic requirements for a multiple separation to be considered as multidimensional were discussed by Giddings in 1990 [1]. Two conditions should be fulfilled:

1) The components of a mixture should be subjected to two (or more) separation steps in which their displacement is governed by different factors.
2) Analytes that have been resolved in the previous step should remain separated until the following separation process is completed.

When two (or more) independent separation mechanisms are used, this will result in a equal number of parameters to define the identity of an analyte [11]. Considering 2D (bidimensional) GC, each analyte is characterized by two independent retention times rather than by a single one (as in 1D GC). The second condition requires the separate analysis of relatively small fractions of eluate from the first column on the second one, in order to maintain the separation already achieved on the first dimension.

If the dimensions are based on different interaction mechanisms, then the separation is said to be "orthogonal" [12]. The slightest correlation between the dimensions will generate redundant information which will affect the global separation. To illustrate the concept of orthogonality, Figure 2.1 represents three degrees of correlation between two separation dimensions. In the case of a totally orthogonal separation, the peaks are distributed over the entire plane (a). The more the dimensions are correlated, the more the distribution will be centered along the diagonal (b). In the extreme case of total correlation (c), the solutes will have a similar or the same retention in the two dimensions, resulting in the equivalent 1D separation along the diagonal.

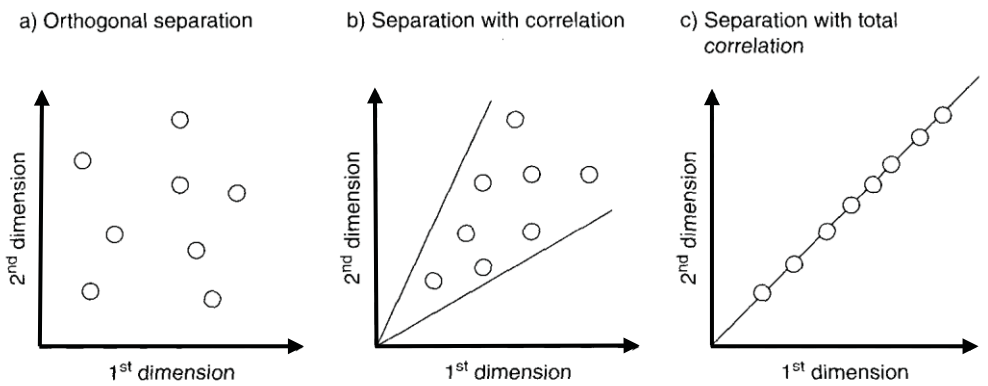

Figure 2.1. Illustration of various degrees of correlation between two separation dimensions [2].

The separation dimensions must be correctly selected to produce efficient multidimensional systems. Giddings introduced the notion of sample dimensionality (S) [9], representing the number of independent variables describing the properties of the sample constituents. If the number and selectivity of the analytical dimensions match well with the sample dimensionality, then the separation will be maximized.

References

[1] J.C. Giddings, J. High Resolut. Chromatogr. 10 (1987) 319.

[2] H. J. Cortes (Editor), Multidimensional chromatography, Techniques and Applications, Marcel Dekker, Inc., New York and Basel, 1990.

[3] Z. Liu, J.B. Phillips, J. Chromatogr. Sci. 29 (1991) 227.

[4] J.C. Giddings, Anal. Chem. 56 (1984) 1258A.

[5] M.M. Bushey, J.W. Jorgenson, Anal. Chem. 62 (1990) 161.

[6] R. Consden, A.H. Gordon, A. J. P. Martin, Biochem. J. 38 (1944) 224.

[7] F. Erni, R. W. Frei, J. Chromatogr. 149 (1978) 561.

[8] J.C. Giddings, J. High Resolut. Chromatogr. 10 (1987) 319.

[9] J.C. Giddings, J. Chromatogr. 703 (1995) 3.

[10] M. Zakaria, M.-F. Gonnord, G. Guiochon, J. Chromatogr. 271 (1983) 127.

[11] P.J. Schoenmakers, P.J. Marriott, J. Beens, LC-GC Eur. 16 (2003) 335.

[12] C.J. Venkatramani, J. Xu and J.B. Phillips, Anal. Chem. 68 (1996) 1486.

Chapter 3

Heart-cutting multidimensional GC-based techniques

3.1 Introduction to multidimensional gas chromatography (MDGC)

The unraveling of naturally-occurring complex samples has been, since a long time, the driving force behind improvement and innovation in the field of separation science. Since the very beginning of GC, it became apparent to chromatographers that single-column separations could not provide enough separation efficiency to clearly resolve every analyte in a complex sample.

Important steps forward were made by replacing packed columns with capillary columns increasing the separation power by at least 10-fold [1], and by coupling gas chromatography with mass spectrometry (MS) [2]. However, such powerful techniques are often insufficient for the full understanding of complex samples. More efficient purification/separation steps would be necessary for easier and more reliable data interpretation.

Separation power can be greatly enhanced through multidimensional chromatography, with both heart-cutting and comprehensive chromatography techniques [3]. Such approaches are attractive, especially when the existing technologies, pushed to their limit, are still insufficient for complex sample analysis. The coupling of the same form of chromatography (both in the heart-cutting and comprehensive modes), such as liquid chromatography (LC-LC, LC×LC) and GC (GC-GC, GC×GC), or of two different forms of chromatography (*e.g.*, LC-GC, LC×GC) has been investigated over the years, both in an off- and on-line manner.

The advantages of combining two independent separation mechanisms, were recognized very early within the chromatography community. Heart-cutting multidimensional gas chromatography was first introduced in 1958 by Simmons and Snyder [4], who described a first-dimension boiling-point separation of C_5-C_8 hydrocarbons and a polarity-based separation of each of the four classes in the second dimension, in four distinct analyses (Figure 3.0). The transfer of chromatographic bands between the two dimensions was achieved

by using a valve-based interface. The results obtained were quite remarkable and it was stated that "separations can be obtained with this column arrangement which are not normally possible with previously described arrangements of single columns and multiple columns connected in series". Although GC column technology has evolved considerably during the last half-century this statement is still fully-valid today.

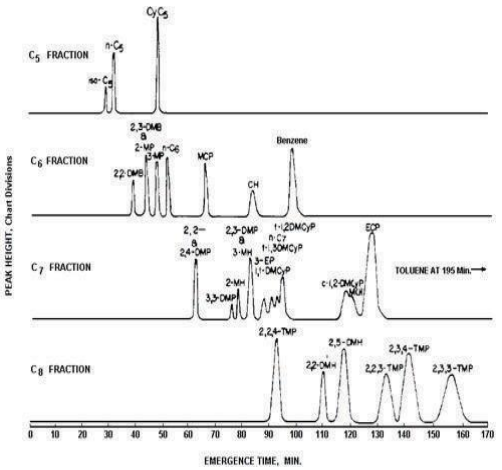

Figure 3.0. Second-dimension GC analyses of C_5-C_8 hydrocarbon groups [4].

The classical heart-cutting MDGC set-up usually consists of two conventional capillary columns (*e.g.*, 30 m × 0.25 mm ID × 0.25 µm d_f), connected in series and characterized by a differing selectivity (*e.g.*, apolar-polar, polar-chiral, etc.). Today, MDGC experiments are for the most part carried out with capillary columns, for clear reasons related to efficiency. Capillaries were employed for the first time, in the MDGC field, in 1964 [5]: two 150 ft columns were connected via a pneumatically-operated diaphragm 6-port valve.

Almost, the columns can be placed in a single or two separate ovens, with the latter solution being certainly the most flexible one. The first double-oven MDGC experiment was carried out nearly 40 years ago [6]. A transfer device is located between the two dimensions, and enables the passage of chromatography bands, from the primary to the secondary column. A cryotrap, situated between the two capillaries, is an option leading the following advantages:

(1) sensitivity improvement through analyte re-concentration;

(2) peak capacity increase, by considerable reduction of the width of primary-column chromatography bands;

(3) concentration of trace-amount compounds, co-eluting (or not) with other constituents, applying subsequent analyses.

It must be added that, for many compounds, focusing can be attained by keeping the second oven at a low temperature during heart-cutting.

The transfer systems until-today developed can be classified in three groups: (I) in-line valve, (II) out-line valve and (III) valveless systems.

In the first group, a valve interfaces the two columns in a direct manner; out-line valves are employed to regulate the direction of gas flow toward the column interface, while valveless systems form a third minor MDGC group. When an MDGC instrument (in- or out-line valve) is in the stand-by mode, a one-dimensional analysis can be carried out; when the configuration is switched to the cutting mode, the primary-column effluent is directed toward the second column. The greater the number of transfers achieved, the higher the possibility of a mix-up of previously separated compounds. Although such an occurrence goes against a golden rule of multidimensional chromatography, namely that all compounds resolved in the first dimension, must remain so in the second, the event is acceptable if all target analytes remain separated.

Classical MDGC is usually employed for the bidimensional analysis of a part of the sample, while the other fraction is of no analytical interest. In short, the primary-column separation can be recognized as a prefractionation step, with no mess involved. Although, in principle, it is possible to carry out sequential cuts on the entire primary column effluent, such an approach is hardly ever used if all the sample constituents require analysis in both dimensions. Other rather unpractical and elaborate alternatives for such an analytical scope have been developed, namely, the use of an array of second dimension capillaries, one for each heart cut, or parallel traps located between the two dimensions, used for storage purposes [7].

Deans realized a major breakthrough at the end of the 1960s, with the introduction of pressure switching [8], what is here designated as an out-line valve system. The invention of the Deans switch brought a series of uneqivocal advantages, such as no temperature limitations, artefact formation, memory effects, or direct contact between valve mechanical parts and sample compounds; furthermore, the contribution of such interfaces toward band broadening was very low; allowing basic MDGC operations such as venting and backflushing.

3.2 Basic instrumentation set-up

Preceding to the descriptions of the commercial systems and applications, attention will be dedicated to the concept of in-series twin-capillary GC, the coupled-column approach proposed by Deans and Scott [9], and recent versions of that technology. Looking at an quite simple sample, composed of two constituents, represented as α and β. If such a sample is analyzed on two conventional capillaries (*e.g.*, 30 m × 0.25 mm I.D.) linked in series, with different selectivities, and under ideal conditions of temperature (with a single oven) and flow, then the possible analytical outcomes are four:

(1) α and β overlap to some degree on both capillaries;
(2) α and β remain entirely resolved on both columns;
(3) α and β are separated on the first column but overlap to some degree on the second;
(4) α and β co-elute to some degree on the first column, and are separated on the second.

In cases I and II, the employment of the second stationary phase is unproductive, while it is entirely negative in the third situation. On the contrary, a clear advantage is reached in the fourth situation. If the previous example is extended to a medium-complexity sample (*e.g.*, 100 compounds), then the number of possible combinations becomes extremely high. However, the final number of compounds that one could expect to resolve would most probably be not that much higher than that attained using a 60 m × 0.25 mm I.D. column, with a single stationary phase. One way to improve the chromatography of a coupled-column system would be to operate each stationary phase using independent temperature programs [10]. A further approach of improving the separation performance of a twin-capillary system can be obtained by manipulation of the gas flows in each column, by using an additional pressure source connected to the columns connection point [9]. A series of attractive papers, based on such an approach, have been described by Sacks and co-workers [10-12]. A scheme representing a series-coupled column ensemble with stop-flow operation is shown in Figure 3.1. The system illustrated is one belonging to the out-line valve MDGC systems. The valve is connected on one side to the columns junction point, and on the other to an aluminum ballast chamber. The pressure in BC is controlled by an electronic pressure controller. An FID is also located between the two chromatography dimensions. If a pressure pulse, equal to that of the injector, is applied to the columns connection point, then a condition of stop-flow will arise in the first column, while elution continues in the second dimension.

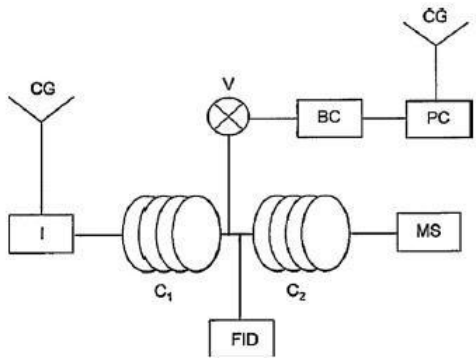

Figure 3.1. Scheme of a coupled column system, with stop-flow operation. Abbreviations: C1 = first dimension; C2 = second dimension; V = pneumatic valve; BC = ballast chamber; PC = pressure controller; I = injector; CG = carrier gas source [11].

The stop-flow MDGC instrument was employed in combination with a third separative dimension, *viz.*, a time-of-flight (ToF) mass spectrometer, in the high-speed analysis of essential oil compounds [13]. Such MS system possess the exclusive capability to unravel coeluting GC peaks through spectral deconvolution. Figure 3.2 shows three chromatograms relative to the analysis of 9 compounds, using the tandem-column ToF MS system. Around 10 % of the first-dimension (7 m × 0.18 mm I.D. × 0.2 µm d_f trifluoropropylmethyl polysiloxane) effluent was directed to an FID (Figure 3.2 a); the single-column GC-FID chromatogram illustrates that peaks 3–4 overlap completely, while compounds 5–6 coelute partially. Looking at the middle total ion-current (TIC) chromatogram, that is an application carried out with no mid-pressure regulation, it can be simply inferred that the chromatography situation has become worse: peaks 1–2, separated on the polar column, co-elute completely on the apolar second column (7 m × 0.18 mm I.D. × 0.2 µm d_f, 5 % phenyl); though peaks 3 and 5 are now totally separated from components 4 and 6, respectively, peaks 4 and 6 now overlap completely; compounds 7-8-9, previously resolved, are now mixed together after their passage on the second capillary.

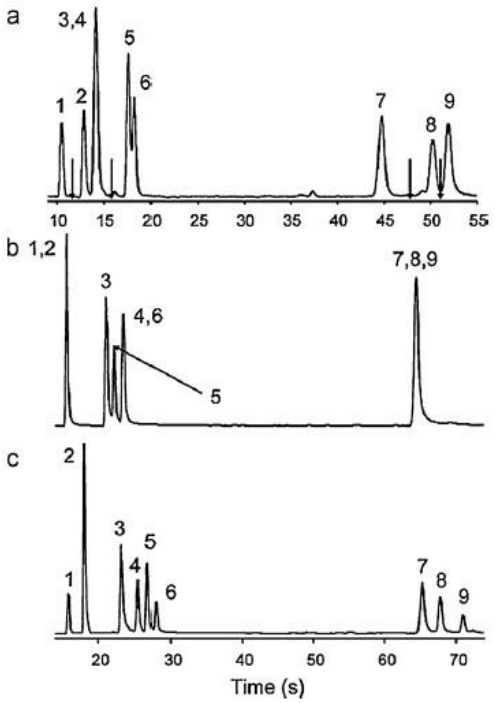

Figure 3.2. Chromatograms relative to the FID primary-column analysis (a), to the total ion-current MS result with no stop-flow operation (b), and to the total ion-current MS analysis with stop-flow operation (c). Peak identification for the essential oil compounds: (1) camphene; (2) furfural; (3) eucalyptol; (4) terpinolene; (5) benzaldehyde; (6) octanal; (7) β-caryophyllene; (8) geranyl acetate; (9) eugenol [13].

A 4-point stop-flow experiment, carried at times indicated by the arrows in Figure 3.2a, enabled the chromatographic separation of all nine volatiles. The first stop-flow operation was made just after the first-dimension elution of peak 1: compound 2 was halted for 5 s in the final primary-column segment. Elution in the first dimension was suspended a further 3 times: once to separate compounds 4 and 6, and the remaining two times to separate compounds 7-8-9. Mass spectral deconvolution was necessary for the chromatogram illustrated in Figure 3.2b, but was clearly not needed in the stop-flow analysis (Figure 3.2c). The stop-flow approach is both simple and attractive, and could be employed as an alternative MDGC method, though currently it is hard to encounter going through the literature.

Recently, an MDGC instrument, characterized by a microfluidic transfer device (Agilent Technologies), has been described [14]. The interface is a thermally stable, leak free, chemically inert, low dead volume, Deans switch,

manufactured through capillary flow technology (CFT): through holes and flow channels are etched into stainless steel plate halves, which are folded, heated to a very high temperature (>1000 °C); then, high pressure is used to generate a diffusion-bonded metal sandwich. The internal channels, created in a similar mode to the production of integrated circuits, are deactivated with a coating layer. Leak-free connections are made by using metal ferrules. Optimum conditions for stand-by, cutting and backflushing processes are created by using electronic pressure control. The interface holds five ports: two are connected to the primary and secondary columns, while another is linked to a restrictor, with the same flow resistance as the second dimension. The latter requisite is important, considering that the pressure drop across the primary column must remain constant during the two operational modes. If pressure-drop differences do occur, then there will be a mismatch between the programmed chromatography- band transfers, which are set on the basis of a preliminary stand-by separation, with those which occur during an MDGC analysis. The restrictor is usually connected to a detector, to monitor the first-dimension separation. The remaining two entrances are fixed, being linked to a two-way solenoid valve. Figure 3.3 shows how the device achieves the bypass (stand-by) and inject (cut) states. The primary flow, which is always lower than the auxiliary flow, enters the interface through the central port.

During the standby mode, the solenoid valve leads the auxiliary flow to the top left part of the Deans switch, which is connected, via an internal channel, to the port linked to the secondary capillary. Once inside the interface, the additional gas flow is divided in two parts, one directed to the second column and the other crosses the internal vertical channel ending up in the restrictor. Prior entry to the restrictor, the auxiliary flow is mixed with the first-dimension flow.

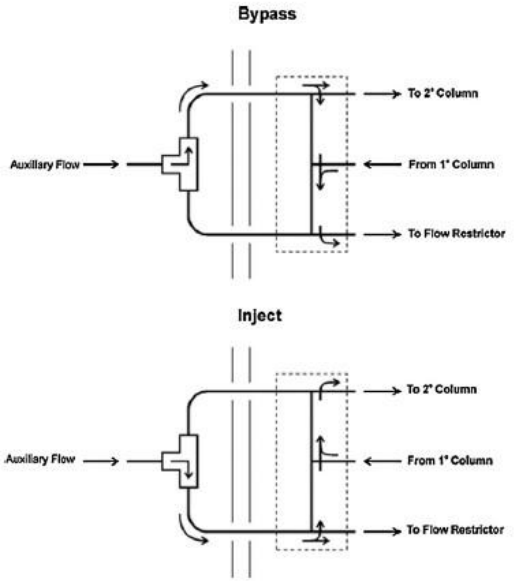

Figure 3.3. Scheme of the Agilent Deans switch in the bypass (stand-by) and inject (cut) modes [14].

When the solenoid valve is switched to the cutting state, the auxiliary flow is directed to the bottom left part of the transfer device, which is connected, via an internal channel, to the port linked to the flow restrictor. Once inside the interface, the auxiliary gas flow is split between the restrictor and the second column. As in the standby mode, the additional flow is mixed with the primary-column flow.

A further commercial system is the integrated "selectable 1D/2D GC–MS system", currently commercialized by Gerstel and characterized by an Agilent capillary flow technology interface and low thermal mass GC modules [15]. The unified system is equipped with dedicated software to deal both with GC–MS and MDGC–MS applications. The main novelty is that the same mass spectrometer is employed in both applications, specifically for stand-by and cutting analysis, meaning that peaks subjected to one- and two-dimensional analysis appear in the same GC–MS chromatogram. Apart from the MS system, other detectors can be used for one- and two-dimensional GC applications. Figure 3.4 shows schemes of the unified instrument: an Agilent GC was equipped with a thermal desorption inlet, two independent LTM units, a CFT Deans switch and a CFT cross-union, to connect the restrictor (0.54 m × 0.10 mm I.D.), the second (5 % phenyl) column (10 m × 0.18 mm I.D. × 0.40 µm d_f), the MS transfer line, and the transfer line to other detectors.

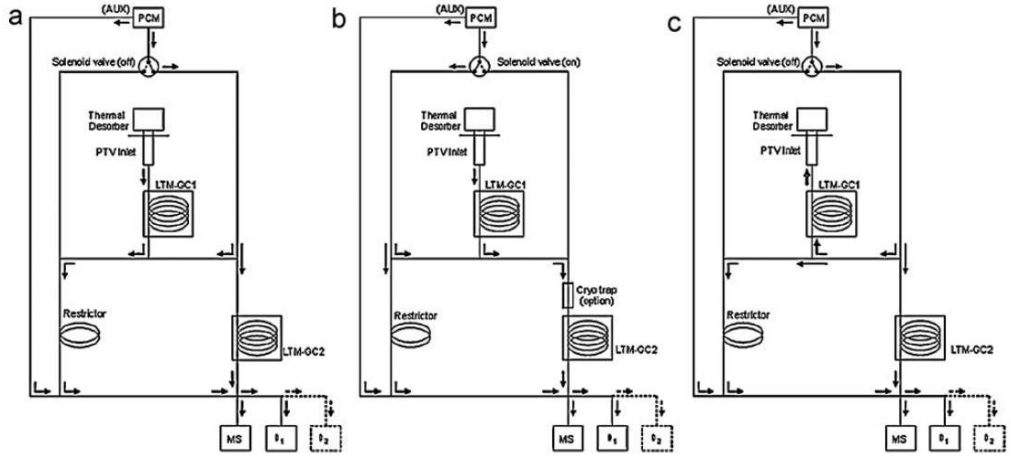

Figure 3.4. Schemes of the Gerstel "selectable 1D/2D GC–MS" system [15]. The one-dimensional GC–MS configuration is reported in (a); the transfer configuration is illustrated in (b); the two- dimensional GC–MS/backflush configuration is shown in (c). Abbreviations are defined in the text .

The Agilent Deans switch connections have been illustrated previously. Apart from the PCM (pressure control module) connection (168.4 kPa) to the transfer device, a further line of the auxiliary pressure source (21.0 kPa) supplied make-up gas to the cross-union. A stand-by GC–MS application was carried out by diverting the "wax" primary column (10 m × 0.18 mm I.D. × 0.30 µm d_f) flow toward the restrictor (Figure 3.4a), while a second-dimension GC–MS analysis was performed by activation of the solenoid valve (Figure 3.4b); if required, the transferred chromatography band can be re-concentrated at the head of the secondary column by using a cryotrap. At the end of the transfer period, the remaining part of the sample was backflushed by decreasing the head pressure to 10 kPa (initially 212.7 kPa), and the second-dimension LTM heating can begin (Figure 3.4c). Though the selectable 1D/2D GC–MS system is certainly interesting it also appears to be characterized by a drawback, mainly the difficulty to perform multiple heart-cuts. The latter operation could be achieved by accumulating more than one heart-cut in the cryotrap (or even at the ambient GC temperature if not very volatile) or by performing a single application for each heart-cut. The successful outcome of the first option would depend on the capability of the second column to separate all the entrapped compounds, while high time costs could characterize the second route. Gerstel also commercializes a more classical heart-cutting MDGC system (MCS: multidimensional column switching system, with a Deans switch, and a primary (monitor) and secondary (main) column detector.

A further effective Deans-switch MDGC system has been developed and introduced by Shimadzu Corporation. The MDGC instrument is commercialized in the double-oven configuration, and is equipped with a quadrupole mass spectrometer. The first and second dimension capillaries are linked by using a low dead-volume, thermally stable and chemically inert stainless steel interface. The latter is housed in the first oven, is characterized by very small dimensions (ca. 3 cm long), is connected to an auxiliary pressure source (2 ports) and to a stand-by detector. Furthermore, a fused-silica restrictor (R_1) is fixed inside, and crosses the interface. Figure 3.5 reports two schemes of the entire Shimadzu transfer system in the stand-by (Figure 3.5a) and cut positions (Figure 3.5b).

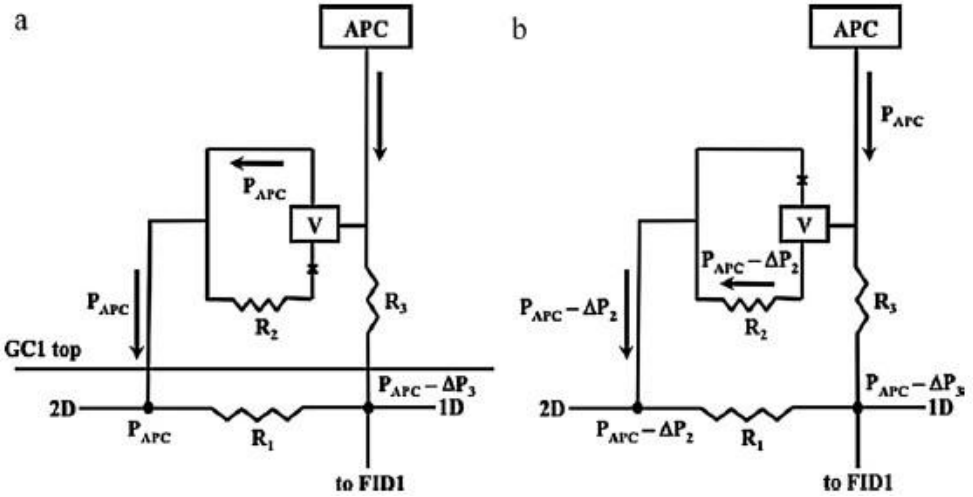

Figure 3.5. Scheme of the Shimadzu Deans switch in the stand-by (a) and cut (b) configurations. Abbreviation definitions are reported in the text [16].

Though the five-port metallic interface is located in the first GC, defined as GC1 (Figure 3.5 a), it is clear that a web of external connections is necessary to create the required MDGC conditions. In both operational modes, an advanced pressure control unit (APC) supplies a gas flow at constant pressure to an external (with respect to the GC oven) fused-silica restrictor (R_3) and to a two-way solenoid valve (V). The latter is connected to two metal branches, one with another fused-silica restrictor (R_2) and one without: R_2 produces a pressure drop, slightly higher than that generated by R_3 ($\Delta P_2 > \Delta P_3$). In the stand-by mode (Figure 3.5a), the APC pressure is reduced on the side of the first dimension (*e.g.*, 100 kPa – ΔP_3), while it reaches the second dimension branch, passing through the solenoid valve, unaltered. Through such a configuration, analytes

eluting from the first (apolar) column are directed to FID1. Once the solenoid valve is activated, the transfer device passes to the cutting mode (Figure 3.5b): the pressure on the first-dimension side of the interface remains unaltered, while the pressure on the second-dimension side becomes 100 kPa – ΔP_2 (a pressure lower than 100 kPa – ΔP_3). It is clear that, under such conditions, the primary-column eluate is free to reach the second (polar) capillary. The instrument is automatically controlled by using a dedicated software that also enables the calculation of fundamental GC parameters, such as gas flows, linear velocities, and analyte recovery.

With respect to the Agilent system, the main differences are that: the capillary linked to the stand-by detector does not need to be characterized by the same flow resistance as that of the secondary column (meaning that if one wants to change the second column, then one does not need to replace the restrictor also); the external design of the (3-restrictor) transfer system is a little more elaborate. However, both the commercial instruments work in an effective manner. Among a series of MDGC experiments, a 14-cut application on perfume allergens will be herein described [16].

Recently, the connection between a series of perfumery ingredients and contact allergy has been the subject of wide scientific discussion [17]. On the basis of European legislation (7th Amendment of the Cosmetic Directive), the 26 most frequently-recognized skin allergens must be reported on the final cosmetic product if specific concentrations are reached: 10 and 100 mg L^{-1} in leave-on and rinse-off products, respectively. Twenty-four compounds, out of the twenty-six, are amenable to GC analysis. Prior to an MDGC experiment it is usual to inject a standard solution of target analytes to define the heart-cut windows. In the case of solutions containing perfume allergens, it is well known that they are characterized by a short life-time due to unstability. To avoid such a problem a valid alternative was found: an alkane mixture was subjected to stand-by MDGC–MS analysis, prior to the injection of the allergen standard solution. Experimental linear retention indices (LRI) were derived for each compound on the primary (5% diphenyl) column; LRI cut windows were developed by adding and subtracting 10 LRI units, with respect to the experimental value. Once an LRI cut window was established, the determination of a time window for each target analyte is straightforward. A total of fourteen cuts were extrapolated for 24 compounds, because the retention time difference between various allergens was only small. Through such an approach, the injection of an allergen solution prior to each MDGC application would not be necessary: it would be only necessary to derive the LRI values through preliminary hydrocarbon analysis. It is obvious that such an approach can be extended to any sample-type. A chromatogram relative to the

first-dimension perfume analysis, after heart-cutting (the position of each cut is shown), is illustrated in Figure 3.6. No retention-time shifts occurred during heart-cutting. The second dimension TIC MDGC-MS result is illustrated in Figure 3.7. As it can be seen, 12 allergens were nicely separated from other matrix interferences. The general mass spectral purity was very good, with MS database similarities always over 90%. Each allergen was subjected to quantification; the data attained were in good agreement with the allergens reported on the perfume container.

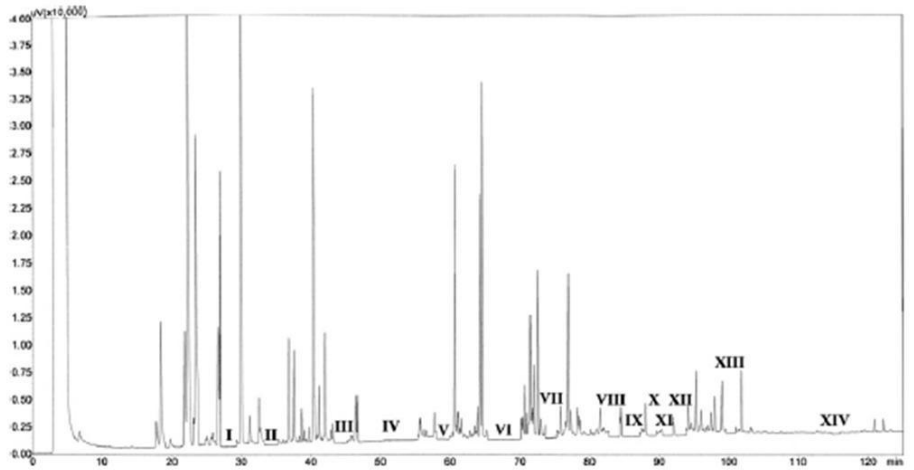

Figure 3.6. Chromatogram relative to a first-dimension perfume analysis, after heart-cutting and with the position of each cut indicated by a Roman number [16].

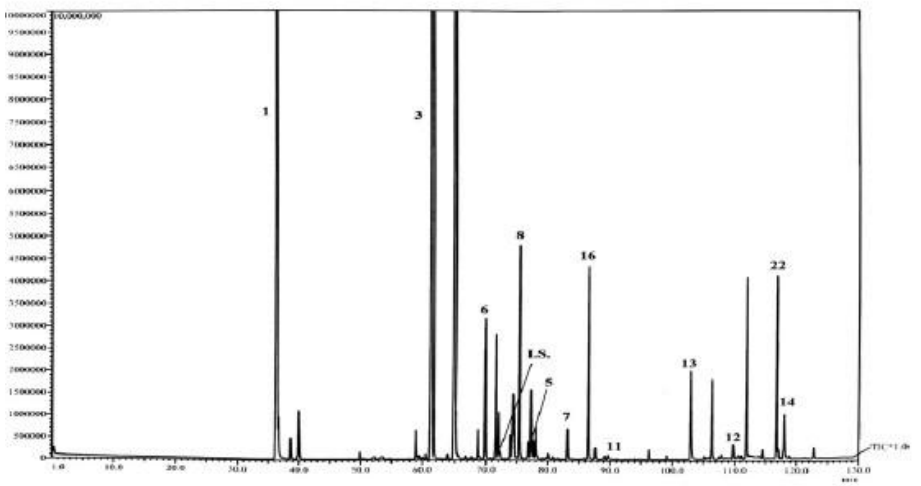

Figure 3.7. TIC chromatogram relative to a second-dimension perfume analysis. For peak identification see Ref. 16.

3.3.0 On-line coupled liquid-gas chromatography

On-line liquid chromatography–gas chromatography (LC–GC) methods are excellent tools for the analysis of complex mixtures. The high sample capacity and wide range of separation mechanisms of LC can be used for the selective clean-up, fractionation and preconcentration of the sample. For the final separation, GC offers high separation efficiency and a variety of selective detection methods. The main benefits from combining the two techniques are relative to the analysis time that is faster, less solvent is needed and the cost *per* analysis decreases. Analysis and sample preparation take place in a closed and usually automated system, where the risks of sample loss and contamination are minimized and, thus, the reliability and repeatability of the analysis are improved. In addition, the negative effects of atmospheric oxygen and moisture are eliminated. One of the main benefits of LC–GC is that, because of the efficient clean-up provided by LC, the whole sample fraction containing the analytes can be transferred to the GC. Since none of the sample material is wasted and the interfering compounds are eliminated, sensitivity is high.

In contrast to conventional GC, the LC fractions transferred to the GC are typically as large as several hundred microlitres. This cannot be done without special interfaces.

At present, most liquid chromatographic analyses are made in the reversed-phase mode (RP). Most LC–GC methods, however, are normal-phase (NP) LC–GC. In part, this is because the organic eluents used in NPLC are typically compatible with GC, making the coupling simpler. Another reason is that many of the samples analyzed by GC require extraction into an organic solvent prior to analysis, and normal-phase separation is the obvious choice. If the whole range of analytical possibilities is to be exploited, then RPLC–GC must be used as well.

On-line LC–GC systems are naturally more complicated than single chromatographic methods. It would be unreasonable, therefore, to use LC–GC for simple analytical problems that are easily solved with traditional methods. Rather, LC–GC is appropriate for samples that are difficult or even impossible to analyze by a single conventional technique. Off-line LC–GC techniques provide a good alternative to conventional techniques, when the sample amount is sufficient and the sensitivity required is not very high. Such methods offer most of the benefits of on-line techniques and the instrumentation is more flexible. The sensitivity is, however, usually lower than in on-line methods because only a part of the sample is injected to the GC. Obviously, sensitivity can be increased through the use of off-line large volume injection. The on-line

technique is always the best choice, however, when a wide series of samples have to be analysed, the amount of sample is limited (as, for example, in human exposure studies), or very high sensitivity is required. Figure 3.8 provides guidelines for choosing an LC–GC method. The main factors to consider in the selection are the complexity of the sample (*i.e.*, the amount of matrix components), the characteristics of the analytes and the selectivity and sensitivity required. The analytes of interest should also be suitable for the final GC analysis, *i.e.*, they should be sufficiently volatile and non-polar or derivatisation should be possible either before the analysis or on-line. The number of samples to be analysed is relevant. If the number is small, there is usually no need for an automated method and the time-consuming development of such a technique. The more complex the sample matrix is, the more efficient the sample clean-up must be and then LC–GC is suited for the task. LC–GC may also be preferable for relatively clean samples if very high sensitivity or selectivity is required for the analysis; for example, if the analytes of interest are present at trace levels or group-type separation of the analytes is needed before the final analysis [18]. Figure 3.9 shows a typical LC–GC apparatus, which consists of a basic LC system, an LC–GC valve interface, and a GC system with solvent vapour exit (SVE). One or two pumps are used in LC and often the separation is monitored with a UV detector. A detailed description of the instrumentation can be found in the paper published by K. Grob in 1991 [19]. Several interfaces have been developed for LC–GC coupling, even though early versions have mostly been abandoned [20-23], and only on-column [24-30], loop-type [31-37], and vaporizer interfaces [38-41], are commonly employed today. The GC part is typically a normal GC equipped with a suitable interface and a solvent vapour exit. When a vaporizer interface is used, the SVE is not always necessary. In the development of an LC–GC method, the LC method is chosen first, bearing in mind the conditions required for transfer and GC analysis.

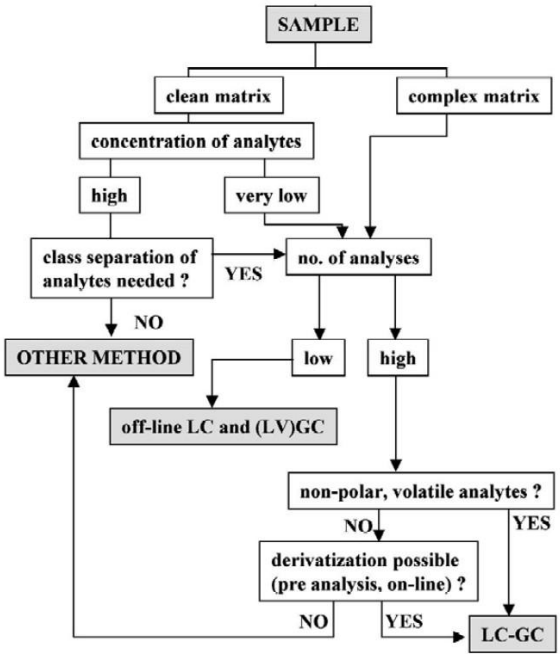

Figure 3.8. Guidelines for choosing an LC-GC method [19].

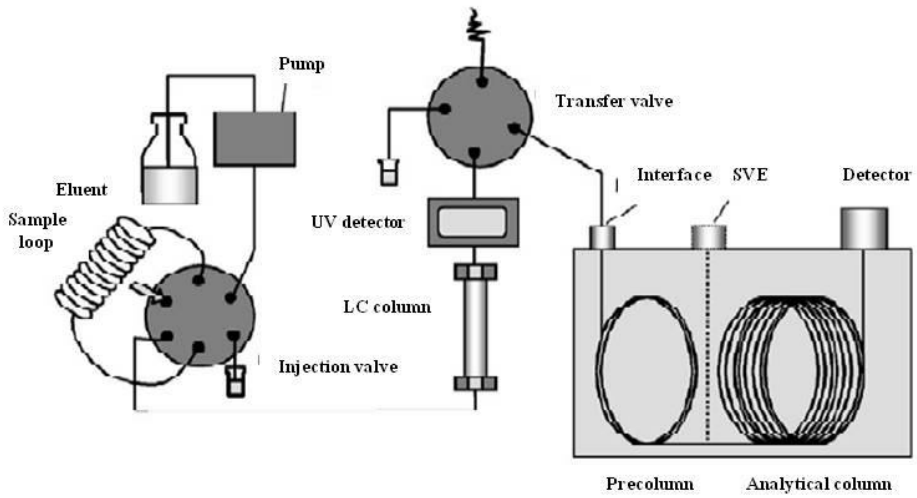

Figure 3.9. An example of a basic LC-GC coupling in an on-line mode [19].

The selection of the interface and evaporation techniques is largely dependent on the volatility of the analytes. In GC, the dimensions of the retention gap and conditions during the transfer must be optimized for the selected interface and

evaporation techniques. The other GC conditions (*i.e.*, column type, temperature program and detection) can then be selected quite independently.

3.3.1 Apparatus and conditions for on-line LC-GC

The LC step can be a simple separation of the target compounds from the bulk of the matrix, or a selective clean-up exploiting the selectivity of the LC column for a concentration or fractionation of the sample. The main LC-separation mechanisms have been intensively explored over the years [42,43].

Normal-phase chromatography has been employed most, since the eluents used are suitable for GC. Few applications using size-exclusion chromatography (SEC) have been published, because this technique involves high solvent volumes, which are not easily managed by the transfer device. Reversed-phase chromatography has been used less, since it requires particular effort to eliminate solvents; however there are a number of applications in this field. Generally, the column dimensions are selected taking into account that the optimum column flow has to fit the evaporation rate necessary for transfer optimization into the GC, especially when the retention-gap technique is used. Consequently, the 2-mm I.D. column seems to be the best compromise for obtaining the optimum column flow (optimum LC flow about 0.3–0.5 mL min^{-1}) and preserving the sensitivity necessary for some applications (*e.g.*, mineral oil contamination). Larger column diameters can be employed but using a different approach: the optimum flow (1–2 mL min^{-1}) is applied until the elution of the fraction of interest starts, then the flow is decreased until the end of the transfer (generally down to 0.1 mL min^{-1}). Backflush is a very important step, especially when NPLC is applied. The bulk of the sample (generally polar by-products) has to be removed from the column efficiently to avoid shifting of the retention time or, what is worse, any trace of the matrix reaching the GC column. MTBE and iso-propanol are very efficient solvents for cleaning silica columns (*i.e.*, triglycerides), but reconditioning with hexane is not easy and is usually time consuming, since it is too weak to remove solvents of such a higher strength (e^0) efficiently, so dichloromethane is usually preferred.

The heart of an LC-GC system is the transfer technique, extensively described in dedicated books [19], and by several reviews as previously reported.

The choice of a suitable interface depends on the volatility of the target analytes and the size of the fractions to be transferred. Nowdays, several different interfaces are present on the market; the reader can refer to the literature for detailed information [19]. A brief description of the programmed-temperature

vaporizer interface (PTV) is herein given because such an interface is reported in the experimental part (Chapter 7) of the present thesis.

In 1979, a new autoinjector interface was introduced at the Pittsburgh Conference [44,45]. The injector was modified with a flow-through side arm syringe. The volume of the fraction was limited (0.1 – 3 µL) since it was injected in a split/splitless flash–vaporization injector. The problem was solved by replacing the conventional LC column with a 1 mm microbore column, by positioning a splitter between the LC and the autoinjector interface, and by operating in the GC split mode. Several years later the LC fraction was significantly increased by using a PTV injector as interface [40]. The LC effluent was sampled from a flow-cell by a large-volume autosampler syringe and automatically injected into a PTV injector, equipped with a liner packed with different adsorbent materials. The solvent transfer can be performed in several modes, namely PTV solvent split, PTV large volume splitless, PTV vapour overflow with or without splitting. de Koning and co-workers reported various problems using the PTV interface [46], in particular recondensation in the split line or/ and in the split valve, which causes an increase in the flow resistance in the split line, and of the pressure in the injector. Consequently, both back-flow of solvent into the carrier gas flow as well as change in the split ratio, make quantification impossible. To solve such problems the split valve is positioned as close as possible to the injector and heated.

The PTV-interface is a helpful alternative to the on-column interface and presents several advantages: the packed liner retains more liquid per unit internal volume and wettability of the packing material is not required. In addition the packing material is more stable than the retention gap, especially with water and non-evaporating by-products, and it prevents high boiling compounds from reaching the GC column. Considering the diffusion of the PTV injector and the flexibility of such an interface in implementing different approaches, ranging from a normal split/splitless injection, to large volume injection and on-line LC–GC, it can be hypothesized that such an interface will enhance the introduction of LC–GC techniques in many laboratories as a routine approach. An LC–GC system exploiting the PTV syringe-type interface is commercialized by Shimadzu (Japan).

References

[1] M. J. E. Golay in: Gas Chromatography, V. J. Coates, H. J. Noebels, I. S. Fagerson (Editors), Academic Press, New York, USA, 1958.

[2] R. S. Gohlke, Anal. Chem. 31 (1959) 535.

[3] L. Mondello, A. C. Lewis, K.D. Bartle (Editors), Multidimensional chromatography, Wiley & Sons, Chichester, England, 2002.

[4] M. C. Simmons, L.R. Snyder, Anal. Chem. 30 (1958) 32.

[5] D.J. McEwen, Anal. Chem. 36 (1964) 279.

[6] D.C. Fenimore, R.R. Freeman, P.R. Loy, Anal. Chem. 45 (1973) 2331.

[7] W. Bertsch, J. High Resolut. Chromatogr. 22 (1999) 647.

[8] D.R. Deans, Chromatographia 1 (1968) 18.

[9] D. R. Deans, I. Scott, Anal. Chem. 45 (1973) 1137.

[10] R. E. Kaiser, L. Leming, L. Blomberg, R. I. Rieder, HRC & CC 8 (1985) 92.

[11] T. Veriotti, M. McGuigan, R. Sacks, Anal. Chem. 73 (2001) 279.

[12] T. Veriotti, R. Sacks, Anal. Chem. 73 (2001) 3045.

[13] T. Veriotti, R. Sacks, Anal. Chem. 75 (2003) 4211.

[14] B. Quimby, J. McCurry, W. Norman, LC GC The Peak April (2007) 7.

[15] K. Sasamoto, N. Ochiai, J. Chromatogr. A 1217 (2010) 2903.

[16] L. Mondello, A. Casilli, P. Q. Tranchida, D. Sciarrone, P. Dugo, G. Dugo, LC GC Eur. 21 (2008) 130.

[17] S. C. Rastogi, T. Menné, J. duus Johansen, Contact Dermatitis 48 (2003) 130.

[18] T. Hyötyläinen, M.-L. Riekkola, J. Chromatogr. A 1000 (2003) 357.

[19] K. Grob, in: On-Line Coupled LC–GC, Huthig, Heidelberg, Germany, 1991.

[20] R. E. Majors, J. Chromatogr. Sci. 18 (1980) 571.

[21] I. A. Fowlis, J. High Resol. Chromatogr. 13 (1990) 213.

[22] T. V. Raglione, J. A. Troskosky, R. A. Hartwick, J. Chromatogr. 409 (1987) 205.

[23] K. Grob, D. Fröchlich, B. Schilling, H. P. Neukom, P. Nägeli, J. Chromatogr. 295 (1984) 55.

[24] F. Munari, A. Trisciani, G. Mapelli, S. Testianu, K. Grob, J. M. Colin, J. High Resolut. Chromatogr. 8 (1985) 601.

[25] H. Siren, H. Hyvönen, M. Saarinen, S. Rovio, M.-L. Riekkola, Chromatographia 34 (1992) 421.

[26] L. Mondello, P. Dugo, K.D. Bartle, B. Frere, G. Dugo, Chromatographia 39 (1994) 529.

[27] L. Mondello, P. Dugo, G. Dugo, K. D. Bartle, J. Chromatog. Sci. 34 (1996) 174.

[28] G. Jongenotter, M. A. T. Kerkhoff, H. C. M. van der Knaap, B. G. M. Vandeginste, J. High Resolut. Chromatogr. 22 (1999) 17.

[29] M. Shimmo, T. Hyötyläinen, K. Hartonen, M.-L. Riekkola, J. Microcol. Sep. 13 (2001) 202.

[30] M. Shimmo, H. Adler, T. Hyötyläinen, K. Hartonen, M. Kulmala, M.- L. Riekkola, Atmos. Environ. 36 (2002) 2985.

[31] K. Grob, J.-M. Stoll, J. High Resolut. Chromatogr. 9 (1986) 518.

[32] F. Munari, K. Grob, J. High Resolut. Chromatogr. 11 (1988) 172.

[33] J. J. Vreuls, G. J. deJong, U. A. Th. Brinkman, Chromatographia 31 (1991) 113.

[34] A. Artho, K. Grob, C. Mariani, Fat Sci. Techol. 5 (1993) 176.

[35] F. Lanuzza, G. Micali, G. Calabro, J. High Resolut. Chromatogr. 19 (1996) 444.

[36] P. Tollbäck, H. Carlsson, C. Östman, J. High Resolut. Chromatogr. 23 (2000) 131.

[37] W. Kamm, F. Dionisi, L.-B. Fay, C. Hischenhuber, H.-G. Schmarr, J. Chromatogr. 918 (2001) 341.

[38] K. Grob, J. High Resolut. Chromatogr. 13 (1990) 540.

[39] K. Grob, M. Bronz, J. Microcol. Sep. 7 (1995) 421.

[40] F. David, P. Hoffmann, P. Sandra, LC–GC Eur. 9 (1999) 550.

[41] S. de Koning, M. van Lieshout, H.-G. Janssen, U. A. Th. Brinkman, J. Microcol. Sep. 12 (2000) 153.

[42] M. Biedermann, K. Grob, J. Chromatogr. A 1255 (2012) 56.

[43] G. Purcaro, S. Moret, L. Conte, J. Chromatogr. A 1255 (2012) 100.

[44] S. P. Cram, A. C. Brown III, E. Freitas, R. E. Majors, E. L. Johnson, Abstract of papers Pittsburgh Conference on Analytical Chemistry and Applied Spectroscopy, Ohio, 1979, Abstract 115.

[45] R. E. Majors, E. L. Johnson, S. P. Cram, A. C. Brown III, E. Freitas, Abstract of papers Pittsburgh Conference on Analytical Chemistry and Applied Spectroscopy, Ohio, 1979, Abstract 116.

[46] S. de Koning, H.-G. Janssen, M. van Deursen, U. A. Th. Brinkman, J. Sep. Sci. 27 (2004) 397.

Chapter 4

Comprehensive two-dimensional gas chromatography

4.1 From MDGC to GC×GC

An on-line multidimensional instrument is generally characterized by the combination of two columns of different selectivity, with a transfer device located between the first and second dimensions.

There are two types of multidimensional gas chromatography: heart-cut GC extensively described in Chapter 3 (MDGC or GC-GC) and comprehensive two-dimensional GC (GC×GC or 2D GC). In MDGC experiments (Figure 4.0 a) two different columns are used, but only a small portion of the material eluting from the first dimension column ("heart-cut") is introduced for further separation onto the second dimension. The number of heart-cuts can be increased, if only the time allowed for the separation of the cuts in the second dimension is proportionally reduced (Figure 4.0 b). When the number of heart-cuts gets high enough (and the time for their separation short enough), one accomplishes a comprehensive separation (Figure 4.0 c), in which the entire sample (or a representative fraction of each sample component) is subjected to separation in both dimensions. Consequently, one can say that GC×GC is in essence an extension of conventional heart-cut GC.

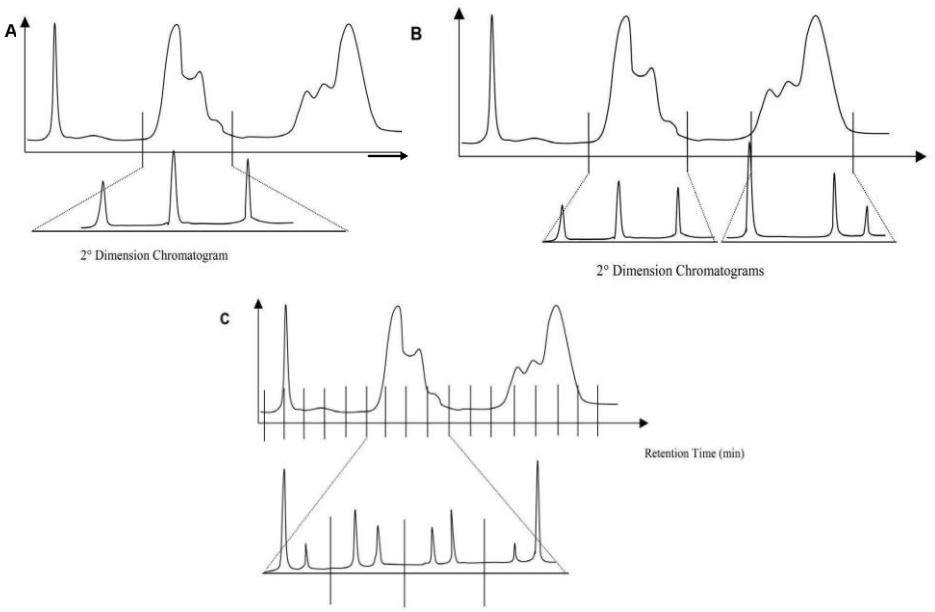

Figure 4.0. The concept of multidimensional GC. (a) single heart-cut GC analysis, where a large portion of the effluent from the primary column with coelutions is diverted to the second dimension column and separated over an extended period of time. (b) dual heart-cut GC analysis, where two regions with coelutions are diverted to the second dimension column, but with less time to perform each separation. (c) comprehensive two-dimensional GC analysis occurs when the size of the sequential heart-cuts is very short, as are the second dimension chromatograms [33].

In truth, the number of samples that can be re-injected onto the second dimension is limited in MDGC, because excessive (or continuous) heart-cutting would cause the loss of a substantial fraction of the primary column resolution [1].

The number of peaks that a chromatographic analysis can resolve can be expressed by the system peak capacity (n_c). In MDGC, the peak capacity equals the sum of that of the first and second dimensions, the latter multiplied by the number (x) of heart-cuts [$n_c^1 + (n_c^2 \times x)$] (see Figure 4.1).

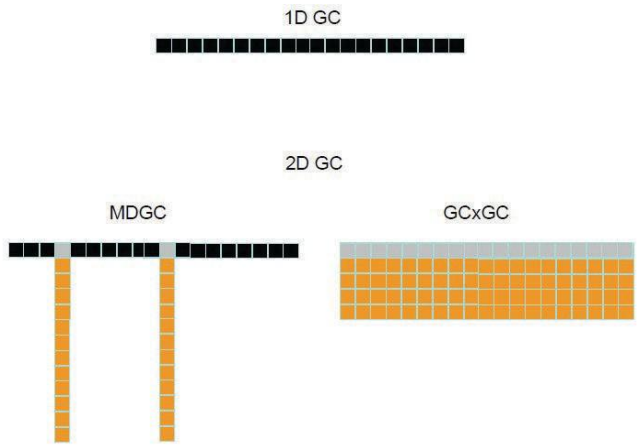

Figure 4.1. Comparison of the 1D GC and the main types of 2D GC (MDGC and GC×GC) [2].

MDGC was used quite widely in the final decades of the twentieth century, but it never became very popular. It probably did not catch on because the instrumental setup, though considered ‘‘fairly simple’’ today, was thought to be too complex for routine use at the time. The main advantages of the MDGC approach are that, in principle, the most powerful second dimension can be selected for each individual target analysis problem, and that there are no time constraints: as regards duration of the run, the second separation is not ‘‘coupled’’ to the first one. However, MDGC has an important limitation, namely the number of heart cuts that can be subjected to a secondary analysis. For such a reason, if the entire initial sample requires analysis in two different dimensions, then a different analytical route must be taken, namely a comprehensive chromatographic approach.

In an ideal comprehensive chromatography system, the total peak capacity becomes that of the first dimension multiplied by that of the second dimension ($n_c^1 \times n_c^2$) (see Figure 4.1). The first example of comprehensive multidimensional chromatography dates back to over 60 years ago. In 1944, chromatography pioneers described a two-dimensional procedure for the analysis of amino-acids on cellulose [3]: “A considerable number of solvents has been tried. The relative positions of the amino-acids in the developed chromatogram depend upon the solvent used. Hence, by development first in one direction with one solvent followed by development in a direction at right angles with another solvent, amino-acids (*e.g.*, a drop of protein hydrolysate) placed near the corner of a sheet of paper become distributed in a pattern across the sheet to give a 2D chromatogram characteristic of the pair of solvents used”.

The combination of solvents to be employed in that two-dimensional analysis was chosen on the basis of RF (retardation factor) values, a parameter (movement of band/movement of solvent front) introduced in that same paper. In fact, the right combination of solvents would enable a more extensive occupation of the two-dimensional space. The amino-acid RF values, for a series of solvent combinations, were used to both to predict and construct what today we would define as "dot plots". A predicted two-dimensional chromatogram, using collidine to develop the first dimension and a phenol-ammonia mixture to develop the second dimension, is illustrated in Figure 4.2 on the left. The excellent agreement between the predicted and experimental results can be appreciated by observing Figure 4.2 on the right.

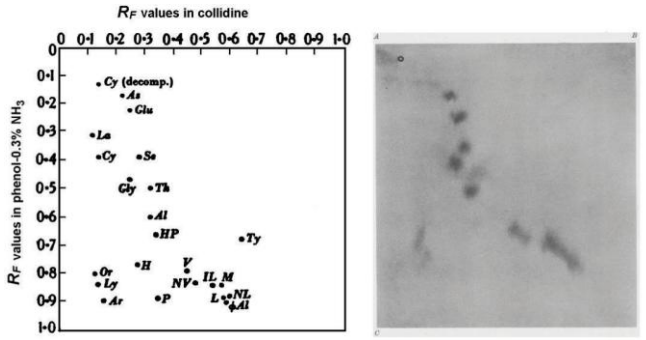

Figure 4.2. Expected positions of a series of amino-acids on a two-dimensional paper chromatogram (on the left) and two-dimensional analysis of 22 amino-acids on paper, developed using collidine in the first dimension and a phenol-ammonia mixture in the second dimension (on the right) [3].

Proceeding onto gas-phase chromatographic separations, comprehensive two-dimensional gas chromatography was invented by Phillips in the early 1990s [4,5], and has been developed to meet the increasing need for complex sample analysis and to address limitations such as peak capacity and restricted specificity of one-dimensional (conventional) GC systems.

Comprehensive chromatographic approaches can by highly useful for the separation of a complex mixture of analytes, as schematically illustrated in Figure 4.3. Let us consider a hypothetical sample that contains a large number of analytes that differ in shape, colour, and size. Following Giddings guidelines [6], the sample can be characterized by a dimensionality of three. Under such conditions, there is practically no chance to separate all the analytes using a conventional single dimension system. By using a 1D system, the separation can either be performed according to size, but then colour and shape will

remain unseparated; or it can be performed according to colour, but then size and shape will remain unseparated. Or, finally, the separation can be performed according to shape, and then size and colour will remain unseparated. A viable approach to achieve the separation of all the constituents of this sample is to use an orthogonal two-dimensional separation system with a dimensionality that can match the dimensionality of the sample [6]. In such a case, one can use most of the available separation space very efficiently to accommodate the separated analytes and create a highly-structured elution pattern.

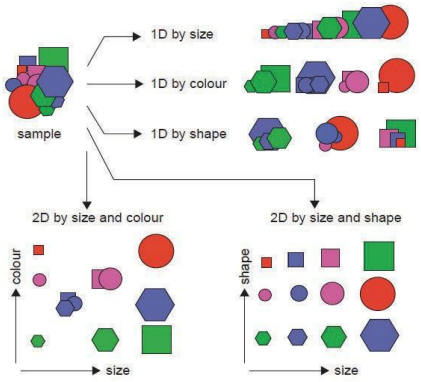

Figure 4.3. Match between separation and sample dimensionality in GC×GC. [10]

In GC×GC, everything starts by injecting and mixing the sample with the carrier gas in the injector. However, rather than entering the detector when exiting the GC column, the solutes arrive at an interface named as modulator, placed between the two separation dimensions (columns) connected in series. The modulator ensures high sampling rates and the transfer of the sample from the first to the second column [7]. The modulator acts as an on-line injector that produces very narrow injection pulses (down to 50 ms peak width) at the second column head. The entire 1D chromatogram is thus ‘‘sliced’’, on the basis of a specific modulation period (PM), and then re-injected onto the second column for a fast GC-type separation [8] (see Figure 4.4 a).

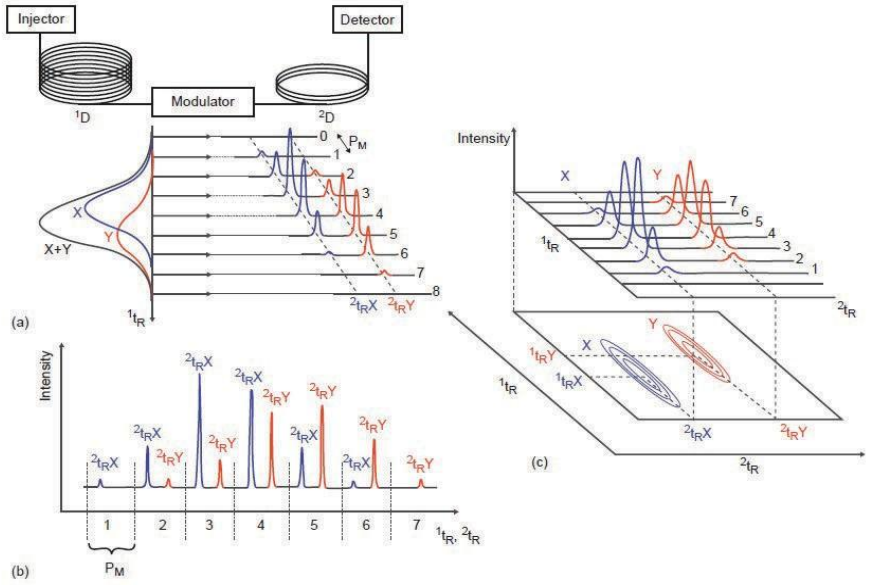

Figure 4.4 a-c. Scheme of the column coupling in a GC×GC setup and of how data are handled [10]. (a) The modulator allows the rapid sampling of the analytes eluting out from the first column and reinjection onto the second. The modulation process is illustrated for two overlapping compounds (X and Y) at a defined first- dimension retention time (^1t). As the modulation process occurs during a defined P_M , narrow bands of sampled analytes enter the second column and are characterized by different second-dimension retention times. (b) Raw data signal as recorded by the detector throughout the entire separation process. (c) Construction of the two-dimensional contour plot from (b).

Ideally, the separation of analytes in the second dimension must be completed before another pulse is injected to avoid overlap of peaks issued from different modulation cycles (an effect called wrap around). It is interesting to note, however, that, as far as no new co-elutions are generated, there is no reason to spend time and effort to avoid wraparound in a separation procedure. And even if a specific chromatographic structure ‘‘wraps around,’’ a trained eye or a dedicated software would easily re-establish a clear picture of the separation space [9]. The most important drawback of wraparound is when peaks overlap and co-elutions occur. The second column analysis is normally much faster than the first one and sometimes a secondary GC oven is used. Because sampling (modulation) occurs during the primary-column separation, the total GC runtime of a GC×GC separation is about the same as in conventional GC. With regard to detection, everything occurs as in classical GC and a trace is monitored continuously. Specifically, a series of high-speed secondary

chromatograms, of a length equal to the PM (3–10 sec), are recorded one after another (Figure 4.4 b). They consist of slices that can be combined to describe the elution pattern by means of a contour plot (Figure 4.4 c).

As discussed, the potential ability to provide a substantially larger peak capacity is not the only advantage of GC×GC over 1D GC. GC×GC processes offer several advantages, such as the formation of highly-organized chromatograms, increased sensitivity, and so on [10-18]. To summarize, the main advantages of GC×GC, over conventional GC methods, are essentially five:

(1) speed - considering the number of resolved peaks /unit of time;

(2) selectivity - two stationary phase of different selectivity are used;

(3) separation - increased resolving power;

(4) sensitivity - the isolation of chemical noise has a considerable influence on sensitivity. Moreover, an analyte band compression effect is generated by modulation, which improves *s/n* ratios (mainly using cryogenic modulation);

(5) spatial order - the contour plot formation of chemically-similar compound patterns for homologous series.

4.2.0 Basic intrumentation set-up

Basically, a GC×GC system can be constructed using the same equipment employed for conventional 1D GC. Samples are introduced by using any type of injector (*e.g.*, split, splitless, large volume, programmed-temperature vaporizor, etc.); the eluate is then fractionated and re-injected through the modulator onto a second capillary column coated with a different stationary phase for further separation. The two columns can be situated in a single oven, or in two different ones, the latter option providing a higher degree of flexibility during method optimization. Dedicated detectors with high acquisition rates, negligible internal volumes, and rapid rise times are required to accurately reconstruct the narrow chromatography bands generated.

Finally, the entire GC×GC process requires data elaboration and visualization (Figure 4.5). Although basic information on the chromatographic performance can be deduced by expert operators from the modulated raw signal, a transformation process is necessary to visualize and elaborate the results. Dedicated software packages stack second-dimension chromatograms side by

side and, considering the modulation time, derive the first and second dimension retention times for each peak. Peak areas are attained by summing the areas relative to each modulated peak while signal intensity is considered as the height of the tallest modulated peaks and can be visualized in a different way:

(1) by the means of colors (color plot);

(2) by contour line (contour plot);

(3) by a three-dimensional plot.

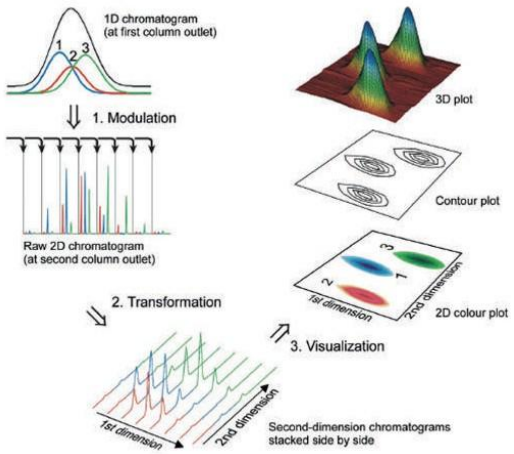

Figure 4.5. Scheme representing GC×GC data manipulation and visualization [104].

4.2.1 Column selection

Although the modulator is the key to successful GC×GC separations, the chromatographic columns play the most significant role in any GC separation. Simply installing the modulator between two columns does not guarantee a good GC×GC separation. Consequently, column combination optimization, focused on stationary-phase chemistry, column dimensions and film thickness, is required to accomplish efficient GC×GC separations.

Usually, GC×GC systems associate a first column with a non-polar stationary phase (*e.g.*, 100% dimethylpolysiloxane), with a polar second column (*e.g.*, polyethylene glycol, 50%diphenyl, 50%dimethylpolysiloxane, etc.) [19,20]. In such a configuration, solutes are generally separated as a function of increasing boiling point in the first dimension. Meanwhile, separation in the second

dimension is carried out under essentially isothermal conditions and governed by the activity coefficient of the analytes. Ideally, analytes should be separated by using two independent (orthogonal) separation mechanisms [21]. When a first column with a non-polar stationary phase is coupled with a second more polar column, the configuration is usually defined as that corresponding to a normal column set (Figure 4.6). Conversely, a reversed set associates a first polar column, with a second non-polar one.

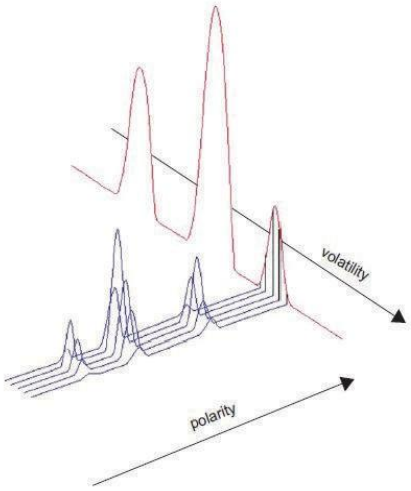

Figure 4.6. Orthogonality in GC×GC [6].

Another important feature of GC×GC is the generation of structured chromatograms in which all compounds are gathered by chemical classes in the retention space. However, for trace-level analysis, the most important goal is to separate the analytes of interest from potential matrix interferences, and structure takes a back seat. Nevertheless, one can conclude that orthogonality and structure are thus not goals in themselves; separation is the goal. As Giddings reported [6],‘‘structure’’ can be obtained under non-orthogonal conditions if the separation dimensions and sample dimensionality are properly matched.

With regard to column dimensions, the primary column is commonly 10 to 60 m long, with an inner diameter in the range of 0.18-0.53 mm and a film thickness in the order of 0.25-1.00 μm. These columns provide peak widths of 5 to 30 s, depending on the experimental conditions [22]. The first dimension is, in fact, often equal to those typically used in conventional 1D GC experiments. The main reason is that it is desirable to have rather large peak widths, to ensure

proper sampling of potentially co-eluting analytes prior to their separation on the ^{2}D column.

On the other hand, the secondary column is usually much shorter, typically 0.5 to 1.5 m length, and has a reduced ID than that of the ^{1}D column, thus allowing for fast analysis. Film thickness is also normally reduced, in the 0.1-0.25 μm range, enabling increased separation efficiencies. In general, it may be true that narrower ID columns provide higher peak capacities than wider columns. In GC×GC, however, when using a micro-bore second column, the pressure drop across the second column is much higher than when using a wider ID column. The main consequence is that the chromatographic process in the first column is much slower, while an excessively high ^{2}D gas linear velocity is generated.

Any existing stationary phases that can be used in GC can also be used in GC×GC. A variety of stationary phases can be selected according to the intended analyte-stationary phase interaction. Many sample-types are characterized by the presence of homologous series of constituents. If the right columns are selected, chemically-similar compounds can form bidimensional patterns, which are a very useful tool for peak identification. Using a straightforward orthogonal set, the non-polar compounds are located in the lower parts of the 2D chromatogram, while the more polar compounds are more retained in the second dimension, and thus are present in the upper part of the contour plot.

The GC×GC analysis of fatty acid methyl esters (FAMEs) is a perfect example to illustrate group-type order [23]; Figure 4.7 shows a complex human plasma fatty acid profile. Homologue compounds are situated in a grid, according to their chemical characteristics; saturated FAMEs are in the lower part of the 2D chromatogram, while an increase in the number of double bonds (DB) in the fatty acid chain intensifies retention in the second dimension. FAMEs are also separated according to the DB position. Compounds with the DB in the same ω position are aligned in parallel diagonal lines, with the higher ω positions eluting before the lower ones (ω6 FAMEs elute before ω3 ones).

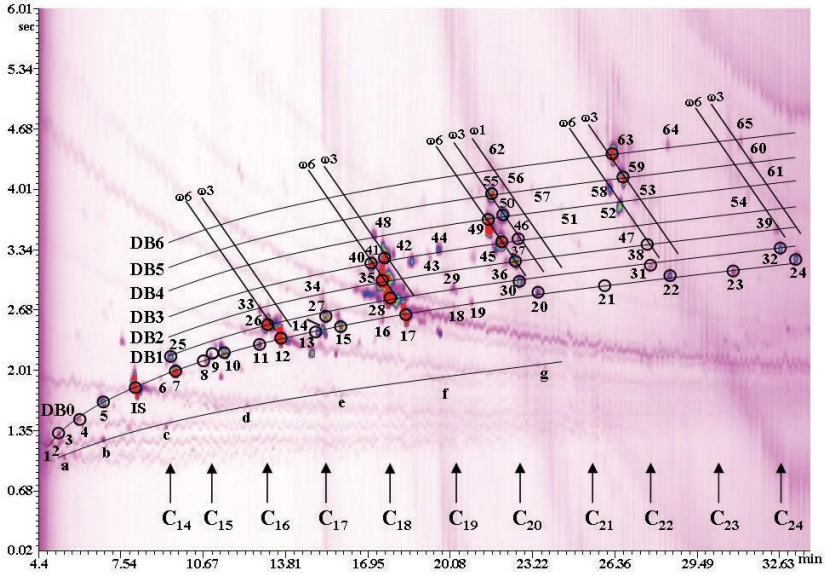

Figure 4.7. GC×GC analysis of human plasma fatty acids. For peak identification see ref. 23.

This ordered structure is of great help for compound identification. The same group [24], in a recent flow modulated GC×GC-qMS application, highlighted the degree of order within the C_{20} carbon-group, in an analysis of menhaden fish oil. Here, some low MS match values (for trace compounds) were acceptable due to the support, for identification, of the ordered elution patterns. For example, the peak indicated by the question mark in Figure 4.8 was not present in the spectra "hit list", most probably due to its low signal. However, the FAME was assigned as $C_{20:3\omega3}$ (compound 37) on the basis of its specific location, at the intersection point between the DB3 and ω3 bands.

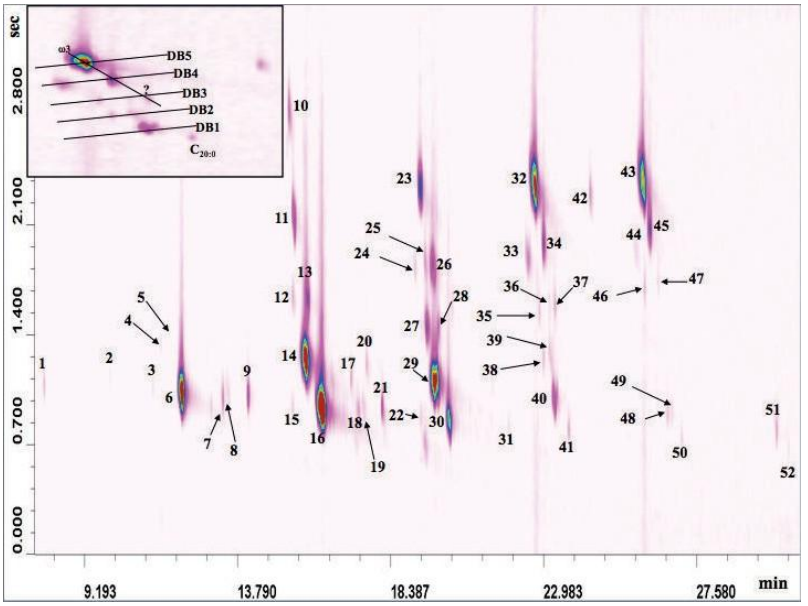

Figure 4.8. Bidimensional chromatogram relative to the flow modulated GC×GC–qMS analysis of menhaden oil FAMEs. For peak identification see ref. 24. The C_{20} group is shown in the inset.

On the other hand, the reversed column set can better satisfy the aims of a specific research. In 2004, Adahchour and co-workers studied and compared a normal and reversed column set for two different complex samples, namely diesel oil and food flavours [25]. For the former sample-type, a reversed ordered structure was obtained, with the different classes (alkanes, mono-aromatics, di-aromatics, etc.) grouped tightly together, giving an advantage when group-type determination is required. When the food flavour samples were analyzed, the reversed approach improved the peak shape of polar compounds, such as aliphatic acids and alcohols, which also improved the ordered structure of the chromatogram. Consequently, the normal and reversed set must both be considered for the determination of target and unknown compounds in complex samples.

Recently, Cordero *et al.* [26] studied the orthogonality and degree of spatial occupation for columns of mixed stationary phases. The authors tested stationary phases coated with mixture ratios of 25 to 75% of polyethylene glycol and dimethyl polysiloxane. They showed that this type of (secondary) column improved the resolution of natural volatile compounds. In addition, medium polarity phases are very useful for analyzing polar compounds with high efficiencies (narrow peaks and less tailing) in contrast to more polar

columns (polyethylene glycol) that can produce distortion in retention that affects their quantification precision. A recent report from Sidisky *et al.* [27], highlighted the promising thermal properties of ionic liquid stationary phases that were used at temperatures of up to 240° C. Also Seeley *et al.* used a high-temperature phosphonium ionic liquid column in a GC×GC application proving that these phases have to be considered as good candidates for the second dimension of a GC×GC setup [28].

Another interesting approach, which can be considered as a good exercise for comparing phase selectivity, is the possibility to use a dual parallel secondary column system by splitting the focused pulse. Such an approach was first described by Seeley *et al.* [29,30], who used an effluent splitter just behind the modulation valve for directing the selected fractions to two parallel and different secondary columns. The resulting approach, called dual-secondary column GC×GC (GC×2GC), produces a pair of two-dimensional chromatograms in a single run.

4.3.0 Transfer devices

The modulator controls the transit of analyte fractions (accumulation and re-injection) between the separation dimensions.

Various technological deveopments have been made throughout the history of GC×GC and two main families can be distiguished: thermal and pneumatic or flow modulators. Another general distinction exists between one- and dual-stage modulators: in the latter case, two events in series occur in two different zones of the modulator. For those modulators which use an auxiliary pressure source, the terms flow/pneumatic will be used indistinctly. Flow modulators are constructed either by using an‘‘in-line’’ switching valve or an “out-line” electrovalve (Deans switch assemblies).

Here, one-stage does not generally associate the storage of primary effluent whilst dual-stage flow modulators temporarily store primary column effluent in a sample loop prior to tranfer to the second column.

Tables 4.0 and 4.1 list the majority of GC×GC modulators until today developed, with their main characteristics.

Table 4.0. Thermal modulators.

Modulator type/Ref.	Year	Characteristics/observations
Thermal desorption [44]	1991	*DS - first GC×GC modulator
Thermal sweeper [49]	1996	DS - first commercial modulator
Thermal desorption [43]	1997	*OS – copper-wire heated
LMCS [45]	1998	DS - first cryogenic GC×GC modulator; liquid CO_2 was used for cooling
Thermal sweeper + cold jet [82]	2000	OS – mobile heating and static cooling; CO_2 was cooled (- 55°C) passing through a coil, immersed in a dry-ice ethanol bath
Two hot + two cold jets [56]	2000	DS - first static cryogenic/heater (air) modulator; liquid N_2 was used for cooling
Two cold jets [83]	2001	DS - static cryogenic modulator; liquid CO_2 was used for cooling
LMCS-design modulator [84]	2001	DS - moving cryogenic GC×GC modulator; liquid CO_2 was used for cooling
A hot + cold jet [57,58]	2002	DS – loop-type cryogenic/ (N_2 gas) heater modulator; N_2 gas was cooled passing through a coil, immersed in a liquid N_2 bath
Two cold jets + two wire heated jets [85]	2002	DS - rotating cryogenic modulator; liquid CO_2 was used for cooling
Sorbent trapping modulator [86]	2002	DS –resistively-heated stainless steel capillary trap, filled with a sorbent
One cold jet [87]	2003	OS - static cryogenic modulator; liquid CO_2 was used for cooling
Two hot jets + a cold jet [88]	2003	DS – loop-type cryogenic/heater (air) modulator; liquid N_2 was used for cooling
Two cold jets [89]	2003	DS - static cryogenic modulator; liquid N_2 was used for cooling
Thermal desorption array [90]	2003	Ten-stage thermal modulator
A cold jet [91-92]	2003 /08	DS - rotating cryogenic modulator; liquid CO_2 was used for cooling
Stop-flow [59]	2004	OS – rotary valve/cryogenic modulator; a valve was used for analyte transfer and liquid N_2 was used for cooling
Stop-flow [60]	2008	DS – a solenoid valve, outside the oven, generated pressure pulses toward the union point between the dimensions; a dual-stage, air-cooled thermal desorption modulator was used for re-concentration
Thermal desorption [93]	2008	DS – the modulator was the same as in Ref. 50
Thermal desorption [94]	2005	OS – electric heating and refrigerated-air cooling modulator tube
Thermal desorption [95]	2006	OS – electric heating and refrigerated-liquid cooling modulator tube
Two cold jets [96]	2009	DS - static modulator with compressed air for cooling
Micro thermal desorption [97]	2010	DS - micro modulator, with heating and cooling, for micro-GC×GC

*DS = dual-stage; OS = one-stage

Table 4.1. Flow modulators.

"In-line" Modulator type/Ref.	**Year**	**Characteristics/ observations**
Six-port diaphragm valve [52]	1998	OS - first PM GC×GC modulator; low duty cycle
Six-port diaphragm valve [59]	2000	DS - first loop (20 mL) PM GC×GC device; 0.8 duty cycle
Six-port diaphragm valve [62]	2003	DS - (low volume) loop modulator; maximum analysis temperature: 270°C; low duty temperature: cycle
Ten-port rotary valve [98]	2003	DS - (low volume) loop modulator; low duty cycle
Eight-port rotary valve [99]	2005	DS - (high volume) dual-loop modulator; duty cycle = 1
Six-port diaphragm valve [100]	2006	DS - loop modulator; maximum analysis temperature:275°C; duty cycle = 1
Two six-port diaphragm valves [65,66]	2007/ 2010	DS - two modulators (same as in Ref. 47) in sequence, used in a GC×GC×GC experiment
Two four-port rotary valves [101]	2008	DS - (high volume) dual-loop modulation achieved with two valves; duty cycle = 1
"Out-line" Modulator type/Ref.		
Two-way three-port solenoid valve [68]	2004	DS - first "out-line" PM GC×GC modulator; two accumulation loops were used; duty cycle = 1
Two-way three-port solenoid valve + two pressure sources [102]	2004	OS - partial-modulation, pulsed-pressure GC×GC interface; the solenoid valve and the analytical columns were connected to a Y-union
Two-way three-port solenoid V [71]	2006	DS - a single accumulation loop was employed: simplified version of the modulator described in Ref. 38
Two-way three-port solenoid valve [77]	2007	DS - the only commercially-available PM GC×GC system; the modulator is based on the interface developed by Seeley et al. [41]
Classical Deans switch [103]	2007	OS - the use of a Deans switch was extended to GC×GC analysis; low duty cycle
Two-way three-port valve [78]solenoid	2010	DS - seven port metallic disc with internal communicating channels; exchangeable external loop
High speed Deans switch [80]	2013	OS - High speed Deans switch for GC×GC analysis; low duty cycle

In Figure 4.9 the need for and the role of the modulator is clear. The direct serial connection of two different columns without a modulator results in a one-dimensional separation because analytes separated on the first column are not prevented from coelution at the exit of the second column (Figure 4.9 B). Their elution order might even be reversed (Figure 4.9 C). The modulator allows the flow of the analytes from the first column to the second column to be controlled, which fundamentally changes the nature of the separation, as illustrated in Figure 4.9 D-G. Following the same separation in the first column (Figure 4.9 D), the modulator traps and focuses the first band (black in Figure 4.9 E), and then injects it onto the second column, before collecting the following band (grey in Figure 4.9 F). The grey band is injected onto the second column only after the black band elutes from it. The grey band is then separated into two bands on the second column, while the spotted band is collected by the

modulator (Figure 4.9 G). This sequence of events assures that separation achieved in the first dimension column is preserved, and additional separation in the second column is possible.

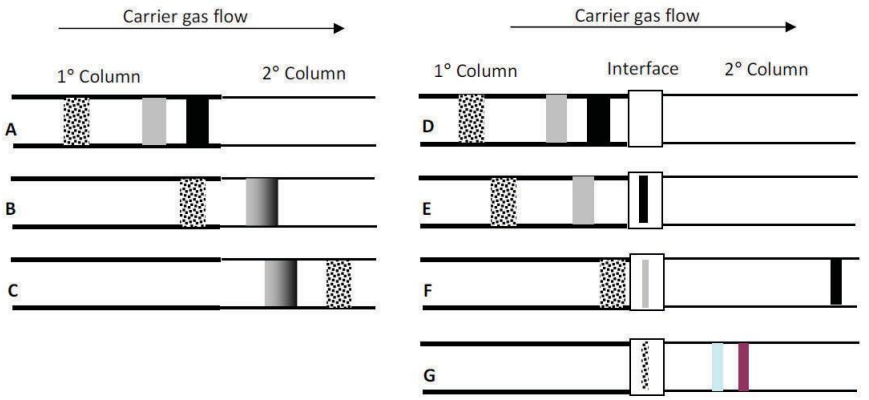

Figure 4.9. The need for the GC×GC interface. (A-C) illustrate how bands separated on one column can recombine or change elution order on the second column if they flow uncontrolled from one to the other. (D-G) illustrate how the interface traps material from the primary column, and then allows discrete bands to pass to the second dimension column while trapping other fractions [33].

To sum up, the role of the modulator is to isolate, re-focus, and inject primary column heart-cuts sequentially onto the second dimension The time taken to complete a single cycle of events is called the modulation period. The preservation of the first dimension separation can only be accomplished if every peak eluting from the primary column is sampled at least three times [31], although 2.5 times has also been proposed as the optimal value [32)]. Górecki *et al.* illustrated the effect of the length of the modulation period on the preservation of the primary column separation in his review in 2004 [33].

4.3.1.0 Thermal Modulators

The term ‘‘thermal modulator’’ is employed for all devices that use a positive and/or negative temperature difference, with respect to the GC-oven temperature to achieve the GC×GC process. Practically all thermal modulators enable a sensitivity enhancement (through a re-concentration effect) and are typically characterized by unit duty-cycle, that is the ratio between the amount of sample exiting and entering the interface. Until 1998 (year of the first cryogenic and pneumatic systems), all the modulators developed were thermal,

and were developed by Phillips and co-workers [34-42] or based on his early models [43].

As is well known, the jump from conventional to comprehensive multi-dimensional GC was first reported in 1991 [34], when Liu and Phillips used a dual-stage thermal-desorption (TD) modulator, exploited successfully in previous research as a sample-input technique [35-36].

The TD interface was constructed using the head of the apolar secondary column (1 m × 0.1 mm ID × 0.5 µm d_f), looped outside the GC oven at ambient temperature and coated with a film of electrically-conductive material, namely gold paint. The modulator was 15 cm in length, divided equally between the two stages. Twin-stage modulation worked as follows (Figure 4.10):

(1) a narrow band of first-column (moderately polar, 21 m × 0.25 mm ID × 0.25 µm d_f) effluent, in this case containing two hypothetical overlapping compounds, was formed at the modulator head (band compression I), at ambient temperature (stage 1a);

(2) re-injection was achieved through an electrical pulse of 20-ms duration (Δ1), directed to the first segment of the modulator (stage 1b), ending the first modulation stage;

(3) the re-mobilized fraction, transported by the carrier gas, hits the second ‘‘cold’’ segment of the modulator (band compression II);

(4) meanwhile, another narrow chromatography plug begins to accumulate at the modulator head, which has rapidly cooled down to ambient temperature (stage 2a);

(5) 100 ms after the previous electrical pulse, a further heating shot (Δ2) is directed to the second modulator segment, launching the narrow band onto the secondary column (stage 2b), thus ending the second modulation stage;

(6) ideally, the different secondary-dimension selectivity will enable the delivery of two separated solutes to the detector; and,

(7) 2 sec after the first electric pulse, the next modulation process was initiated.

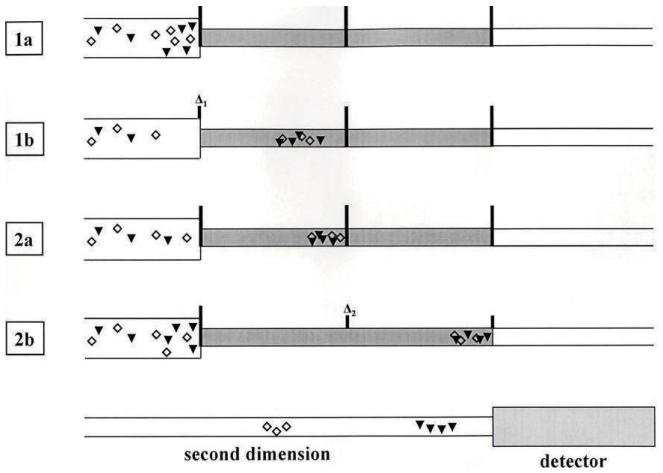

Figure 4.10. Twin-stage thermal desorption-modulation process on two compounds, co- eluting in the first dimension [43].

Phillips published additional GC×GC studies [37-38], using the primordial thermal modulator. Though excellent results were attained, the lab-made modulator was not robust, with burnouts often being an adverse result.

One of the most significant thermal modulators, also because it was the first to be commercialized (Zoex Corporation), was the thermal sweeper [39-42]. This rotating device was first described in 1996 [39], subjected to further technical development over the sequential years, and appeared in its final version in 1999 [42]. The thermal sweeper, illustrated in Figure 4.11, consisted of a slotted heater (4), rotated by means of a shaft (5). Chromatography band entrapment and focusing were achieved at the GC temperature, on a modulator capillary (3) with a thick stationary-phase coating (phase-ratio focusing), located between the two dimensions (1/2). The dual-stage process was achieved through the anti-clockwise rotation of the heater over the modulator capillary:

(1) primary-column solutes accumulate within the first part of the modulator capillary at the GC-oven temperature (a);

(2) before breakthrough occurs, the heater (275°C) rotates over the upstream end of the modulator capillary, generating a heart-cut;

(3) the previously accumulated band of analytes moves rapidly into the mobile phase (*k* values are dramatically reduced), and is swept downstream (b);

(4) the re-mobilized analytes are transported by the carrier gas, which moves faster than the heater, and undergo strong deceleration/compression at a point of the modulator capillary (*k* values increase to a value of ~40), ahead of the heater, at the GC-oven temperature (c);

(5) during the last modulation process, the focused band is injected onto the second dimension by the passage of the heater over the downstream part of the modulator capillary (d).

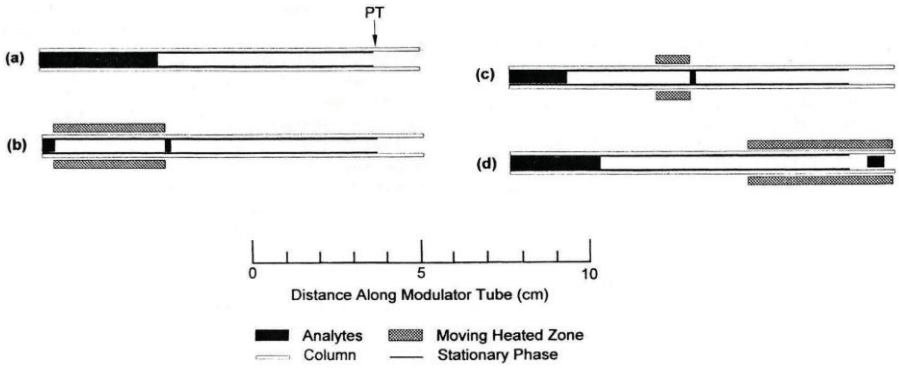

Figure 4.11. The thermal sweeper-modulation process: (a) accumulation; (b) cut; (c) compression; and, (d) re-injection. PT = Phase termination [43].

Although the thermal sweeper proved to be useful, it was found that, out of five prototypes, only two worked continuously for two years [42].

In general, the thermal sweeper was not suited to accumulating the more volatile compounds; moreover, the maximum GC-oven temperature had to be about 100°C lower than the highest operational temperature of the stationary phase.

4.3.1.1 Cryogenic interfaces

Following the introduction of the first cryogenic modulators, the use of the thermal sweeper rapidly declined, and it has not been available commercially for several years.

The longitudinally-modulated cryogenic system (LMCS) was first reported as a device capable of increasing GC signal-to-noise (*s/n*) ratios (Figure 4.12) [44]: the detector-end part of a 30 m × 0.22 mm ID × 1.25 µm d_f non-polar capillary was threaded through a moving 5-cm cryo-trap, which entrapped/focused effluent fractions through an internal CO_2 flow, generating intense cooling. Following the entrapment step, the cold region was exposed to the GC-oven heat through the longitudinal movement of the trap along the column, and, thus, the entrapped analyte was launched onto the final 40-cm segment of the column. The use of the LMCS device increased the peak height of C14:0 fatty acid methyl ester by ~ 9 times, while modulated and non- modulated *s/n* ratios for pentadecane were 56:1 and 7:1, respectively. The authors also reported the appearance of an unknown peak assigned to column bleed; the capacity of cryogenic modulation (CM) to isolate column bleed, from the sample components, was to be greatly emphasized in the following years.

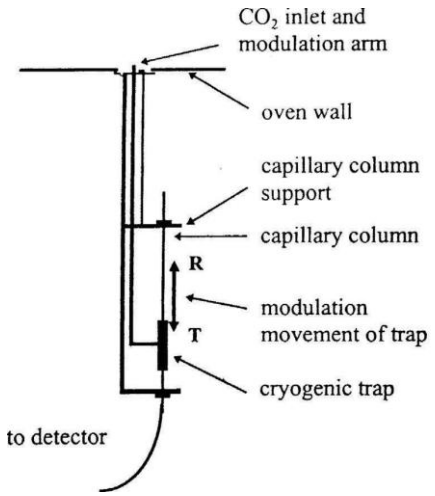

Figure 4.12. The longitudinally-modulated cryogenic system. Solutes are focused when the trap is in the T position, and released when the trap reaches the R position [44].

In 1998, Kinghorn and Marriott connected a 30 m × 0.25 mm ID × 0.25 µm d_f non-polar capillary to a polar 0.6 m × 0.10 ID mm × 0.10 µm d_f one; the first 5-

cm of the secondary column was thread through an LMCS, with the movement of the trap occurring every 7.5 sec, thus enabling comprehensive 2D GC analysis of kerosene [45]. The advantages of the LMCS device, compared to the thermal sweeper, were:

(1) more efficient entrapment/focusing (a general value of -100° C, with respect to the GC temperature, was applied);

(2) no GC-oven-temperature limitations, except that related to the less thermally-stable stationary phase employed; and,

(3) less elaborate construction.

However, the additional expense related to the consumption of CO_2 was a negative aspect, boosting the cost/analysis. In general, the lack of additional heating, for efficient re-mobilization, can be considered a shortcoming if higher MW analytes are analyzed (entrapment on an uncoated column can help). Furthermore, ^{2}D peak widths are usually greater compared to liquid N_2 + heater modulators [*e.g.*, loop-type and quad-jet], if both GC×GC systems are operated under identical conditions. The fact that the modulator is moving is an additional disadvantage.

Ledford developed a dual-stage static modulator, equipped with cold and hot jets [46]: the modulator employed two cold and two hot jets, situated at the head of the second column and pulsed in an alternate mode. The first stage of (liquid N_2) cooling, which enabled the re-concentration of a primary column chromatography band (here defined CB1), was attained by activation of the cold jet upstream [the hot jet (air) downstream was simultaneously activated]. At the end of the first entrapment process, the upstream hot and downstream cold jets were activated, enabling re-mobilization and then second-stage entrapment of CB1. At the end of the second entrapment process, the upstream cold and downstream hot jets were turned on, allowing the first-stage entrapment of another chromatography band (called CB2) and the second-dimension analysis of CB1. Immobility was, in itself, an advantage, while the modulation quality was excellent, enabling the generation of very narrow, second-dimension analyte plugs. Moreover, highly volatile compounds (*e.g.*, propane and butane) were easily entrapped by the low temperatures generated by liquid N_2 (down to -190°C). The need for and the high consumption of liquid N_2 gas (contained in bulky Dewars) were certainly disadvantages. A commercial version of the quad-jet modulator is mounted on LECO Corporation GC×GC instruments.

Shortly after the introduction of the quad-jet modulator, Ledford *et al*. proposed a dual-stage interface, equipped with a cold and hot jet, named as loop-type modulator [47]. The latter is commercialized by Zoex Corporation, and we describe its most recent version [48]. The two stages are created by looping a segment (1-1.5 m) of capillary column (modulator tube) through the pathway of a cold jet of N_2 gas (Figure 4.13).

Though the modulator loop can be created by using the last part of the first dimension, or the initial segment of the second, such options are not advisable because breakages can occur when a capillary column is coiled tightly (columns are expensive). A better choice is to use an uncoated column, or a segment of stationary-phase-coated capillary. The focusing gas, which is cooled in a heat exchange coil located in a small liquid-N_2 Dewar, flows continuously throughout the GC×GC analysis. The cold jet is directed vertically downward onto the modulator tube, thus generating two cold spots; the cold jet is diverted from the cold spots by a hot jet of nitrogen gas, which is activated for a brief period (*e.g.*, 300–375 ms), in a periodic manner (*e.g.*, every 4-6 s, corresponding to the modulation period). The hot jet is located perpendicularly to the cold one, and rapidly heats the cold spots, remobilizing the entrapped analytes (Figure 4.13).

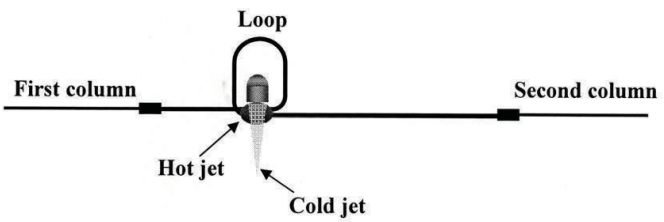

Figure 4.13. Loop-type modulator. The cold N_2 flow is directed downwards, while the hot N_2 flow is directed toward the reader [48].

Recently, Zoex Corporation has commercialized a loop-type modulator with no liquid N_2 requirements (ZX2): cooling of the N_2 gas is achieved by using a refrigeration unit, with a reported minimum temperature of -90°C, sufficient for the entrapment of C_7 alkane. The need for N_2 gas remains, with a reported maximum consumption of 18 standard L/min (SLPM) (http:// www.zoex.com/docs/pdf/ZX2-Product-Specs.pdf).

The loop-type modulator works essentially in the same way as the quad-jet system, using only two jets: analytes entrapped in the upstream cold spot are

injected in the modulator tube by activation of the hot jet. Before the analytes reach the downstream spot, the hot jet is deactivated, a new cold spot is created, and the previously remobilized analytes are subjected to a further re-concentration step. The following activation of the hot jet injects the entrapped chromatography band onto the second dimension.

The concept of stop-flow modulation, published in 2004 by Harynuk and Gorecki [49], added an option to the existing modulation modes. The stop-flow approach was interesting because it enabled decoupling of the first and second-dimension separations, and offered the possibility of optimizing each analytical process separately. For example, long modulation periods could be applied without the risk of insufficient first-dimension sampling. Figure 4.14 shows the stop-flow GC×GC instrument; the outlet of the primary column (apolar, 30 m × 0.25 mm ID × 0.25 µm d_f), and the inlet of the secondary capillary (polar, 1.5 m × 0.25 mm ID × 0.25 µm d_f) were attached to two ports (3 and 4, respectively) of a twin-stage six-port valve, with three ports plugged (1, 2 and 6). The valve was located in a chamber heated at 300°C, while a single liquid-N_2 jet was employed to focus the chromatography bands exiting port 4. An additional supply of carrier gas to the valve was attained by using a transfer line, made of deactivated fused silica, and with the same flow resistance as that of the primary column. The transfer line was connected on one side to the carrier-gas tubing, via a T-union, and on the other to port 5 of the valve. As can be seen from Figure 4.14, when the modulator is in the ‘‘sample position’’ the primary-column effluent is transferred onto the second dimension, and is entrapped by the cold jet. When the valve is switched to the ‘‘stop position’’ the flow in the first dimension undergoes an interruption (port 2 is plugged), the cold jet is deactivated and the flow in the second dimension is maintained by the auxiliary carrier-gas supply.

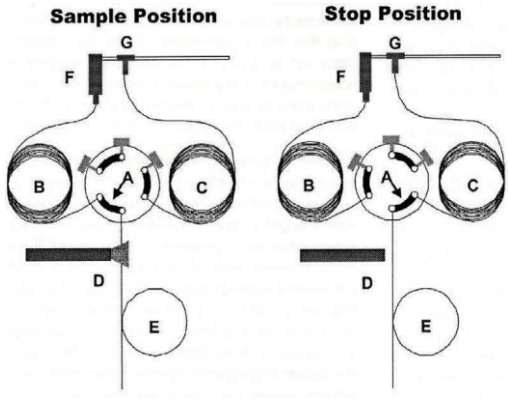

Figure 4.14. Stop-flow valve/cryogenic modulator: six-port valve with three positions plugged in the two states [49].

The performance of the valve/cryogenic modulator was evaluated in the analysis of C_5–C_{13} alkanes; the ^{1}D effluent was subjected to transfer for 2 s (sample position), and then interrupted for 4 s (stop position), leading to a 6-s analysis time in the second dimension. Using such modulation conditions would mean that an hypothetical 8-s peak would be sampled at least four times, instead of the maximum two times by using a ‘‘traditional’’ 6-s modulation period. The drawbacks are:

(1) the rather elaborate instrumental configuration of the stop-flow approach;
(2) the limited rotary valve duration;
(3) the formation of artifact peaks (derived from the valve polymer); and,
(4) the extended analysis times.

Issues (2)-(4) were circumvented by eliminating the valve from the column sequence [48], using a system based on previous stop-flow GC research carried out by the group of Sacks [49]. The flow in the primary column was stopped by using an external solenoid valve, which generated sequential pressure pulses at the union point between the first and second dimension. Consequently, it was not necessary to use the rotary valve Figure 4.15. A dual-stage, air-cooled, thermal-desorption modulator, located on top of the GC oven, was employed to re-concentrate the first-dimension chromatography bands. The overall disadvantages of the new stop-flow system were certainly reduced. However, it is clear that the instrumentation was rather elaborate and total analysis times remained longer.

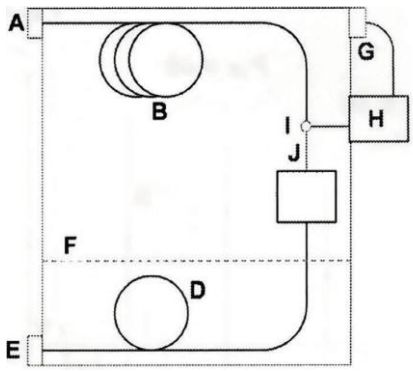

Figure 4.15. A stop-flow GC×GC system with pneumatic switching [50]. Instrumental components include (A) injector, (B) 1D column, (C) modulator, (D) 2D column, (E) detector, (F) optional second oven, (G) cool on-column injector as an auxiliary gas pressure source, (H) a solenoid valve, (I) a three-port junction, and (J) a restricting transfer capillary from the junction to the modulator.

4.3.2.0 Flow modulators

Although cryogenic modulation is effective, it is also rather costly. Consequently, the concept and the development of cryogenic-free, low-cost modulation is of great interest. Pneumatic modulation (PM) or flow modulation (FM) (both PM and FM terms are used indistinctly) is rather well-known throughout the GC×GC community and, for a variety of reasons, has always been considered as a ‘‘poor relation’’ of twin-stage CM. It is important to highlight the differences between the PM processes developed.

Two main characteristics can be identified, namely those which employ an ‘‘in-line’’ column-set, using valve/es (valve- based) and those characterized by a valve located ‘‘out- line’’ (Deans switch).

The first stop-flow approach, proposed by Harynuk and Górecki [49], can be considered a hybrid ‘‘in-line’’ valve pneumatic/cryogenic GC×GC method, while the later stop-flow technique [50] can be considered as a mixed ‘‘out-line’’ pneumatic/thermal-desorption GC×GC method.

Furthermore, ‘‘in-line’’ valve PM approaches can be achieved by storing primary-column effluent in an accumulation loop, prior to re-injection (two-step process), or by direct transfer of first-dimension plugs (one- step process). Although the ‘‘out-line’’ hybrid application reported was based on direct transfer [50], ‘‘out-line’’ PM analyses are, with few exceptions, usually carried out by using a storage loop or chamber.

4.3.2.1 Valve-based devices (low duty cycle)

It is curious that PM was described for the first time in the same year as the LMCS [52]. In an investigation focused on chemometrics, Bruckner *et al.* employed four ports of a six-port diaphragm valve (located in the GC oven) to achieve PM GC×GC analysis (Figure 4.16). A 4.9 m × 0.53 mm ID × 3.0 µm d_f apolar column and a 0.85 m × 0.18 mm ID × 0.15 µm d_f polar capillary were used in the first and second dimensions, respectively. The other two valve ports were connected to an auxiliary pressure source and to a waste line. Excessively high gas flows in the second dimension were avoided by using a split line (0.5 m × 0.180 mm ID fused-silica column).

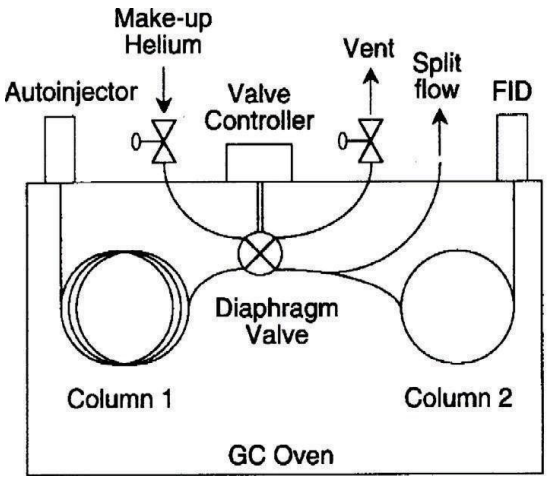

Figure 4.16. The first PM device (in the ‘‘waste’’ mode) [52].

Modulation was carried out with a chromatography band being transferred onto the secondary column for a 50-ms period at the beginning of each modulation process. At the end of the brief injection period, the valve was switched to the other position, and the primary-column effluent was directed to waste (450 msec). The auxiliary pressure unit maintained elution conditions in the second dimension. Figure 4.17 shows a bidimensional chromatogram relative to a fast white gas GC×GC experiment. Even if 95% of the primary column flow was lost, the experiment can be considered as ‘‘comprehensive’’ because the first dimension chromatography profile was maintained due to the high modulation frequency. Apart from the sensitivity issue, a disadvantage of the PM method was the restricted operational temperature of the valve.

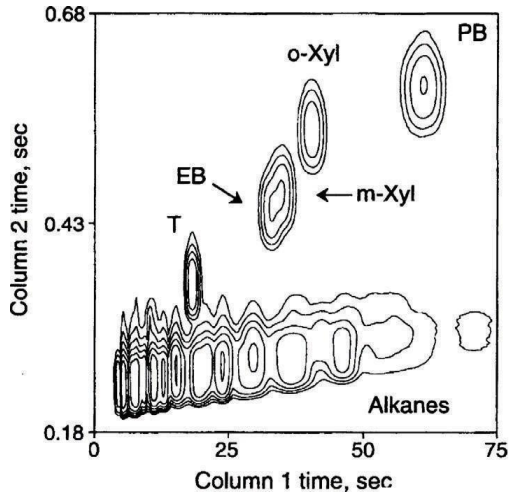

Figure 4.17. Fast PM GC×GC analysis of white gas [52].

In 2000, Seeley's group reported the first dual-stage and high duty-cycle (0.8) valve PM device, defining the approach as differential flow modulation [53], because of an independent gas flow was used in each dimension. The novel PM device comprised a six-port, two-position, diaphragm valve, equipped with a 20-µL stainless-steel sampling loop, connected to a waste line and an additional pressure source, and located between the detector platform and the GC oven (Figure 4.18).

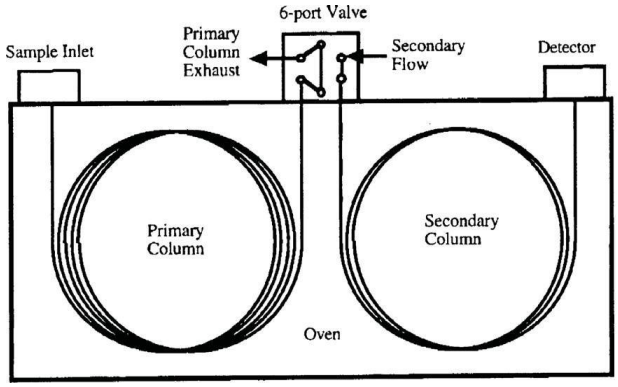

Figure 4.18. The first loop PM GC×GC device [53].

The part of the valve containing non-wetted components was situated outside the oven and was maintained at 125° C by using a heater. Inside the oven, the interface was attached to a 10 m × 0.25 mm ID × 1.4 µm d_f (6% cyanopropylphenyl, 94% dimethylpolysiloxane) primary column and a 5 m × 0.25 mm ID × 0.25 µm d_f polyethylene glycol capillary or a 5 m × 0.25 mm ID × 0.50 µm d_f trifluoropropylmethyl polysiloxane capillary. The authors used the valve in the accumulation and injection states for 80% and 20% of the modulation period, respectively (the valve is in the accumulation state in Fig. 4.18). During the injection state, while the previously accumulated chromatography plug was launched onto the second dimension exploiting a high gas flow (15 mL/min), the primary-column effluent (0.75 mL/min) was directed to waste. The employment of a 0.25 mm ID secondary column was necessary to cope with the high secondary-column gas flows. Figure 4.19 shows a 2D chromatogram relative to a mixture of standard compounds, analyzed using the polyethylene glycol column in the second dimension. Peak widths at half height between 45 ms and 65 ms were generated by the GC×GC system. Obviously, sensitivity losses were reduced with respect to the modulator developed by Synovec's group [52-59].

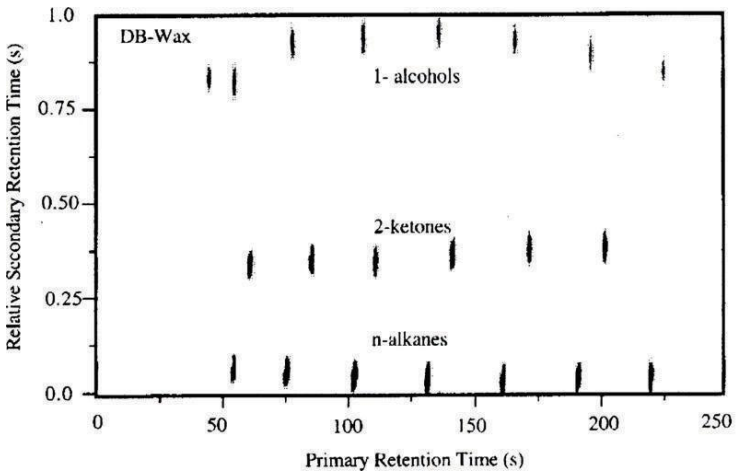

Figure 4.19. Loop FM GC×GC analysis of a mixture of primary alcohols (C_1–C_8), 2-ketones (C_3–C_8) and n-alkanes (C_5–C_{11}) [53].

The fact that the pneumatic modulator was unsuitable for analytes requiring a GC oven temperature over 200° C was a disadvantage (in common with the previous device developed by Synovec's group). The disadvantage related to the high secondary-column flows was partially resolved in a series of later PM

GC×GC studies by splitting the flow between two secondary analytical capillaries (GC×2GC) [60-61].

In 2003 and 2004, Synovec's group employed a high-speed, six-port diaphragm valve, equipped with a low-capacity accumulation loop, in a series of flow-modulation studies, exploiting a low duty cycle PM [62-64]. In particular, the first combination of PM GC×GC with a time-of-flight (ToF) MS [62] had the wetted portions of the valve (equipped with a 5-μL loop) mounted inside the oven, while the temperature-sensitive O-ring part was located outside.

It is obvious that the flows generated were necessarily within the pumping capacity (maximum operational limit: 10 mL/min) of the ToF MS. A modulation period of 2.5 s was applied, while only 10% of the primary-column effluent was injected onto the secondary capillary. Breakthrough was reported by the authors for the more abundant compounds, an effect most probably related to the low loop volume.

Apart from the disadvantages (limited duty-cycle and loop volume), the most important advantage of the modulator was the extended analysis temperature range (up to 270° C).

A general final comment can be made on the current-day employment of in-line valve systems: the only device still employed on a rather regular basis (in publishing terms) is the low duty-cycle PM developed by Synovec's group in 2003 [62]. For example, in 2007 and 2010, two six-port diaphragm valves were used in sequence to generate comprehensive three-dimensional GC separations (GC×GC×GC) [65-66].

4.3.2.2 Deans switch assemblies (unit duty cycle)

Out-line valve systems have provided the most interesting and promising PM GC×GC results. The concept of out-line valve systems departs from the possibility to play around with mid-point pressures by means of a Deans switch [67]. In 2004, a breakthrough occurred, with the construction of a novel thermally-stable PM device [68]. The interface was constructed using stainless-steel tubing, four T-unions, segments of uncoated fused-silica capillaries, and a two-way solenoid valve, the latter located outside the GC oven (Figure 4.20).

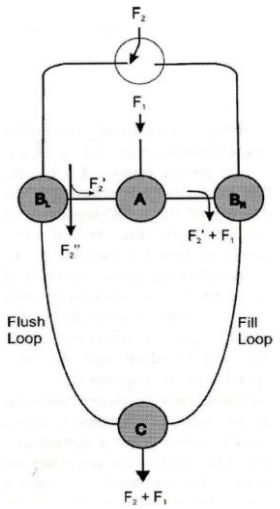

Figure 4.20. The first ‘‘out-line’’ PM GC×GC modulator in one of its two states [58].

The outlet ports of the electro-valve were linked to the lateral T-unions by using two 20 cm segments of stainless-steel tubing (0.5 mm ID). The outlet of the primary column was linked to the central union (A), the latter connected to the lateral unions (B_L/B_R) through two 4 cm × 0.15 mm ID fused-silica columns. Two accumulation loops (15 cm × 0.53 mm ID) bridged the lateral unions and the lower union (C). Considering Figure 4.20, union A receives the primary column flow (F_1), while the auxiliary flow (F_2), which is much higher than F_1, is directed by the solenoid valve towards union B_L. The auxiliary flow is divided into two parts at union B_L: a small portion ($F_2^{'}$) directs the primary-column flow toward the ‘‘fill loop’’ ($F_2^{'} + F_1$), while the main part of the flow ($F_2^{''}$) flushes the other. Optimal modulation conditions are achieved when $F_2^{'}$ is slightly higher than F_1, directing the primary-column effluent into the loop. The gas flow exiting the two loops, namely $F_2^{''} + F_2^{'} + F_1$ ($F_2 + F_1$), is directed onto the second dimension. When the solenoid valve state is changed, the fill-flush process is inversed. A series of examples were illustrated including a diesel application in which a non-polar 27 m × 0.25 mm ID × 0.25 µm d_f capillary column (5% diphenyl) was employed in the first dimension (flow: 0.9 mL/min) and a polar 5.7 m × 0.25 mm ID × 0.10 µm d_f column (polyethylene glycol) was used as second dimension. A 26.4 mL/min flow exited at union C, and was divided between the secondary analytical column and a 1.4 m × 0.25 mm ID uncoated capillary (1:4 ratio). The modulator required high auxiliary flows for efficient loop flushing, while flow splitting was useful to operate at acceptable 2D linear velocities. A typical PM GC×GC diesel chromatogram (modulation period: 2 s) was shown, characterized by the presence of very narrow peaks (on

average 70 ms at half height). Other papers followed the initial work and were focused on an evaluation study [69], and the analysis of gasoline aromatics [70]. Although this PM device was of elaborate construction, requiring fine flow tuning, it laid the basis for later more efficient, less complex PM systems. In 2006, Seeley *et al.* introduced an interesting dual-stage flow modulator [71], which was a simplified version of the system previously described by Bueno and Seeley [68]. The PM device (Figure 4.21) was constructed using three deactivated fused-silica columns, two micro-volume T-unions and a two-way solenoid valve (located outside the GC oven), connected to an auxiliary pressure source. The output ports of the solenoid valve were connected to the unions by using two fused-silica segments. One of the T-unions was linked to the primary-column outlet (upstream), while the other directed the flow to the second dimension (downstream). A fused-silica segment, bridged between the two unions, acted as sample loop (volume = ~24 µL). A non-polar 15 m × 0.25 mm ID × 0.50 µm d_f capillary was used in the first dimension (flow: 1.0 mL/min), while two polar 5 m × 0.25 mm ID columns were employed in the second dimension, one with a 0.25 µm polyethylene glycol film and the other with a 0.50 µm poly(methyltrifluoropropylsiloxane) film. When the modulator was in the ‘‘fill’’ state, the auxiliary flow (20 mL/min) was directed to the downstream union, and the primary-column effluent (~ 17 µL/s) flowed freely within the loop; the accumulation period (1.4 s) was lower than the time necessary for the effluent to reach the bottom union (~1.5 s). When the solenoid valve was switched for a brief period (0.1 sec), the auxiliary flow flushed the content of the loop onto the head of the second dimension. The pressure pulse, during the injection stage, temporarily stopped the 1D flow. The 21 mL/min flow exiting the modulator was split between the two columns, corresponding to a linear velocity value of ~240 cm/s at the beginning of the experiment (40°C).

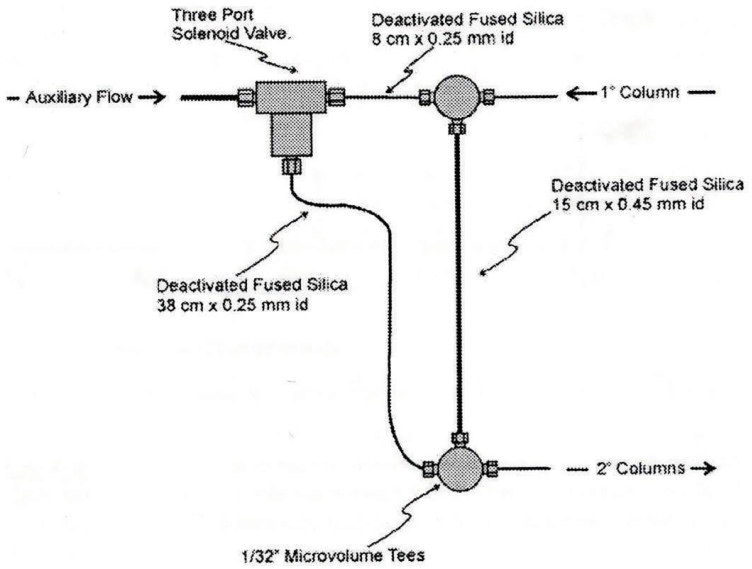

Figure 4.21. The ‘‘out-line’’ single-loop, dual-stage FM device introduced by Seeley [71].

The dual-stage PM system proposed by Seeley *et al.* was characterized by:

(1) stability at high GC temperatures;

(2) simple construction;

(3) duty-cycle = 1.

The disadvantages related mainly to the complexity of method optimization, the rather high second-dimension gas linear velocity, and the low modulation period. However, the novel modulator was very promising and was exploited successfully in PM GC×GC applications [72,73].

A series of pneumatic-modulation GC×GC works were based on the original research of Seeley *et al.* [71]:

1) Amirav’s group used a rather large storage column (50 cm × 0.53 mm ID) and brass T-unions for the necessary modulator connections in applications with flame-ionization and triple-quadrupole MS detection [74,75];

2) Harvey *et al.* proposed a symmetric flow-path modulator {*i.e.*, the use of transfer lines and storage loop of the same ID (0.25 mm) [76]}. The authors

affirmed that such a configuration was used to limit flow perturbation issues (causing detector instability).

Agilent Technologies introduced a pneumatic modulator based on Seeley's design (the only commercially-available PM GC×GC system), constructed using capillary-flow technology [77]. A planar metal structure contained an internal collection chamber, was connected (in a permanent manner) *via* two metal branches to a solenoid valve, which received a controlled gas supply from an auxiliary electronic pressure-control module. The collection chamber was filled periodically with primary-column effluent when the solenoid valve was in the collection mode (*i.e.*, when the auxiliary pressure was applied to the outlet of the storage chamber). At the end of the collection period, the internal ''loop'' was flushed by using a very high gas flow (typically 20 mL/min), generated by switching the valve to the flush mode (the auxiliary pressure was applied to the inlet of the storage chamber), the duration of which was usually 0.1–0.2 s. The interface was a simpler version of the device proposed by Seeley *et al.* [71] (the PM principles were essentially the same), with simplicity being the main advantage. The fact that the accumulation chamber was fixed, with no possibility for the operator to modify its volume, was a disadvantage. Loop volume and length, as will be demonstrated later (Chapter 8) is also a PM GC×GC method parameter to be optimized, in relation to the specific combination of columns, gas flows and modulation time parameters. As can be seen, the period 2006–07 was very active in terms of PM developments.

In 2010, Tranchida *et al.* proposed a flexible loop-type PM device [78], with the characteristics and the advantages of the two previously described interfaces [71,77], plus the possibility to optimize flows, using a waste branch bridging the interface and a needle valve [78]. Figure 4.22 shows the seven-port PM device. The interface was formed of a metallic disc (2.5 cm diameter, 7 mm thickness), and internal rectangular channels (250 μm width/75 μm depth), connecting ports 1-2-3 and 4-5- 6/7. A three-way electrovalve is located outside the GC oven and is connected to an advanced pressure control (APC) unit. Two metallic branches connect the valve to the interface in positions 2 and 5. The primary and secondary columns are linked to positions 1 and 6, respectively. A 40 μL stainless-steel loop (20 cm × 0.71 mm OD × 0.51 mm ID) bridged positions 3 and 4; the size of the loop is chosen considering the modulation period, first-column flow and second- column dimensions. It is noteworthy that the flow exiting the loop is divided between the channels linked to ports 6 and 7. Flow splitting depends on needle-valve regulation and remains unaltered during the analysis because the valve-restriction parts are located within the GC oven.

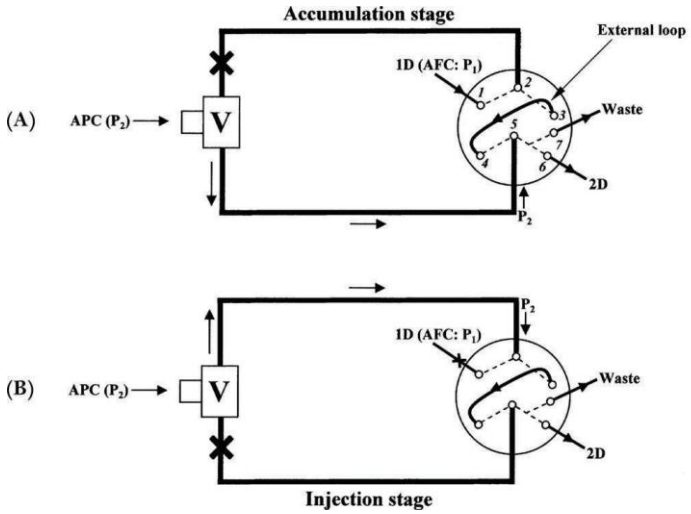

Figure 4.22. Seven-port PM device (proposed by Tranchida *et al.* [78]) in the accumulation (A) and injection (B) modes. Abbreviations: V: three-way solenoid valve; APC: advanced pressure controller.

The principles of the dual-stage PM process relate to the original research work of Seeley *et al.* [71]. A twin-oven PM enantio-GC×polar-GC-FID method (employing a 40 µL loop) was used for the analysis of essential oils. The optimized PM method was characterized by a primary-column linear velocity and flow (50°C) of ~40.5 cm/s (constant velocity conditions) and 8.7 µL/s (0.52 mL/min), respectively. The authors affirmed that a micro-bore ^{1}D was employed because:

(1) low flows generate optimum separation conditions and enable longer accumulation periods; and,
(2) efficiency increases with an ID reduction.

With respect to the second-dimension configuration, a 0.25 mm ID analytical column was used because high flows were generated. Finally, the reasons for using a waste line were:

(1) the loop pressure release was much more rapid during flushing;
(2) to emulate a high split-ratio injection; and,
(3) to generate acceptable second-dimension linear velocities: a value of ~180 cm/s (~5.5 mL/min) was calculated, with about 95% of the effluent directed to waste.

The loop flow was estimated to be 111 mL/min, while a 0.2-s injection period was exploited for efficient flushing. The optimized PM method (modulation period 3.4 s) was applied to spearmint oil analysis Figure 4.23.

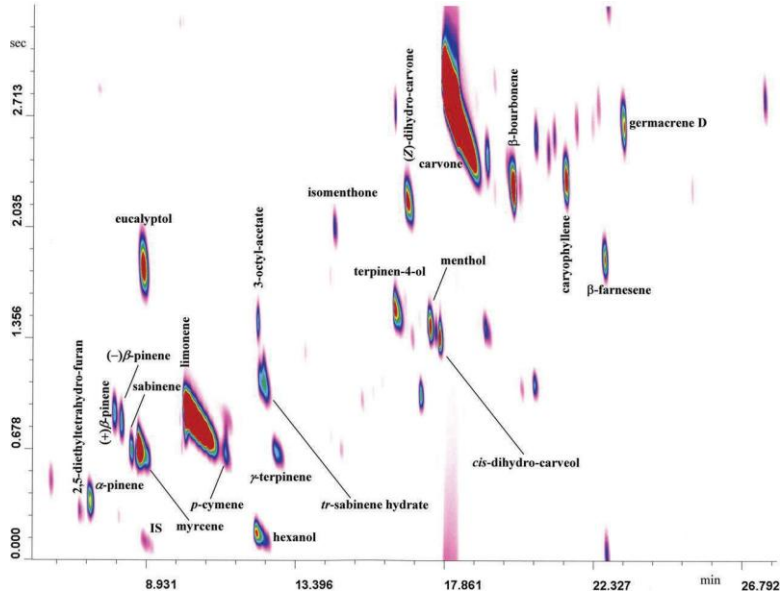

Figure 4.23. Dual-oven split-flow FM GC×GC-FID spearmint-oil analysis [78].

The authors concluded that further research was necessary to optimize the PM process, in particular the limitation of sensitivity losses. They emphasized that additional work was also required to define the best column dimensions and to reduce the complexity of the optimization step.

Very recently, Seeley and co-workers reported the use of a high-speed Deans switch, exploited as GC×GC modulator, shown in Figure 4.24 [80]. The device was constructed from a 1/32” cross union and a 1/32” tee union. A 2.0 cm × 0.53 mm piece of deactivated metal capillary, referred to as the joining capillary, was held in place between the two fittings.

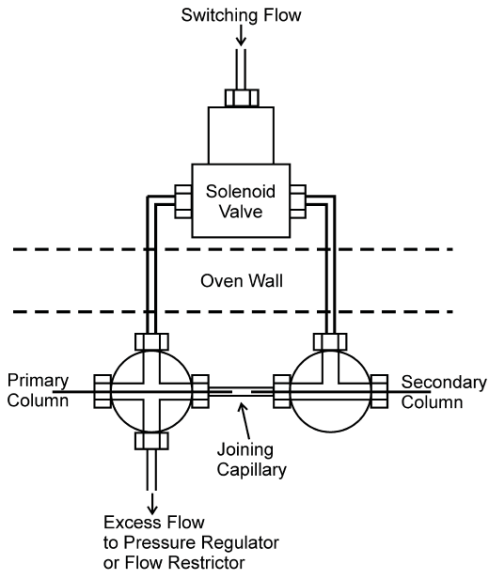

Figure 4.24. Basic construction of the high-speed Deans switch [80].

Even though reduced secondary column gas flows (i.e., 2 mL/min) were generated, the interface was characterized by a main disadvantage, namely a low duty cycle (*i.e.*, 0.1). Such works highlight the need for high duty-cycle modulators, with gas flow requirements which are compatible with commonly-used MS systems.

4.4 Detector technologies

The detector is obviously another important GC×GC system component. In addition to classical GC detector specifications, a GC×GC detector must offer high sampling rates, such as those required for high-speed GC analysis, for proper peak recontruction. A brief discussion about the most commonly-employed detectors in the GC×GC field will follow.

The most commonly employed detector in GC×GC has been the flame ionization detector (FID), which is capable of very high acquisition rates, easily above 100 Hz. The FID is a universal detector, with a response proportional to the compound carbon content, thus suitable for most quantitative applications. For instance, in petrochemical applications the FID is the most suitable detector [104-107], since such samples are formed of far too many compounds and these are not available as pure standards for quantification purposes using other

detectors, such as the mass spectrometer (MS). Indeed, when group-type 2D chromatograms are obtained, the FID can be easily employed for tentative peak classification. The group type is assigned according to retention time correspondence with even one standard, and then FID quantification can easily be performed. Biedermann and Grob exploited GC×GC-FID [108], and group-type pattern formation, for the quantification of mineral oil constituents contained in a contaminated sunflower oil. GC×GC-FID has been employed in several fields, such as environmental [109-111], industrial [112], and food [113,114].

Selective detectors are useful in trace analysis, since sensitivity can be greatly enhanced. The electron capture detector (ECD) is characterized by a high sensitivity for organic molecules, containing electronegative functional groups (halogens, phosphorous and nitro-groups). The main concern, in coupling such a detector, has been related to a rather high internal volume, which can cause band broadening. Rather recently, Agilent Technology has presented a newly-designed ECD, the micro-ECD (μ-ECD), with a miniaturized internal volume (150 μL); the μ-ECD responds more rapidly to peak flux change and is compatible with reduced columns flows. In 1999, the performance of the μ-ECD was evaluated by Klee and co-workers [115], in a monodimensional GC system. Internal dead-volumes played an important but not exclusive role on band broadening. In fact, careful optimization of the GC×GC system is also fundamental, as demonstrated in 2003 by Kristenson and co-workers [116], who evaluated and compared the performance of six modulator-types (sweeper, LMCS, quad-jet, dual-jet CO_2, semi-rotating cryo, loop), coupled with three commercially-available ECDs. The detectors were characterized by extremely different internal volumes, namely 150 μL, 450 μL, and 1.5 mL for the Agilent, Thermo Finnigan, and Shimadzu ECD, respectively. The authors demonstrated that peak broadening can be greatly limited by adjusting the make-up flow properly. Several applications have been published, using GC×GC-ECD to improve detection limits in the trace analysis of organochlorine (OCs), organophosphorus (OPs), and polychlorinated biphenyl (PCBs) contaminants [117-122].

The nitrogen-phosphorous detector (NPD) is structurally similar to the FID, except for a ceramic bead above the jet, containing an alkali metal salt, which catalyses the electron transfer to nitrogen and phosphorus compounds, forming negative ions in a flameless gaseous environment. Ions are then directed to a collector electrode. NPD temperature and gas flow modification can reduce the peak tailing that often occurs, due to the temporary adsorption of decomposition product on the ceramic bead [123]. The NPD has been used for pesticide analysis in GC×GC [124], and in gas-oil samples [125].

The sulphur chemiluminescence (SCD) and nitrogen-chemiluminescence detector (NCD) are S- and N- compound-selective detectors. Oxidation and combustion, under hydrogen-rich conditions, generate the corresponding oxide compound, which reacts with ozone to form an electronically-excited dioxide derivative. The latter generates light energy when returning back to ground state: SO_2 in the blue region of the spectrum and NO_2 in the red and infra-red region. In 2004, Blomberg and co-workers analysed dibenzothiophene, using SCD and FID simultaneously [126]. The authors found that system electronics, rather than the detector dead volume, caused band broadening. Once the problem was resolved, by using a modified electrometer, sulphur compounds were analyzed in a series of fuel products. The NCD has been employed to characterize N-compounds in a diesel sample, in particular carbazoles and indoles [127].

The atomic emission detector (AED) is a multi-element system, with the possibility to measure up to 23 elements. The capillary GC column ends into a microwave-induced helium plasma chamber where all the elements contained in a sample are atomized and excited. Characteristic atomic emission spectra pass through a diffraction grating and are detected by a photodiode array. Although the AED is characterized by a rather limited acquisition frequency, namely 10 Hz, it was coupled to a GC×GC system for pesticides analysis [128]. To meet the low sampling rate of the detector, and with the aim of obtaining quantitative data, the authors induced band broadening by connecting a 0.7 m × 0.25 mm ID uncoated column to the end of the 0.6 m × 0.10 mm ID polar second dimension.

A discussion apart has to be made on mass spectrometry, the most informative detection system, considered as an additional third dimension by GC×GC users. The coupling of an MS instrument, to a GC×GC system, has been highly desirable since the birth of comprehensive 2D GC, to add structural information to the great separation power. The first attempt was made in 1999 by Frysinger and Gaines [129], who used a quadrupole MS with a very low acquisition speed (2.43 scan/s). The authors intentionally broadened the ^{2}D peaks, to a minimum 1 s baseline width, by using a thick second-dimension stationary phase and by slowing down the heating rate (0.5°C/min); under such conditions, less than 3 data points per peak were obtained. The authors concluded that a time-of-flight (ToF) MS would be the ideal solution to satisfy the requirements of GC×GC narrow peaks. A year later, van Deursen and co-workers described the first GC×GC-ToF MS application [130], focused on kerosene analysis. The ToF MS process generates a complete spectrum from every ion pulse from the ion source; up to 500 spectra/s can be produced, thus a huge quantity of information needs collection. However, to optimize a ToF MS method, in terms of

acquisition rate, a compromise among different parameters must be made, namely I) data points per peak, which have to be sufficient for a reliable peak reconstruction; II) sensitivity, which decreases with an increase of the spectral production rate; III) data file size, because higher acquisition rates generate large data file, handled with difficulty by normal computers. Consequently, in GC×GC-ToF MS experiments an acquisition rate of 50 Hz is a frequent compromise. The acquisition of complete spectra and the absence of peak skewing enable the exploitation of deconvolution, a useful tool to unravel peak overlapping. Beside these pre-requisites, slight resolution (at least 5 ms) and a sufficient number of data points (at least 4) are required to deconvolute between peaks. The main software employed for deconvolution purposes are the LECO ChromaTOF and AMDIS. Although ToF MS fully satisfies GC×GC acquisition rate requirements, researchers and instrument developers have made substiantial efforts to use the quadrupole (q)MS, by carefully tuning the qMS parameters, in relation to the specific GC×GC application, and by improving the scan-rate components, respectively. With regard to qMS, there are advantages: low cost, robustness, availability of commercial MS databases. In a quadrupole analyzer, the scan data acquisition rate (Hz) is defined as 1000 divided by the scan time (ms) and the inter-scan delay (ms) (Equation 4.0), where the scan time depends on the mass range (set by the operator) and on the q-scan speed (instrument parameter) (Equation 4.1).

$$Data\ acquisition\ rate(Hz) = \frac{100}{scan\ time\ (ms) + inter\ scan\ delay(ms)} \qquad \text{(Eq. 4.0)}$$

$$Scan\ time\ (s) = \frac{Mass\ range\ scanned(amu)}{scan\ speed\ (amu/s)} \qquad \text{(Eq. 4.1)}$$

The interscan delay is defined as the time required to re-set the initial voltage, prior to the next scan. Figure 4.25 shows a graph illustrating the quadrupole MS acquisition process.

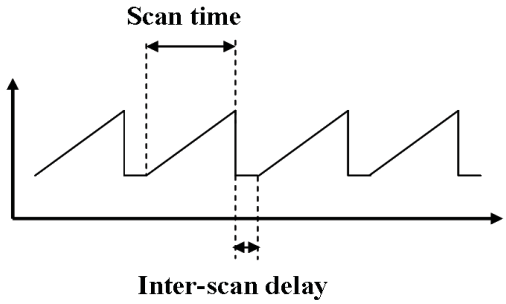

Figure 4.25. Graph illustrating the qMS full-scan acquisition process [131].

Several authors have tried to push the performance of the qMS by playing with the scanned mass range [132-136]. For example, Shellie and co-workers attained between 18.5 and 20 scan/s [132,133], using a 4000 amu/s qMS scan speed and by reducing the mass range, in essential oil and environmental applications. Cordero and co-workers [135], in 2007, although using a qMS with a high scan speed (11,111 amu/s) in allergen analysis, had to reduce the mass range scanned (40-240 *m/z*), to achieve 18.52 scan/s, due to the relatively high inter-scan delay (30 ms). Mondello and co-workers analysed a commercial perfume [136], using GC×GC in combination with a rapid-scanning qMS (10,000 amu/s). Thanks to the relatively low inter-scan delay (calculated to be 14 ms), an acquisition frequency of 20 Hz was achieved using a "normal" mass range (40-400 *m/z*). Considering its limitations, the qMS has been considered suitable only for qualitative purpose. The single ion monitoring (SIM) mode has been often used to meet the requirements for quantitative analysis, since higher acquisition rates can be attained. In the SIM mode, acquisition speed is composed of the dwell time, which is the time spent acquiring the specific ion, and the inter-channel delay, the time to set the voltage for the next acquisition level.

Rather recently, the performance of a novel very-rapid qMS, with a 20,000 amu/s scan speed and a very low inter-scan delay (5 ms), has been reported [137]. GC×GC-qMS quantification of perfume allergens was described: an average of more than 15 data points per peak were obtained, through the application of a 50-Hz acquisition rate and a 40-340 *m/z* mass range.

References

[1] L. Mondello, A.C. Lewis, K.D. Bartle (Eds.), Multidimensional chromatography, Chichester, John Wiley & Sons, 2002.

[2] L. Ramos, Udo A.Th. Brinkman, Multidimensionality in Gas Chromatography: General Concepts, In Comprehensive Analytical Chemistry Vol. 55, Elsevier, Amsterdam, (2009).

[3] R. Consden, A.H. Gordon, A.J.P. Martin, Biochem. J. 38 (1944) 224.

[4] Z. Liu, J.B. Phillips, J. Chromatogr. Sci. 29 (1991) 227.

[5] J.B. Phillips, Z. Liu, Chromatographic Technique and Apparatus, USA Patent 5, 135, 549, 1992.

[6] J.C. Giddings, J. Chromatogr. 703 (1995) 3.

[7] P.J. Schoenmakers, P.J. Marriott, J. Beens, LC-GC Eur. 16 (2003) 335.

[8] J.F. Focant, E. Reiner, K. MacPherson, T. Kolic, A. Sjödin, D.G. Patterson, S. Reese Jr., F. Dorman, J. Cochran, Talanta 63 (2004) 1231.

[9] J.F. Focant, A. Sjödin, W.E. Turner, D.G. Patterson Jr, Anal. Chem. 76 (2004) 6313.

[10] M. Adahchour, J. Beens, U.A.Th. Brinkman, J. Chromatogr. A 1186 (2008) 67.

[11] J.-M.D. Dimandja, Anal. Chem. 76 (2004) 167A.

[12] J.-F. Focant, A. Sjödin, D.G. Patterson, J. Chromatogr. A 1040 (2004) 227.

[13] P.J. Marriott, D. P. Morrison, R. Shellie, V.S. Dunn, E. Sari, D. Ryan, LC-GC Eur. 15 (2003), 209.

[14] P.J. Marriott, P.D. Morrison, LC-GC North Amer. 24 (2006) 1067.

[15] L. Mondello, A. Casilli, P.Q. Tranchida, P. Dugo, G. Dugo, J. Chromatogr. A 1019 (2003) 187.

[16] D. Ryan, R. Shellie, P.Q. Tranchida, A. Casilli, L. Mondello, P.J. Marriott, J. Chromatogr. A 1054 (2004) 57.

[17] P.Q. Tranchida, G. Purcaro, L. Conte, P. Dugo, G. Dugo, L. Mondello, Anal. Chem. 81 (2009) 8529.

[18] J. Beens, J. Blomberg, P.J. Schoenmakers, J. High Resolut. Chromatogr. 23 (2000) 182.

[19] P. Korytár, P. Haglund, J. de Boer, U.A.Th. Brinkman, Trends Anal. Chem. 25 (2006) 373.

[20] J. Dallüge, J. Beens, U.A.Th. Brinkman, J. Chromatogr. A, 1000 (2003) 69.

[21] F. Ern, R.W. Frei, J. Chromatogr. 149 (1978) 561.

[22] J.V. Seeley, J. Chromatogr. A 962 (2002) 21.

[23] P.Q. Tranchida, R. Costa, P. Donato, D. Sciarrone, C. Ragonese, P. Dugo, G. Dugo, L. Mondello, J. Sep. Sci. 31 (2008) 3347.

[24] P.Q. Tranchida, F.A. Franchina, P. Dugo, L. Mondello, J. Chromatogr. A 1255 (2012) 171.

[25] M. Adahchour, J. Beens, R.J.J. Vreuls, A.M. Batenburg, U.A.Th. Brinkman, J. Chromatogr. A 1054 (2004) 47.

[26] C. Cordero, P. Rubiolo, B. Sgorbini, M. Galli, C. Bicchi, J. Chromatogr. A 1132 (2006) 268.

[27] L.M. Sidisky, C.A. Baney, J.L. Desorcie, K.K. Stenerson, Organohalog. Compd. 70 (2008) 2183.

[28] J.V. Seeley, S.K. Seeley, E.K. Libby, Z.S. Breitbach, Anal. Bioanal. Chem. 390 (2008) 323.

[29] J.V. Seeley, F.J. Kramp and K.S. Sharpe, J. Sep. Sci. 24 (2001) 444.

[30] J.V. Seeley, F.J. Kramp, K.S. Sharpe and S.K. Seeley, J. Sep. Sci. 25 (2002) 53.

[31] R.E. Murphy, M.R. Schure, J.P. Foley, Anal. Chem. 70 (1998) 1585.

[32] L.M. Blumberg, J. Chromatogr. A 985 (2003) 29.

[33] T. Górecki, J. Harynuk, O.J. Paníc, Sep. Sci. 27 (2004) 359.

[34] Z. Liu, J.B. Phillips, J. Chromatogr. Sci. 29 (1991) 227.

[35] Z. Liu, J.B. Phillips, J. Microcol. Sep. 1 (1989) 249.

[36] Z. Liu, M. Zhang, J.B. Phillips, J. Chromatogr. Sci. 28 (1990) 567.

[37] Z. Liu, S.R. Sirimanne, D.G. Patterson Jr., L.L. Needham, J.B. Phillips, Anal. Chem. 66 (1994) 3086.

[38] J.B. Phillips, J. Xu, J. Chromatogr. A 703 (1995) 327.

[39] J.B. Phillips, E. Ledford, Field Anal. Chem. Technol. 1 (1996) 23.

[40] H.-J. de Geus, J. de Boer, J.B. Phillips, E.B. Ledford Jr., U.A.Th. Brinkman, J. High Resolut. Chromatogr. 21 (1998) 411.

[41] J. Blomberg, P.J. Schoenmakers, J. Beens, R. Tijssen, J. High Resolut. Chromatogr. 20 (1997) 539.

[42] J.B. Phillips, R.B. Gaines, J. Blomberg, F.W.M. van der Wielen, J.-M. Dimandja, V. Green, J. Granger, D. Patterson, L. Racovalis, H.-J. de Geus, J. de Boer, P. Haglund, J. Lipsky, V. Sinha, E.B. Ledford Jr., J. High Resolut. Chromatogr. 22 (1999) 3.

[43] P. Tranchida, G. Purcaro, P. Dugo, L. Mondello, Trends in Anal. Chem 30 (2011) 1437.

[44] R.M. Kinghorn, P.J. Marriott, J. High Resolut. Chromatogr. 21 (1998) 32.

[45] R.M. Kinghorn, P.J. Marriott, J. High Resolut. Chromatogr. 21 (1998) 620.

[46] E.B. Ledford Jr., 23rd International Symposium on Capillary Chromatography, 5–10 June 2000, Riva del Garda, Italy.

[47] E.B. Ledford, C. Billesbach, J. Termaat, Pittcon 2002, 17–22 March 2002, New Orleans, LA, USA.

[48] E.B. Ledford, J.R. Termaat, C.A. Billesbach, Zoex Technical Note KT030606-1 (http://www.zoex.com/applications/techni- cal_notes.asp).

[49] J. Harynuk, T. Górecki, J. Sep. Sci. 27 (2004) 431.

[50] N. Oldridge, O. Paníc, T. Górecki, J. Sep. Sci. 31 (2008) 3375.

[51] T. Veriotti, R. Sacks, Anal. Chem. 73 (2008) 3045.

[52] C.A. Bruckner, B.J. Prazen, R.E. Synovec, Anal. Chem. 70 (1998) 2796.

[53] J.V. Seeley, F. Kramp, C.J. Hicks, Anal. Chem. 72 (2000) 4346.

[54] B.J. Prazen, C.A. Bruckner, R.E. Synovec, B.R. Kowalski, J. Microcol. Sep. 11 (1999) 97.

[55] C.G. Fraga, B.J. Prazen, R.E. Synovec, J. High Resolut. Chromatogr. 23 (2000) 215.

[56] C.G. Fraga, B.J. Prazen, R.E. Synovec, Anal. Chem. 72 (2000) 4154.

[57] B.J. Prazen, K.J. Johnson, A. Weber, R.E. Synovec, Anal. Chem. 73 (2001) 5677.

[58] C.G Fraga, C.A. Bruckner, R.E. Synovec, Anal. Chem. 73 (2001) 675

[59] C.G. Fraga, B.J. Prazen, R.E. Synovec, Anal. Chem. 73 (2001) 5833.

[60] J.V. Seeley, F.J. Kramp, K.S. Sharpe, J. Sep. Sci. 24 (2001) 444.

[61] J.V. Seeley, F.J. Kramp, K.S. Sharpe, J. Sep. Sci. 25 (2002) 53.

[62] A.E. Sinha, K.J. Johnson, B.J. Prazen, S.V. Lucas, C.G. Fraga, R.E. Synovec, J. Chromatogr. A 983 (2003) 195.

[63] A.E. Sinha, B.J. Prazen, C.G. Fraga, R.E. Synovec, J. Chromatogr. A 1019 (2003) 79.

[64] A.E. Sinha, J.L. Hope, B.J. Prazen, C.G. Fraga, E.J. Nilsson, R.E. Synovec, J. Chromatogr. A 1056 (2004) 145.

[65] N.E. Watson, W.C. Siegler, J.C. Hoggard, R.E. Synovec, Anal. Chem. 79 (2007) 8270.

[66] W.C. Siegler, J.A. Crank, D.W. Armstrong, R.E. Synovec, J. Chromatogr. A 1217 (2010) 3144.

[67] D.R. Deans, Chromatographia 1 (1968) 18.

[68] P.A. Bueno, J.V. Seeley, J. Chromatogr. A 1027 (2004) 3.

[69] R.W. LaClair, P.A. Bueno, J.V. Seeley, J. Sep. Sci. 27 (2004) 389.

[70] N.J. Micyus, J.D. McCurry, J.V. Seeley, J. Chromatogr. A 1086 (2005) 115.

[71] H. Cai, S.D. Stearns, Anal. Chem. 76 (2004) 6064.

[72] J.V. Seeley, S.K. Seeley, E.M. Libby, J.D. McCurry, J. Chromatogr. Sci. 45 (2007) 650.

[73] J.V. Seeley, E.M. Libby, S.K. Seeley, J.D. McCurry, J. Sep. Sci. 31 (2008) 3337.

[74] M. Poliak, M. Kochman, A. Amirav, J. Chromatogr. A 1186 (2008) 189.

[75] M. Poliak, A.B. Fialkov, A. Amirav, J. Chromatogr. A 1210 (2008) 108.

[76] P.McA. Harvey, R.A. Shellie, P.R. Haddad, J. Chromatogr. Sci. 48 (2010) 245.

[77] B. Quimby, J. McCurry, W. Norman, LC-GC the peak April (2007) 7.

[78] P.Q. Tranchida, G. Purcaro, A. Visco, L. Conte, P. Dugo, P. Dawes, G. Dugo, L. Mondello, J. Chromatogr. A 1218 (2011) 3140.

[79] A. Ghosh, C. T. Bates, S. K. Seeley, J. V. Seeley, J. Chromatogr A 1291 (2013) 146.

[80] P.Q. Tranchida, A. Casilli, P. Dugo, G. Dugo, L. Mondello, Anal. Chem. 79 (2007) 2266.

[81] J.V. Seeley, J. Chromatogr. A 962 (2002) 21.

[82] E.B. Ledford Jr., C. Billesbach, J. High Resolut. Chromatogr. 21 (2000) 202.

[83] J. Beens, M. Adahchour, R.J.J. Vreuls, K. van Altena, U.A.Th. Brinkman, J. Chromatogr. A 919 (2001) 127.

[84] J. Beens, J. Dallüge, M. Adahchour, R.J.J. Vreuls, U.A.Th. Brinkman, J. Microcol. Sep. 13 (2001) 134.

[85] T. Hyötyläinen, M. Kallio, K. Hartonen, M. Jussila, S. Palonen, M.- L. Riekkola, Anal. Chem. 74 (2002) 4441.

[86] J. Harynuk, T. Górecki, J. Sep. Sci. 25 (2002) 304.

[87] M. Adahchour, J. Beens, U.A.Th. Brinkman, Analyst 128 (2003) 213.

[88] J. Harynuk, T. Górecki, J. Chromatogr. A 1019 (2003) 53.

[89] M. Pursch, P. Eckerle, J. Biel, R. Streck, H. Cortes, K. Sun, B. Winniford, J. Chromatogr. A 1019 (2003) 43.

[90] B.V. Burger, T. Snyman, W.J.G. Burger, W.F. van Rooyen, J. Sep. Sci. 26 (2003) 23.

[91] M. Kallio, T. Hyötyläinen, M. Jussila, K. Hartonen, S. Palonen, M.- L. Riekkola, Anal. Bioanal. Chem. 375 (2003) 725.

[92] M. Kallio, T. Hyötyläinen, P. Raimi, M. Jussila, Anal. Bioanal. Chem. 391 (2008) 2357.

[93] A.H. Goldstein, D.R. Worton, B.J. Williams, S.V. Hering, N.M. Kreisberg, O. Paníc, T. Górecki, J. Chromatogr. A 1186 (2008) 340.

[94] M. Libardoni, J.H. Waite, R. Sacks, Anal. Chem. 77 (2005) 2786.

[95] M. Libardoni, E. Hasselbrink, J. Hunter Waite, R. Sacks, J. Sep. Sci. 29 (2006) 1001.

[96] I.R. Pizzutti, R.J.J. Vreuls, A. de Kok, R. Roehrs, S. Martel, C.A. Friggi, R. Zanella, J. Chromatogr. A 1216 (2009) 3305.

[97] S.-J. Kim, S.M. Reidy, B.P. Block, K.D. Wise, E.T. Zellers, K. Kurabayashi, Lab Chip 10 (2010) 1647.

[98] J.F. Hamilton, A.C. Lewis, K.D. Bartle, J. Sep. Sci. 26 (2003) 578.

[99] J.W. Diehl, F.P. Di Sanzo, J. Chromatogr. A 1080 (2005) 157.

[100] R.E. Mohler, B.J. Prazen, R.E. Synovec, Anal. Chim. Acta 555 (2006) 68.

[101] F.C.-Y. Wang, J. Chromatogr. A 1188 (2008) 274.

[102] H. Cai, S.D. Stearns, Anal. Chem. 76 (2004) 6064.

[103] J.V. Seeley, N.J. Micyus, S.V. Bandurski, S.K. Seeley, J.D. McCurry, Anal. Chem. 79 (2007) 1840.

[104] M. Adahchour, J. Beens, R.J.J. Vreuls, U.A.Th. Brinkman, Trends in Anal. Chem. 25 (2006) 540.

[105] E. Engel, J. Ratel, P. Blinet, S.-T. Chin, G. Rose, P.J. Marriott J. Chromatogr. A 1311 (2013) 140.

[106] J.B. Phillips, J. Xu, J. Chromatogr. A 703 (1995) 327.

[107] C. von Mühlen, W. Khummueng, C.A. Zini, E.B. Caramao, P.J. Marriot, J. Sep. Sci. 29 (2006) 1909.

[108] M. Biedermann, K. Grob, J. Sep. Sci. 32 (2009) 3726.

[109] C.M. Reddy, T.I. Eglinton, A. Hounshell, K.K. White, L. Xu, R.B. Gaines, G.S. Frysinger, Environ. Sci. Technol. 36 (2002) 4754.

[110] G.S. Frysinger, R.B. Gaines, L. Xu, C.M. Reddy, Environ. Sci. Technol., 37 (2003) 1653.

[111] G.F. Slater, H.K.White, T.I.Eglinton, C.M. Reddy, Environ. Sci. Technol. 39 (2005) 2552.

[112] C. Vendeuvre, F. Bertoncini, L. Duval, J.L. Duplan, D. Thiébaut, M.-C. Hennion, J. Chromatogr. A 1056 (2004) 155.

[113] P.Q. Tranchida, A. Giannino, M. Mondello, D. Sciarrone, P. Dugo, G. Dugo, L. Mondello, J. Sep. Sci. 31 (2008) 1797.

[114] B. Vlaeminck, J. Harynuk, V. Fievez, P.J. Marriott, Eur. J. Lipid Sci. Technol. 109 (2007) 757.

[115] M.S. Klee, M.D. Williams, I. Chang, J. Murphy, J. High Res. Chromatogr. 22 (1999) 24.

[116] E.M. Kristenson, P. Korytár, C. Danielsson, M. Kallio, M. Brandt, J. Mäkelä, R.J.J. Vreuls, J. Beens, U.A.Th. Brinkman, J. Chromatogr. A 1019 (2003) 65.

[117] J. Zrostlikova, S.J. Lehotay, J. Hajslova, J. Sep. Sci. 25 (2002) 527.

[118] X. Quan, S. Chen, B. Platzer, J. Chen, M. Gfrerer, Spectrochim. Acta 57B (2002) 189.

[119] K. Conka, B. Drobna, A. Kocan, J. Petrik, J. Chromatogr. A 1084 (2005) 33.

[120] J. Aybar-Munoz, E. Fernandez-Gonzalez, L.E. Garcia-Ayuso, A. Gonzalez-Casado, L. Cuadros-Rodriguez, Chromatographia 61 (2005) 505.

[121] B. Gomara, L. Ramos, M.J. Gonzalez, J. Chromatogr. B 766 (2002) 279.

[122] T. Kusakabe, T. Saito, S. Takeichi, Tokai J. Exp. Clinical Med. 28 (2003) 131.

[123] C.F. Poole, in: The Essence of Chromatography, Elsevier, Amsterdam (2003) p. 66-67.

[124] W. Khummueng, C. Trenerry, G. Rose, P.J. Marriott, J. Chromatogr. A 1131 (2006) 203.

[125] C. von Mühlen, E.C. de Oliveira, P.D. Morrison, C.A. Zini, E.B. Caramao, P.J. Marriott, J. Sep. Sci. 30 (2007) 3223.

[126] J. Blomberg, T. Riemersma, M. van Zuijlen, H. Chaabani, J. Chromatogr. A 1050 (2004) 77.

[127] F.C.Y. Wang, W.K. Robbinson, M.A. Greaney, J. Sep. Sci. 27 (2004) 468.

[128] L.L.P. Van Stee, J. Beens, R.J.J. Vreuls, U.A.Th. Brinkman, J. Chromatogr. A 1019 (2003) 89.

[129] G.S. Frysinger, R.B. Gaines, J. High Resolut. Chromatogr. 22 (1999) 251.

[130] M. van Deursen, J. Beens, J. Reijenga, P. Lipman, C. Cramers, J. Blomberg, J. High Resol. Chromatogr. 23 (2000) 507.

[131] G. Purcaro, P. Q. Tranchida, C. Ragonese, L. Conte, P.Dugo, G. Dugo, L. Mondello, Anal. Chem., 82 (2010) 8583.

[132] R. Shellie, P.J. Marriott, C.W. Huie, J. Sep. Sci. 26 (2003) 1185.

[133] R. Shellie, P.J. Marriott, Analyst 128 (2003) 879.

[134] M. Kallio, T. Hyötyläinen, M. Lehtonen, M. Jussila, K. Hartonen, M. Shimmo, M.-L. Riekkola, J. Chromatogr. A 1019 (2003) 251.

[135] C. Cordero, C. Bicchi, D. Joulain, P. Rubiolo, J. Chromatogr. A 1150 (2007) 37.

[136] L. Mondello, A. Casilli, P.Q. Tranchida, G. Dugo, P. Dugo, J. Chromatogr. A 1067 (2005) 235.

[137] G. Purcaro, P.Q. Tranchida, P. Dugo, E. La Camera, G. Bisignano, L. Conte, L. Mondello, J. Sep. Sci. 33 (2010) 2334.

Chapter 5
Preparative gas chromatography (prep-GC)

5.1 Introduction

Preparative chromatography can be a very ambiguous term and its meaning will often depend on the *raison d'être* for its use. To the forensic chemist, preparative chromatography may mean the isolation of only a few micrograms of material for structure elucidation by subsequent spectroscopic examination. To the biochemist, it may mean the isolation of a few milligrams of a substance required for assessing its physiological activity. In contrast, to the organic chemist, preparative chromatography will often mean the isolation of 5 or perhaps even 50 gr or more of a pure intermediate for subsequent synthetic work (this can be particularly important in the separation of chiral mixtures). Thus, the amount of material that is separated does not necessarily determine whether the separation can be classed as preparative or not. It is interesting to note that the technique of chromatography, originally invented by Tswett in the initial part of the 900s, was not initially developed for analytical purposes, but for the isolation of some specific pigments from plant extracts.

Preparative gas chromatography (prep-GC) is an important tool for separation and purification of components of a mixture for further uses such as structure elucidation or for recovery of bulk materials in a pure form for commercial applications. Prep-GC allows to collect single compounds, or zones of compounds isolated from a sample after GC separation. Sample collection includes preparative fraction collectors (PFC) into vials, trapping onto capillary columns or using sorbent materials attached to the end of the column. After the collection step, structure elucidation is usually the following step in preparative gas chromatography; different analytical techniques such as MS, Fourier transform infrared spectroscopy (FTIR), nuclear magnetic resonance (NMR), X-ray analysis, are used for such a purpose. Prep-GC can be achieved on packed columns, allowing for large sample masses to be injected, capillary GC column for greater component separation, or multidimensional methods where two or more capillary columns having different stationary phases are coupled. The most productive ways used in the past for prep-GC applications were linked to the use of a single packed column [1].

A scheme of a prep-GC system is showed in Figure 5.0. The method must incorporate a suitable collection or trapping device (C) which may often be

operated at a sub-ambient temperature. It is useful to have some way to monitor the progress of the GC analysis, so a detector with a switching system is also incorporated. The switching device allows selection of the component(s) for transfer to the collection system.

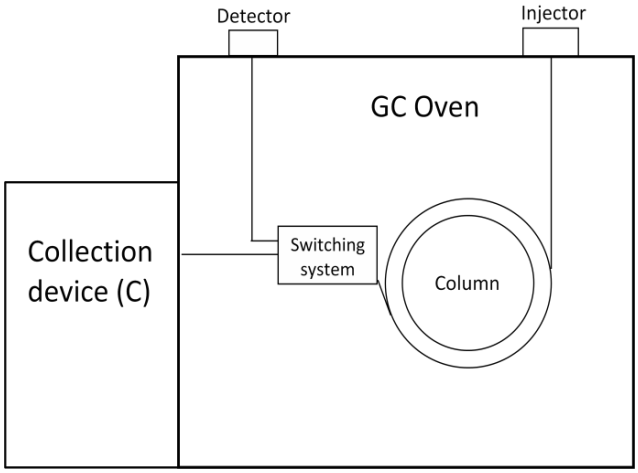

Figure 5.0. Scheme of a classical preparative GC system.

An alternative view of this process is shown in Figure 5.1. The first column effluent is cut or sampled directly into the collection device C or onto a secondary column, with as many or as few target regions (T_1–T_4) as necessary during the isolation step. The method can be repeated many times to increase the amount of material collected [2].

As aforementioned, preparative scale GC can range from the use of analytical scale methods, where sufficient material has to be collected to perform subsequent characterization methods with off-line spectroscopic or microscale methods, to the true large-scale prep-GC methods capable of producing kilograms of material per hour.

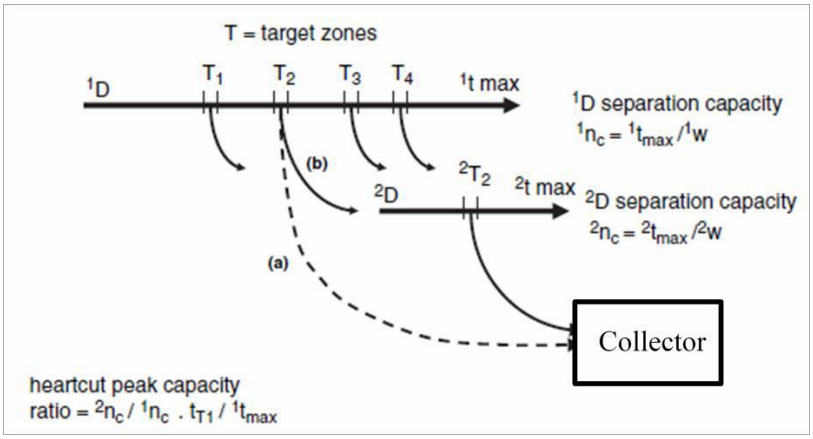

Figure 5.1. Transfer of selected zones T from a first column (1D) to a) a collection device or b) a second column (2D) and then to the collection device. The process can be repeated many times during a single GC analysis [2].

Packed columns allow a large volume of stationary phase to be loaded into the column, which in turn prevents column overloading. Thus, relatively large volumes of relatively high concentration samples can be injected onto the column. Capillary columns can accommodate only small volumes and solute amounts to prevent overloading of the phase. Overloading leads to asymmetric peak shapes and causes reduced resolution of neighboring peaks. This is not a negative issue in itself if the peaks remain separated, but if peaks progressively merge as a result of trying to increase sample load, then the ability to isolate a pure component in the presence of a closely eluting peak diminishes.

A linear peak is defined as one that has a linear isotherm, *i.e.*, where the relationship in Equation 5.0 between the distribution constant K and the concentrations in the stationary (C_S) and mobile (C_M) phases is constant:

$$K = \frac{Cs}{CM} \qquad \text{Eq. 5.0}$$

The relationship between K and the retention factor ($k = t'_R/t_M$) and the phase ratio ($\beta = V_M/V_S$) is:

$$K = k\beta \qquad \text{Eq. 5.1}$$

for linear chromatography. This means that the retention time under linear chromatography conditions is constant. This also means that the resolution (R_S) of neighboring peaks in packed columns is constant for even large amounts of injected solute. The width (at half height or base width, W_B) of a peak under linear chromatography conditions should also not change.

Although packed columns might be the obvious approach to implement prep-GC, many applications require a more efficient separation method. In such a case, the best choice is the use of a high-resolution capillary column, that can be either of megabore dimensions (0.53 mm I.D.) or a narrower bore (0.25–0.32 mm I.D.). In most cases, the most logical approach is to use a smaller phase ratio (β) column (thicker film) to allow larger injected amounts than are possible with high β columns.

As aforemention, the collection of the effluent from the GC column can be achieved in many ways. The most common techniques are: (a) to direct the GC flow through a sorbent trap, with the use of a solvent for recovery, (b) collection into a solvent reservoir of the eluting pure compounds, (c) use of a phase-coated capillary column so that the solute undergoes trapping in the phase according to classic chromatographic principles. Probably the more popular method is to use a cooled region in which to collect the solute. It is possible to combine a number of the above approaches, *e.g.*, cooling down a sorbent, solvent, or phase-coated capillary trap. Nojima *et al.* evaluated a selection of different capillary trapping columns [3], with and without phase coating, and with different phase thickness. A prep-GC system was described, with a short megabore column as an efficient sample-trapping device, the open tubular trap (OTT). Different trapping capillary phase thicknesses were tested, from 0.5 to 5.0 μm, and were compared with a deactivated (uncoated) capillary tube. The effectiveness of trapping a range of ester, alcohol, and alkane compounds over an extended range of carbon numbers was evaluated. A 5.0 μm phase thickness of non-polar DB-1 phase was able to trap compounds with a retention index above 1000, whereas the thinner film-trapping capillaries could only successfully trap compounds of higher carbon number and retention index (*e.g.*, 1100, 1200, etc.).

Prep-GC experiments with capillary columns normally require multiple injections into the GC, with the selected zone isolated from the matrix in each of these injections. It has been reported that multiple injections of up to 800 or more can be made [4]. The only requirement, in this case, is the stability of the system over such an extended time.

5.2 Multidimensional preparative gas chromatography

Preparative applications in MDGC are less common than in one-dimensional chromatography, because fewer laboratories are involved in multidimensional chromatography. However, if one or more target analytes are obscured by matrix interferences then prep-MDGC is a highly suitable choice.

There are no particular limitations to developing a prep-MDGC method, and the higher resolving power afforded by MDGC should make this approach beneficial if the high purity of the collected components is required. The combination of a packed column to a capillary one in prep-MDGC experiments is logical, since the large sample capacity of the packed GC column is combined with the high resolution of capillary column. Such an approach is highly useful for trace components. The prep-GC isolation of trace-amount compounds puts extra demands on the spectroscopic method in terms of sensitivity; the more sensitive the detection method (with capability to identify at lower concentrations), the smaller the mass of component that needs to be collected, and the fewer the injections required.

One of the most well-known applications of prep-GC is the off-line combination with NMR. It is noteworthy that recent developments in the on-line coupling of GC with NMR have been made [5,6]. In the field of prep-MDGC, many papers have been published over the years. For instance, Eyres *et al.* developed a novel prep-MDGC method to isolate gernaiol from an essential oil sample (Figure 5.3) [7]. Geraniol overlapped with six other compounds on the first column, using an essential oil mixture made up of lavender and peppermint oils to test the MDGC approach.

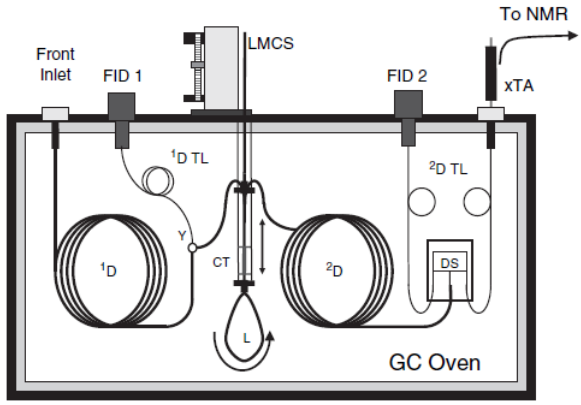

Figure 5.2. Design of a prep-MDGC system for the isolation of a single pure compound from a complex mixture [7].

At the end of the second column, a Deans switch was used to divert geraniol into an external trapping assembly (uncoated capillary assembly). From 50 to 100 injections were made to collect a sufficient quantity of geraniol for NMR analysis, using one-and two- dimensional NMR. The method was then tested to resolve dimethoxybenzene (DMB) from a similar essential oil mixture (Figure 5.3) [8].

In a further demonstration, 1- and 2-methyl naphthalene were resolved from coeluting alkanes, cyclic alkanes, and other components in a crude oil. The two compounds have essentially the same mass spectra, but the NMR data are dissimilar. The same group then demonstrated that multiple components could be collected by switching the Deans switch a number of times during the chromatogram, again with multiple injections. Consequently, a new sub-mixture to be generated. The sample was the same as the geraniol mixture above-mentioned.

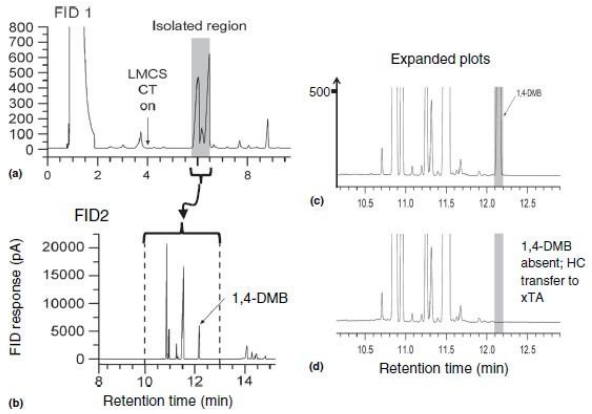

Figure 5.3. Example of capillary prep-GC sampling of dimethylbenzene in peppermint oil, showing the unresolved zone of peaks (a) recorded at FID1 , which are isolated and transferred to a second column for better resolution (b). The expanded trace (c) shows the isolated zone as recorded on FID2, and in (d) DMB is transferred to an external trapping assembly (xTA) for preparative collection [7].

Werkhoff *et al.* used a prep-MDGC method applied to yellow passion fruit [9]. The enrichment method allowed 47 sulfur-containing volatiles to be identified in yellow passion fruits, with 35 of these components shown to be present in the tropical fruit flavor for the first time. A total of 23 of these sulfur-bearing compounds had not been previously reported as constituents of food flavors, and hence were proposed as new natural components.

References

[1] R. Schmidt, M. Roeder, O. Oeckler, A. Simon, V. Schurig, Chirality 12 (2000) 751.

[2] P. Marriott, Preparative gas chromatography as a sample preparation approach, in: Comprehensive Sampling and Sample Preparation: Analytical Techniques for Scientists, J. Pawliszyn (Editor), Elsevier, Amsterdam Netherlands, 2012, 971-982.

[3] S. Nojima, C. Apperson, C. Schal, J. Chem. Ecol. 34 (2008) 418.

[4] J. Roeraade, S. Blomberg, H. D. J. Pietersma, J. Chromatogr. 356 (1986) 271.

[5] M. Kühnle, D. Kreidler, K. Czesla, P. Schuler, V. Shurig, K. Albert, Chirality 22 (2010) 808.

[6] M. D. Grynbaum, D. Kreidler, J. Rehbein, A. Purea, P. Schuler, W. Schaal, H. Czesla, A. Webb, V. Schurig, K. Albert, Anal. Chem. 79 (2007) 2708.

[7] G. T. Eyres, S. Urban, P. D. Morrison, J.-P. Dufour, P. J. Marriott, Anal. Chem. 80 (2008) 6293.

[8] G. T. Eyres, S. Urban, P. D. Morrison, P. J. Marriott, J. Chromatogr. A 1215 (2008) 168.

[9] P. Werkhoff, M. Guntert, G. Krammer, H. Sommer, J. Kaulen, J. Agric. Food Chem. 46 (1998) 1076.

Page intentionally left blank

Chapter 6

Gas chromatography-olfactometry (GC-O)

6.1 Introduction

The human nose perception of volatile compounds, released from foods and fragrances, depends on the extension of the release from the matrix and the odour properties of the compounds. It is known that only a small portion of the large number of volatiles occurring in a fragrant matrix contributes to its overall perceived odour [1,2]. Further, these molecules do not contribute equally to the overall flavour profile of a sample, hence, a large GC peak area, generated by a chemical detector does not necessarily correspond to high odour intensities, due to differences in intensity/concentration relationships. Consequently the general interest of researchers was directed to the determination of the contribution of single constituents to the overall flavour of a sample. In general, the sensory importance of an odour-active compound depends on its concentration in the matrix, and on its human nose limit of detection. Moreover, the unpredictable extent of interaction of flavour molecules with each other, and with other food constituents (lipids, proteins, carbohydrates, etc.) must also be considered.

GC-O is the most appropriate analytical solution to such issues, as it enables the assessment of odour-active components in complex mixtures, through the specific correlation of an olfactive sensation with a chromatographic peak; this is possible because the eluted substances are perceived simultaneously by two detectors, one of them being the human olfactory system. Consequently, GC-O provides not only an instrumental, but also a sensorial analysis. The latter is defined as a science responsible for the quantification of the human responses to the stimuli perceived by the senses of sight, smell, taste, touch and audition [3,4]. When coupled to analytical techniques, such as in GC-O, it becomes a precise, descriptive approach to characterise stimuli, evaluating and measuring impressions, as also an important process which enables the comprehension and quantification of sensorial characteristics. The introduction and diffusion of GC-O, proved to be vital for development in the research field of odour-active compounds, providing valuable information on the chromatogram locations on which to focus attention and resources. GC-O is a unique analytical technique

which associates the resolution power of capillary GC with the selectivity and sensitivity of the human nose.

6.2 Overview of the human olfactive system

The human sense of smell has often been regarded as the least refined of all the human senses, and far inferior to that of other animals [5]. For many species of insects and animals a sense of smell determines their day-to-day survival. For mankind the strength of social interactions has been determined for centuries by bodily odours, so that perfumed materials have been significant creators of wealth. As a consequence, in humans, the odours are often viewed as related to aesthetics, and capable of eliciting enduring thoughts and memories. For most organisms, however, the sense of smell is a primal sense that affords them the ability to detect food, predators, and mates. Whether primal or aesthetic, all organisms have evolved a mechanism to recognize olfactory information in the environment and transmit it to the brain, where it is processed creating an internal representation of the external world. The discriminatory capacity of mammalian olfactory system is such that thousands of volatile chemicals are perceived as having distinct odours. Due to the great efforts over the last decade using various experimental approaches [6,7-9], the complex pathways of this intriguing system are emerging, including the mechanisms through which the brain decodes and discriminates odorants.

In vertebrates, the detection of odours starts in the olfactory sensory neurons (OSNs) located in the olfactory epithelium, also named regio olfactoria, situated in the roof of the nasal cavities of the nose (Figure 6.0). Each OSN has 8 to 20 cilia that are considered as the first active site of the olfactory pathway and contain the odorant receptor (OR) proteins, also defined as odorant binding proteins (OBPs).

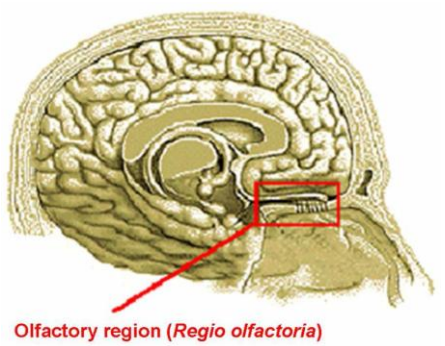

Figure 6.0. Olfactory epithelium [10].

Chemicals dispersed in the air may interact with the OBPs according to their concentration and properties. One proposed role of these proteins is that they bind lipophilically to odorants in the aqueous/lipid mucous increasing the concentration and then facilitating the transport through the mucous layer to the receptors in the olfactory membrane. Further hypothesis are that they bind to the ligand and to the receptor, assisting in the transport across the olfactory membrane, or that they may act as a filter to prevent the saturation of the receptor [10].

The binding of an odorant to an OR triggers the activation of a classical G-protein-based transduction cascade *via* elevation of intracellular cyclic nucleotides. ORs are transmembrane proteins that belong to the large superfamily of G-protein-coupled receptors (GPCRs) [11].

The binding of odorant molecules to a transmembrane receptor causes a conformational change in the receptor, leading to an interaction with a heterotrimeric GPCR. As a consequence the guanosine diphosphate (GDP) is replaced by a guanosine triphosphate (GTP), being so in its active state. Once GTP is bound, the α subunit protein activates the enzyme adenylyl cyclase (AC). Activated AC cyclases adenosine triphosphate (ATP) into the neurotransmitter cyclic-3',5'-adenosylmonophosphate (cAMP). The neurotransmitter cAMP, acts then as a second messenger and activate cyclic nucleotide-gated (CNG) cation channels, allowing the flow of extracellular inorganic ions (Ca^{2+} and Na^{+}) (Figure 6.1). These ions move across the cellular membrane into the olfactory neuronal cell generating a membrane signal potential leading to an electrical signal that represents a transfer of the chemosensory information to the olfactory bulb via the axons. The ultimate result is the depolarization of the OSN and the initiation and propagation of action potentials. [12,15].

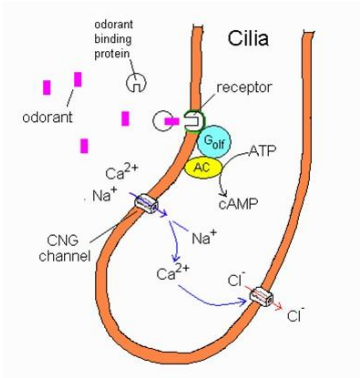

Figure 6.1. The cAMP-mediated signal transduction pathway in olfactory sensory neurons [11].

The action potential generated in the cAMP transduction cascade is then propagated along the axon, which crosses through a thin bone known as the cribiform plate, and into the forebrain, more specifically into the olfactory bulb, where it synapses with second-order neurons. The axons of the latter expressing the same OR converge forming synaptic structures called glomeruli [6], also defined as the primary olfactory area of the brain. The glomeruli are connected in groups that converge into mitral cells; confer Figure 6.2. Through long nerve processes, the mitral cells send the information to several parts of the brain. This suggests that olfactory information is first roughly organized into large sets in the nose and then reorganized in the olfactory bulb into a sensory map, which is identical in different individuals.

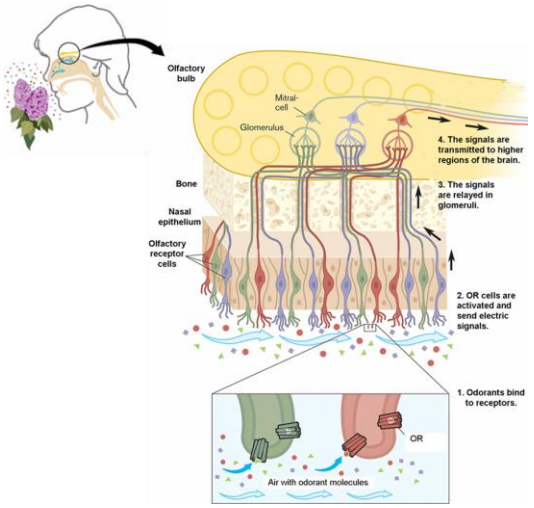

Figure 6.2. Scheme of the signal transduction [16].

The nerve signals sent to different parts of the brain in turn reach defined micro regions in the brain cortex. There the information from several types of ORs is combined into a pattern characteristic for each odour; Table 6.0 was extracted from the publication of Buck [17], with the aim to better illustrate odour recognition mechanisms. This OR combinations are interpreted, leading to the conscious experience of a recognizable odour.

Table 6.0. Distinct odorants are detected by different combinations [17].

Compounds	ORs														Odour description
	1	**2**	**3**	**4**	**5**	**6**	**7**	**8**	**9**	**10**	**11**	**12**	**13**	**14**	
hexanoic acid					■										rancid, sweaty, sour, goat-like, fatty
hexanol		■				■									sweet, herbal, woody, Cognac, Scotch
heptanoic acid	■			■	■		■			■	■				rancid, sweaty, sour, fatty
heptanol		■			■	■									violet, sweet, woody, herbal, fresh, fatty
octanoic acid	■			■	■		■	■		■	■	■			rancid, sour, repulsive, sweaty, fatty
octanol				■	■		■			■					sweet, orange, rose, fatty, fresh, powerful,
nonanoic acid	■			■	■		■	■		■		■		■	waxy, cheese, nut-like, fatty
nonanol				■	■		■			■		■			fresh, rose, oily, floral, citronella oil, fatty

The researchers Axel and Buck stated that each olfactory receptor cell possesses only one type of OR, and each OR can detect a limited number of odorant substances. The olfactory receptor cells are therefore highly specialized for a few odours. Furthermore, most odours are composed of multiple odorant molecules, and each odorant molecule activates several ORs. This leads to a combinatorial code forming an "odorant pattern" – somewhat like the colours in a patchwork quilt or in a mosaic. This is the basis for human's ability to recognize and form memories of approximately 10,000 different odours [18].

Over the years a number of theories relating odorant quality to molecular structure have been proposed; although they are not going to be dealt with in this thesis, it is worth to cite the most prominent theories, which are the steric theory [20,21], the vibrational theory [22], and the vibrational induced electron tunnelling spectroscope theory [23].

The knowledge of the mammalian olfactory system is as yet incomplete, although spectacular progress has been made in the last few years through the application of molecular biology techniques, there is still much to be discovered.

6.3 GC-O hardware

The description of a gas chromatograph modified for the sniffing of its effluent to determine volatile odour activity, was first published in 1964 by Fuller, Steltenkamp and Tisserand [24]. The gas chromatograph was equipped with a non-destructive thermal conductivity detection (TCD) system with the outlet connected to a sniffing port (also called olfactometry port). The latter was located inside a telephone booth, in order to isolate the evaluator from the potential influences of odorants present in the ambient. In 1971, a more

sophisticated GC-O system was reported; humid air was added to the GC effluent, thus avoiding nasal mucosa dry-out [25]. Further improvements included the use of a Venturi tube, to maintain capillary column resolution and to deliver, ergonomically, the effluent to the evaluator.

In general, GC-O is carried out on a standard GC equipped with a sniffing port (Figure 6.3) in substitution of, or in addition to, the conventional detector. When a flame ionisation detector or a mass spectrometer is also used to record the signal, the analytical column effluent is split and transferred to the detector and to the human nose. The splitting of the columns effluent is enabled through the installation of a splitting unit at the column outlet. Among the most common splitter types are the T-union (Figure 6.4 A) and the four port splitter (Figure 6.4 B to D). In the case a T-union is used, one port is connected to the analytical column outlet and the two remaining ports to the conventional detector and to the transfer line; in the four-port splitter, the fourth port is connected to an auxiliary gas outlet. The flow division occurs according to the splitting unit and the dimensions of the uncoated columns (length and internal diameter).

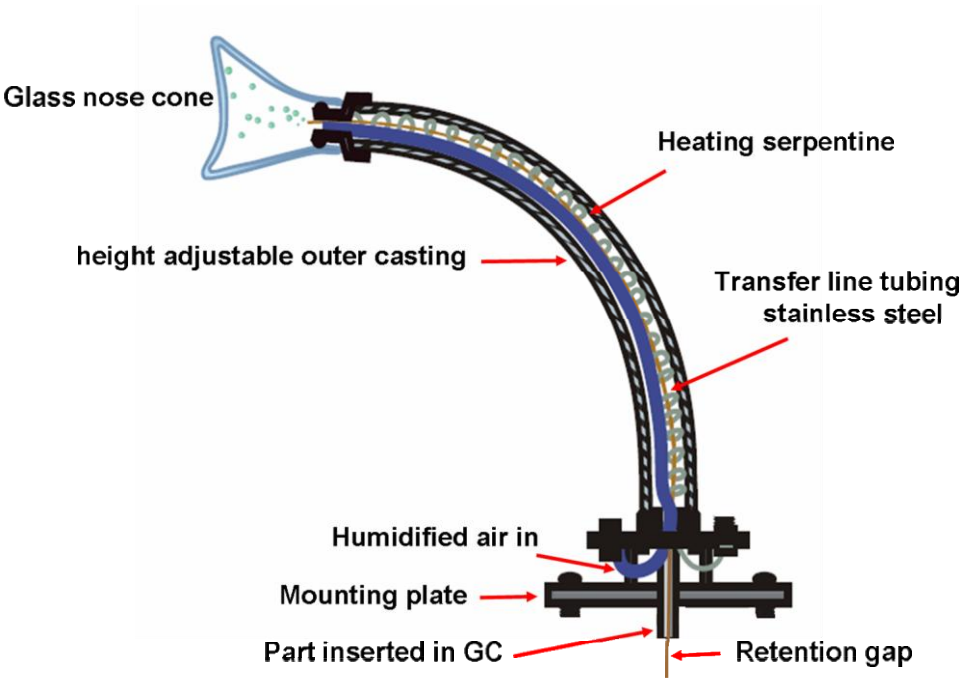

Figure 6.3. Scheme of a sniffing port device (ODO II, SGE International Pty. Ltd.).

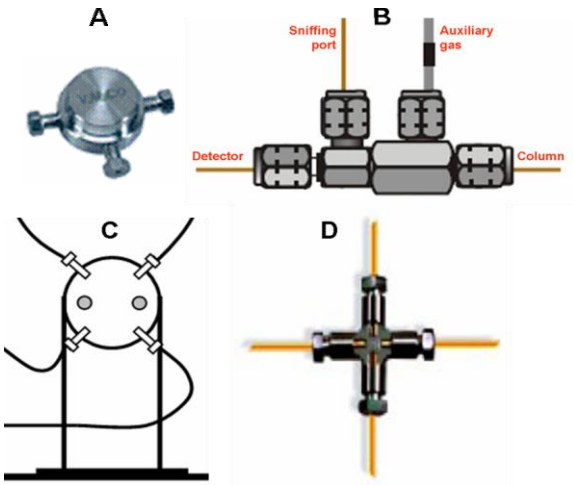

Figure 6.4. Splitting unit types used in GC-O: (A) T-union (Valco), (B) column flow splitter of the olfactometry port ODO II (SGE), (C) standing splitting unit of the olfactometry port Phaser (ATAS GL International), and (D) cross union of the olfactometry port ODP 2 (Gerstel).

The sniffing port is ergonomically-designed, possesses a nose-cone shape, to which the eluting volatiles are directed *via* a connecting transfer line. The nose-cone is typically positioned at a short distance, about 30 to 60 cm, from the instrument. Moreover, since the transfer line extends outside the oven, it must be heated to avoid that late eluting compounds with high boiling points condensate [26].

In the past, a mask was used to facilitate sniffing [27], nowadays sniffing ports typically use a glass cone or a polytetrafluoroethylene – PTFE (Teflon®) sleeve. It has been suggested that the design of the nose piece may influence the flow characteristics of the gas and therefore the sensory perception [28]. The position of the nose-cone must be such that the assessor feels comfortable; standing or sitting positions during analysis is subjective, and may also depend on the length, flexibility and adjustability of the transfer line. The assessor's comfort is particularly important when considering that GC-O runs may be longer than 30 min. In addition, to avoid discomfort the assessor should be far enough from the top of the hot GC oven, where the smell of hot metal may interfere. To achieve best comfort and performance, it is preferable that the sniffing port extends from the side of the GC rather than from its top.

A further important aspect, early realised, was the fact that the carrier gas eluting from a GC is typically hot and dry, causing drying of the nose, and considerable discomfort. for the assessors, and as such, affecting sensitivity. This issue was addressed by using humidified air as a make-up carrier gas to

deliver the odorants to the human assessors [25]. Nowadays, volatiles are typically directed to the nose in a stream of heated and humidified air; about 50% to 75% of relative humidity. Moreover, multi-sniffing systems have been developed, characterized by 2, 3 or 4 ports, enabling the simultaneous olfactive analysis made by more than one panellist. In such systems, the flow entering the splitter is divided into equal parts toward different thermostated transfer lines of identical size [29].

GC-O systems are often used in addition to either an FID or a mass spectrometer [2,29]. With regard to detectors, splitting column flow between the olfactory port and a mass spectral detector provides simultaneous identification of odour-active compounds [30,31]. Another variation is to use an in-line, non-destructive detector such as a TCD [32], or a photo-ionisation detector (PID) [33].

It is worth highlighting that in consideration of possible processes of analyte condensation or adsorption, as also a possible use of the system for environmental analyses (CEN – Comite Européen de Normalisation/European Committee for Standardization EN 13725 of 1999), the sniffing port should be constructed of components made of glass, stainless steel, and/or Teflon® [34].

6.4 Panel of evaluators

Sensory analysis involves human subjects as a measuring tool. This presents an immediate problem due to the innate variability between individuals, not only as a result of their previous experiences and expectations, but also their sensibility [4]. To circumvent such a drawback, odour panels consist of individuals that are selected and screened for specific anosmia. One modality for screening evaluators is by using the standard solution set proposed by Friedrich *et al.* [35]. In the case no insensitivities are found, the panellists are introduced to two sensorial properties, quality and intensity.

Odour quality shall be described according to the odour families that compose the aromatic wheel, or according to Kraft *et al.* [36], the olfactive spectrum (Figure 6.5). An odour family may be described as a class of odours which, due to the presence of certain features, are related to each other. The families may also present sub-classifications, enabling a more detailed description of an olfactive impression. With regard to intensity, a sensation triggered by an odour shall be measured through its rating on an intensity interval scale.

Figure 6.5. Olfactive spectrum [36].

Commonly the evaluators are trained by sniffing different dilutions of standard compounds selected according to their significance for each odour category. In such a manner, the evaluators learn to correlate the odour elicited by key standard compounds to their common descriptors, such as cis-3-hexenol as green, grassy, linalool as floral, etc.

In sensorial analysis, the verbal expression of quality and intensity is of great importance in order to define the responses deriving from human perception. Furthermore, considering that the olfactory ability between humans may be significantly different, to normalise the vocabulary between panellists the quality attribution of an odour sensation is generally based on glossaries of olfactive descriptors. Commonly, each group of researchers, either academic or industrial, establishes their own glossary, generally matrix specific, to be adopted by the panel.

Furthermore, if intensity measurements have to be carried out, panellists have to learn how to estimate intensity by using the aforementioned intensity interval scale, such as the three-point [37], five-point [38] and nine-point [39] scales, in the evaluation of different dilutions of standard compounds. These scales, also named as structured scales, discriminate intensity according to scores; *e.g.*, in the five-point scale 1 stands for extremely weak, 2 for weak, 3 for moderate, 4 for strong, and 5 for extremely strong. It is preferable is to use a scale that permits to achieve a normal distribution of values; the number of points of difference a scale provides will determine the subsequent ability to statistically analyse data.

A further example of scale is the rather subjective semi-structured scale in which only the maximum and minimum values are established, respectively very strong and odourless. Intensity estimation through the use of a sliding 60 cm scale and a fingerspan scale have also been reported [40]. In the latter case, the assessors estimate the maximum intensity of an eluting odour by using their

own fingerspan as a scale; the thumb is held still and the intensity signal is generated by moving the finger along a rheostat.

The main disadvantage in sensorial analysis is the lack of objectivity, since the discrimination, association and development of an olfactive memory vary according to each individual; additionally, the absence of a universal odour language contributes to discrepancies in odour descriptions. Finally, the assessor comfort and the possibility to perform analyses free of distractions is of great importance to attain maximum performance. Drawbacks arise when long sniffing sessions are carried out; commonly analyses are divided in sessions with intervals to avoid lassitude. It can occur that panellists do not perceive an odour because they simply miss the eluting compound due to a lack of concentration or due to their breathing cycle [41].

For such reasons, continuous training of the panellist is required to promptly recognise odours, describe them uniformly and attribute to each an intensity rate. According to Meeilgaard, Civille and Carr [3], the following aspects may contribute to discrepancies:

(1) Adaptation which is related to the saturation of the olfactive receptors;

(2) Age of the panellist, the loss of the sense of smell along the years is to be considered. There is a marked sensitivity decrease after seventy, that becomes pronounced for octogenarians;

(3) Gender, women commonly have greater odour sensitivity;

(4) Space, the analysis should be executed in rooms with controlled temperature, adequate exhaustion and pressure. The sniffing port should be easily accessible permitting a comfortable position for the panellist;

(5) The panellists must be aware of their importance and function, and continuously develop their olfactive memory.

The number of evaluators forming a panel is a rather controversial matter; dilution methods are often performed using only one to three assessors, while in detection frequency techniques higher reliability is attained with eight to ten assessors. A large number of trained panellists is also required for intensity evaluations since a high variability may be commonly observed between panellists.

6.5 Sample preparation for GC-O analysis

A series of considerations have to be made on a rather laborious, but significant step of flavour and fragrance GC analysis, namely sample preparation. The isolation procedure should yield a product which is representative of the odour profile of the sample; therefore, the choice of an appropriate sample preparation method becomes crucial. According to the properties of the matrix, sample preparation may include mincing, homogenization, centrifugation, steam distillation (SD), solvent extraction (SE), fractionation of solvent extracts, simultaneous distillation-extraction (SDE), supercritical fluid extraction (SFE), pressurized-fluid extraction, Soxhlet extraction, solvent assisted flavour evaporation (SAFE), microwave-assisted hydrodistillation (MAHD), direct thermal desorption (DTD), headspace techniques (HS), cryofocussing, solid-phase microextraction (SPME), matrix solid-phase dispersion (MSPD), among others.

Commonly, distillation and SE methods are considered to yield the near complete flavour of food extracts, which is not always of relevance for the determination of a characteristic odour profile. In order to obtain more representative samples, SDE is widely applied; providing elegant and rapid extractions, through which the recovered isolates, after being concentrated, are ready to be injected into the GC system. However, the analyst has to deal with decomposition of labile compounds, loss of highly volatile compounds and heat-induced artifact formation. The latter drawback can be contrasted by the use of a modified system, an SDE under static vacuum (SDE-SV), which allows extractions at 30-35 °C. In addition, the use of SDE-SV, although being more time-consuming, eliminates the concentration step prior to sample injection.

In general, the extracts obtained by SE can be very complex, leading to many GC co-elutions, making the identification of individual odour-active compounds difficult. The fractionation of such extracts is a time-consuming, but reasonable mode to overcome excessive complexity. The fractionation of extracts may be accomplished in several manners, such as by washing a food extract with a dilute acid, base, and either sodium metabisulphite or 2,4-dinitrophenylhydrazine, promoting the elimination of acids, bases or carbonyl compounds from the extract, respectively. If each wash solution is then re-extracted with solvent, the fractions containing only acids, bases or carbonyls may be recovered, even though multiple manipulations of the extract may cause the loss of highly volatile compounds. Further aspects should be considered with regards to SE methods, as the possible loss of the more volatile compounds during solvent removal, the need of large sample amounts in order to attain concentrated extracts, and the presence of non-volatile and high-

boiling compounds in the extract, or impurities from the solvent. Furthermore, in GC-O analysis the solvent peak may cover early eluting odour-active volatiles.

On the other hand, samples extracted by means of SD methods are commonly free of non-volatile or high-boiling compounds, and therefore do not contaminate GC liners and columns. Moreover, the sample can be concentrated, thus enabling the detection of trace components. However, poor extraction of highly polar or hydrophilic compounds (acids and alcohols) may occur, as also artifact formation due to thermal degradation. With regard to odour assessment, SD methods may not be suitable for fresh material extraction, such as fruits and vegetables, as the extract will elicit an odour that is more similar to a cooked, rather than to fresh fruit or vegetable odour.

A further very popular method is SAFE, which may be applied after SE techniques or be used as an individual extraction method for solvent extracts or food matrices. A common application is on aqueous foods, such as milk, fruit pulps or matrices with high oil content. This technique removes volatiles under low temperature and high vacuum conditions. The extract is then collected into flasks which are cryogenically cooled with liquid nitrogen. The attained material should be representative of the original sample; uncooked, but without high boiling compounds and colour. Some attention and time should be devoted to the cleaning of the system, in order to avoid contamination of liners and columns.

HS methods, which are also frequently applied, may be divided into static (SHS) and dynamic (DHS) headspace analyses; the former is characterised by the sampling of the atmosphere around the headspace of a matrix, located in a vial, after equilibrium has been achieved; the latter removes larger amounts of volatiles by sweeping the sample with a carrier gas flow, with a concentration step carried out prior to GC analyses. HS techniques are a valuable tool for GC-O analysis combining simplicity, solvent-free procedures, requirement of small sample amounts, and no artifact formation. However, the relative concentration of volatile components in the headspace does not correspond to the concentration in the sample due to the differences in volatility of flavour compounds. A further technique, worthy of note is SPME, a widely applied solvent-free method which exploits the high adsorption power of a fused silica fibre coated with a specific extraction phase, which is selected according to the type of sample [42,43]. However, the use of SPME as isolation method prior to GC-O analysis, presents some limits due to the possible non-representative nature of the extracts. The chemical profile of the collected volatiles depends upon the type, thickness and length of the fiber, as well as on the sampling time

and temperature. Although a series of volatile isolation methods are known, the most appropriate way to attain an optimum recovery of the odorant chemicals is the employment of more than one extraction technique.

6.6 GC-O data measurement methods

Over the last decades, GC-O has been widely used in combination with sophisticated olfactometric methods which have been developed to estimate the sensory contribution of a odour-active compounds. These methods are commonly classified in four categories: dilution, time-intensity, detection frequency, and posterior intensity methods [2,44-46]. Dilution analysis, the most applied method, is based on successive dilutions of an aroma extract until no odour is perceived by the panellists. This procedure, usually performed by a reduced number of assessors, is mainly represented by CHARM (combined hedonic aroma response method), developed by Acree and co-workers [47], and AEDA (aroma extraction dilution analysis), first presented by Ullrich and Grosch [48]. In AEDA samples are evaluated by the panellists in increasing dilution order and the impact of an odour-active compound is given by its dilution factor (FD) value. The results are represented as a diagram, the FD factor is plotted against the retention time in the form of the retention index (RI) and the diagram is called a FD chromatogram or aromagram, as exemplified in Figure 6.6A, or simply by listing the FD values. On the other hand, in CHARM analysis the dilutions are presented to the panellists in a randomized order, avoiding bias introduced by the knowledge of the dilution being analysed. The panellists record the start and end of each detected odour; the detection duration for each individual is then compiled, and an aromagram is generated by plotting the duration of the odour sensation against the dilution value (Figure 6.6B). CHARM values can be calculated according to Equation 6.0, where n is the number of coincident responses between panellists and d is the dilution value. The later is analogous to the FD value in AEDA.

$$c = d^{n-1} \qquad \text{Eq. 6.0}$$

AEDA presents limitations, such as the non-consideration of odorant losses during the isolation procedure, or the reduction of synergistic or suppressive effects of distinct compounds initially present in the real sample. With regard to

CHARM, limitations can be observed in quantification analyses, which require the replication of the experiment by at least three different trained assessors.

Time-intensity methods, such as OSME (Greek word for odour), are based on the immediate recording of the intensity as a function of time by moving the cursor of a variable resistor [49]. In OSME odour-active compounds intensity information is attained in a single run, although the results are reliable only if trained assessors are used.

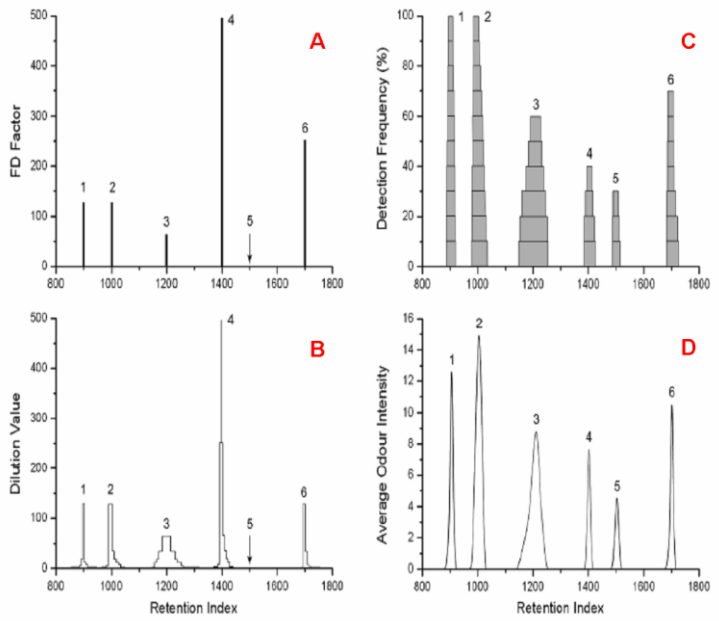

Figure 6.6. Results simulated for six compounds using four different GC-O methods: (A) AEDA, (B) CHARM, (C) detection frequency, and (D) OSME [45].

A further approach, namely the detection frequency method [50,51], uses the number of evaluators detecting an odour-active compound in the GC effluent as a measure of its intensity. This GC-O analysis is performed with a panel composed of 8 to 10 assessors. It must be added that the results attained are not based on real intensities and are limited by the scale of measurement. A presentation of the results attained with the detection frequency method is shown in Figure 6.6C. At a particular concentration and odour intensity, a compound may be perceived by all assessors, but as the concentration and the odour intensity may continue to increase, however, the detection frequency cannot. Based on the detection frequency method, the nasal impact frequency

(NIF) approach was developed [52,53]. The NIF technique does not require a trained panel, no intensity scale has to be learned by the evaluators, and therefore no intensity measurement is performed. Consequently, peak intensities are not related to odour intensity, but to their detection frequency. Commonly, peak heights and areas are defined as NIF and SNIF (surface of nasal impact frequency), respectively. Each panellist participates in 1/n of the final results (n stands for the number of panellists); if NIF is 100%, then all n panellists detected the odorant [52].

Another GC-O technique, is the posterior intensity method [54], such a technique proposes the measurement of the odour intensity, and its comparison with respect to a previously-determined scale. This posterior registration of the perceived intensity may cause a considerable variance between assessors. The attained results may generally be well correlated with detection frequency method results, and to a lesser extent, with dilution methods.

The choice of the GC-O method is of extreme importance for the correct characterization of a sample, since the application of different methods to an identical sample can distinctly select and rank the odour-active compounds according to their odour potency and/or intensity. Commonly, detection frequency and posterior intensity methods result in similar odour intensity/concentration relationships, while dilution analysis investigate and attribute odour potencies.

6.7 Relationship between odorant concentration and odour intensity

As is well-known, odours can be defined by distinct parameters; one of the terms used is threshold concentration, which can be further described at three levels, namely detection, recognition, and difference thresholds. Detection threshold is defined as the lowest concentration or intensity that is perceived by the panellist, while recognition threshold is the lowest concentration or intensity at which a substance or an olfactive quality attribute can be identified and described. Finally, difference threshold is the magnitude of a stimulus above which there is no increase in the perceived intensity of the appropriate quality for that stimulus.

The thresholds of volatile compounds may differ by many orders of magnitude (parts per trillion at the low extreme to odourless compounds). Therefore, in a sample composed of many different volatile compounds, some flavour and fragrance chemicals may present an increased intensity in odour-activity

according to a proportional increment of their concentration, while with others the change in intensity may be, for example, less marked.

The dependence of intensity upon concentration is related a constant which quantifies odours, and is denominated as slope. The idea of slope as a constant, which is characteristic of a substance, assumes the validity of the Stevens's power law [55]. This law states that equal changes in stimulus magnitude (Φ) produce the corresponding change in perceived intensity (Ψ); k is a constant and n is the Steven's exponent, as presented in Equation 6.1.

$$\Psi = k\Phi^n \qquad \text{Eq. 6.1}$$

It has to be noted that the slope depends upon the method by which it was determined. Generally, a relatively high value for the slope indicates a strong dependence of intensity upon concentration, while a low-slope odorant is typically not very powerful when assessed in the undiluted form. Two theoretical concentration-intensity curves are presented in Figures 6.8 and 6.9. Figure 6.8 reports a sigmoidally-shaped curve in a plot of log concentration against perceived intensity. There is an initial part of the function where the response at concentration levels below and just passing through the threshold rises slowly from the baseline; then, there is a rapidly-increasing part of the function when the threshold is passed and changes in intensity can be relatively easily perceived; finally, at higher concentrations the function becomes eventually flat as the human ability to perceive change at high concentrations diminishes. At this point, one could consider the human detector to be saturated. The first inflection point can be considered as an empirical definition of threshold. Figure 6.9 presents a straight line in a log concentration – log perceived intensity plot, due to the application of the Stevens's power law; *n* indicates the relationship between concentration and perceived intensity.

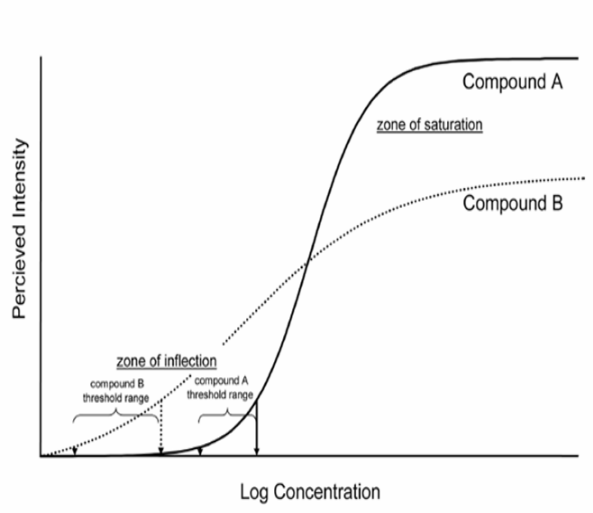

Figure 6.8. Theoretical concentration-intensity curve plotting log concentration against perceived intensity [44].

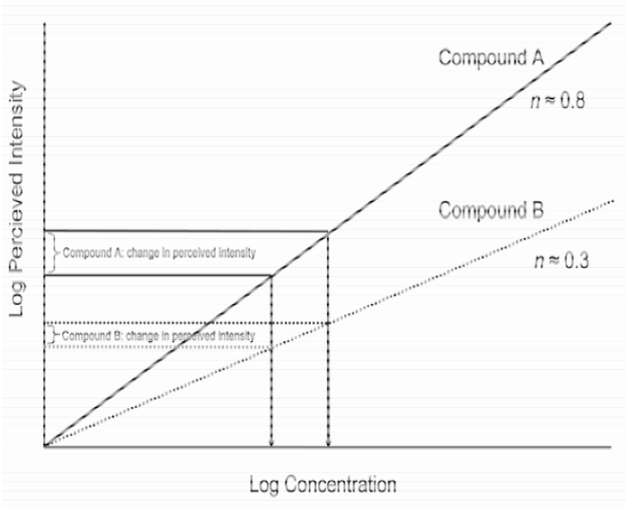

Figure 6.9. Theoretical concentration-intensity curve plotting log concentration against log of perceived intensity, where n is the slope of the line [46].

In 1957, Patton and Josephson first proposed an estimation of the importance of a flavour chemical to a food based on the ratio of its concentration in that food to its threshold concentration in that same matrix [56]. In 1963, in relation to such an approach, Rothe and Thomas proposed the odour activity value (OAVs), with the aim to better correlate the concentration of an odorant with its

detection threshold value [57]; the latter is defined as the lowest concentration or intensity that is perceived by the panellist [58]. Odour activity value (OAV) is the measure of importance of a specific compound to the odour of a sample (*e.g*. food), calculated as the ratio between the concentration of individual substance in a sample and the threshold concentration of this substance dissolved in water, in oil or mixed with starch, depending on which of these materials dominates in the food.

It is clear that the theoretical intensity of an odorant under any specific set of conditions could be roughly expressed in terms of its OAV. However, the difficult and time-consuming determination of threshold values, which vary among and within panellists [59], led to controversies related to the use of OAVs as indicators of the percent contribution an analyte to the overall odour of a sample.

The screening of significant odorants, especially with regard to food analysis, has not only been extensively made by performing GC-O dilution methods, but also through the OAV concept. As described previously, in dilution methods a dilution series of the original aroma extract from a particular matrix are evaluated and the key odorants are ranked in order of potency. The highest dilution at which a substance is sniffed is represented by its FD value; the latter value is considered as proportional to the OAV evaluated in air [58]. Both methodologies are applied in the determination of the aroma compounds which most likely contribute to the overall odour of a sample.

The synergistic or suppressive effects of different odorants in a sample are not considered in the determination of OAVs and GC-O analysis. The sample preparation steps may deprive the real matrix of some of its characteristics. The compounds detected as odour-active in GC-O analyses are most likely to be significant. However, the investigated extract could be too concentrated, and so a specific compound may result as odour-active in a GC-O application, but not so in the real-world sample; on the other hand, a compound might not be determined as odour-active in a GC-O application, due to an insufficient concentration of the extract, and still contribute to the odour of the sample.

With regard to food samples, in order to attain a complete evaluation of key odorants, further sensorial analysis should be performed, such as studies of recombination models and omission experiments. In the former, the aroma model system for a specific food sample is prepared based on the combination of previously achieved AEDA or CHARM values, and/ or OAVs. Odorants showing higher values are used to formulate a recombined model, which is then compared to the real food product for similarities or differences. The omission experiments, on the other hand, deal with the preparation of an aroma model for

a specific sample in which one or more odorants are omitted. In such an approach, the panellists must compare the reduced model, with the complete one, and indicate the perceived sensorial differences [60].

References

[1] W. Grosch, Flavour Fragr. J. 9 (1994) 147.

[2] S. M. van Ruth, Biomolec. Eng. 17 (2001) 121.

[3] M. Meilgaard, G. V. Civille, B.T. Carr, Sensory Evaluation Techniques. CRC Press, Boca Raton, 1991.

[4] A. Richardson, In The Chemistry of Fragrances, D. H. Pybus, C. S. Sell (eds.). Royal Society of Chemistry, Cambridge, 1999.

[5] Aristotle, In The Parva Naturalia, J.I. Beare (ed.). The Works of Aristotle, Volume III, Clarendon Press, Oxford, 1908.

[6] B. Malnic, J. Hirono, T. Sato, L.B. Buck, Cell 96 (1999) 713.

[7] S. L. Sullivan, L. Dryer, J. Neurobiol. 30 (1996) 20.

[8] G. Sicard, A. C. Holley, Brain Res. 292 (1984) 283.

[9] S. Bieri, K. Monastyrskaia, B. Schilling, Chem. Senses 29 (2004) 483.

[10] J.C. Leffingwell, Olfaction - Update No. 5. Leffingwell Reports 2. www.leffingwell.com (access date: December 10th, 2005).

[11] D. L. Nelson, M. M. Cox, Lehninger Principles of Biochemistry. Palgrave Macmillan, Hampshire, 2004.

[12] S. Firestein, Nature 413 (2001) 211.

[13] D. Schild, D. Restrepo, Physiol. Rev. 78 (1998) 429.

[14] T. Kurahashi, K. W. Yau, Nature 363 (1993) 71.

[15] S. Firestein, Current Biol. 6 (1996) 666.

[16] L. B. Buck, R. Axel, Press Release Noble Prize in Physiology or Medicine for 2004. http://nobelprize.org/nobel-prizes/medicine/ laureates/2004/press.html (access date: January 10th 2005).

[17] L. B. Buck, Cell 100 (2000) 611.

[18] L. B. Buck, R. Axel, Cell 65 (1991) 175.

[19] C. M. McGinley, Enforceable Permit Odor Limits. The Air and Waste Management Association Environmental Permitting Symposium II, Chicago, IL, 2000.

[20] L. Pauling, Chem. Eng. News 24 (1946) 1375.

[21] R.W. Moncrieff, Am. Perfumer 54 (1949) 453.

[22] G.M. Dyson, Chem. Ind. 57 (1938) 647.

[23] L. Turin, Chem Sens. 21 (1996) 773.

[24] G.H. Fuller, R. S. Seltenkamp, G.A. Tisserand. Ann. NY Acad. Sci. 116 (1964) 711.

[25] A. Dravnieks, A. O'Donnell, J. Agric. Food Chem. 19 (1971) 1049.

[26] N. Abbott, P. X. Étiévant, S. Issanchou, D. Langlois, J. Agric. Food Chem. 41 (1993) 1698.

[27] F. Drawert, N. Cristoph, In Analysis of Volatiles: Methods and Applications, P. Schreier (ed.). Walter de Gruyter, Berlin/New York, 1984.

[28] K. Hanaoka, J. M. Sieffermann, P. Giampaoli, J. Agric. Food Chem. 48 (2000) 2368.

[29] C. Debonville, B. Orsier, I. Flament, A. Chaintreau, Anal. Chem. 74 (2002) 2345.

[30] L. S. Ettre, J. V. Hinshaw, Basic relationships of Gas Chromatography Advanstar Data, Cleveland, 1993.

[31] H. M. McNair, J. M. Miller, Basic Gas Chromatography. Wiley & Sons, New York, 1998.

[32] O. Nishimura, J. Agric. Food Chem. 43 (1995) 2941.

[33] D.W. Wright, In Techniques for Analyzing Food Aroma (Food Science and Technology), R. Marsili (ed.). Marcel Dekker, New York, 1997.

[34] C. M. McGinley, M. A. McGinley, Modeling, Analysis & Management of Odors, Pre-printed Manuscript of the Air and Waste Management Association, 2001 Annual Conference Technical Program Session No: EE-6b, Session, 2001.

[35] J. E. Friedrich, T. E. Acree, E. H. Lavin, In Gas Chromatography-Olfactometry: The State of the Art., J. V. Leland, P. Schieberle, A. Buettner, T. E. Acree (eds.). American Chemical Society, Washington, D.C., 2001.

[36] P. Kraft, J. A. Bajgrowicz, C. Denis, G. Fráter, Angew. Chem. Int. Ed. 39 (2000) 2980.

[37] J. Pet'ka, V. Ferreira, J. Cacho, Flavour Fragr. J. 20 (2005) 278.

[38] D. Tonder, M. A. Petersen, L. Poll, C. E. Olsen, Food Chem. 61 (1998) 223.

[39] S.M. van Ruth, C. H. O'Connor, Food Chem. 74 (2001).

[40] H. Guichard, E. Guichard, D. Langlois, S. Issanchou, N. Abbott. Z, Lebensm. Unters. Forsch. 201 (1995) 344.

[41] K. Hanaoka, N. Vallet, P. Giampaoli, B. Heyd, P. MacLeod, Food Chem. 72 (2001).

[42] H. Kataoka, H. L. Lord, J. Pawliszyn, J. Chromatogr. A 880 (2000) 35.

[43] W. Wardencki, M. Michulec, J. Curylo, Int. J. Food Sci. Technol. 39 (2004) 703.

[44] V. Ferreira, J. Pet'ka, M. Aznar, J. Agric. Food Chem. 50 (2002) 1508.

[45] S. Le Guen, C. Prost, M.J. Demaimay, J. Agric. Food Chem. 48 (2000) 1307.

[46] C. M. Delahunty, G. Eyres, J. P. Dufour, J. Sep. Sci. 29 (2006) 2107.

[47] T.E. Acree, J. Barnard, D, Cunningham. Food Chem. 14 (1984) 273.

[48] F. Ullrich, W. Grosch. Z, Lebensm. Unters. Forsch 184 (1987) 277.

[49] M.R. McDaniel, R. Miranda-Lopez, B.T. Watson, N.J. Micheals, L.M. Libbey, In Flavors and Off-Flavors (Developments in Food Science Vol. 24), G. Charalambous (ed.). Elsevier Science Publishers, Amsterdam, 1992.

[50] J. P. H. Linssen, J. L. G. M. Janssens, J. P. Roozen, M. A. Posthumus, Food Chem. 46 (1993) 367.

[51] J.P.H. Linssen, J. L. G. M. Janssens, J.P. Roozen, M.A. Posthumus, Food Chem. 8 (1993) 1.

[52] P. Pollien, A. Ott, F. Montigon, M. Baumgartner, R. Munoz-Box, A. Chaintreau, J. Agric. Food Chem. 45 (1997) 2630.

[53] A. Ott, L. B. Fay, A. Chaintreau, J. Agric. Food Chem. 45 (1997) 850.

[54] D.J. Casimir, F. B. Whitfield, Int. Fruchtsaftunion 15 (1978) 325.

[55] S.S. Stevens, Psychol. Rev. 64 (1957) 153.

[56] D.J. S. Patton, Food Res. 22 (1957) 316.

[57] M. Rothe, B. Thomas, Lebensm. Unters. Forsch. 119 (1963) 302.

[58] V. Audouin, F. Bonnet, Z.M. Vickers, G.A. Reineccius, In In Gas Chromatography Olfactometry: The State of the Art., J. V. Leland, P. Schieberle, A. Buettner, T. E. Acree (eds.). American Chemical Society, Washington, D.C., 2001.

[59] P. Schieberle, K. Gassenmeier, H. Guth, A. Sen, W. Grosch, Lebensm. Wiss. Technol. 26 (1993) 347.

[60] M. Czerny, F. Mayer, W. Grosch, J. Agric. Food Chem. 47 (1999) 695.

Page intentionally left blank

Chapter 7

Research in the field of preparative chromatography

7.1 Performance evaluation of a multidimensional preparative chromatographic system for the collection of volatile constituents: summary

The present section discusses the multi-collection of the most important sesquiterpene alcohols belonging to sandalwood essential oil: (*Z*)-α-santalol, (*Z*)-α-trans bergamotol, (*Z*)-β-santalol, epi-(*Z*)-β-santalol, α-bisabolol, (*Z*)-lanceol, and (*Z*)-nuciferol. A versatile multidimensional preparative system, based on the hyphenation of liquid and gas chromatography techniques, was operated in the LC–GC–GC-prep or GC–GC–GC-prep configuration, depending on the concentration to be collected from the sample. The system was equipped with a silica LC column in combination with polyethylene glycol-poly(5%diphenyl/95% dimethylsiloxane)-medium polarity ionic liquid or β-cyclodextrin based GC stationary phases. The GC–GC–GC-prep configuration was employed for the collection of four components, by using a conventional split/splitless injector, while the LC–GC–GC-prep approach was used for three low abundant components (<5%), to increase the quantity collected in a single run, by the LC injection of a high sample amount. All target compounds, whose determination is hindered by the lack of commercial standards, were collected at milligram levels and with a high degree of purity (>87%).

7.2 Introduction

Plants belonging to the genus Santalum (Santalaceae) are ever-green parasitic trees consisting of about 25 species that are distributed in India, Indonesia, Malaysia and Australia [1]. Sandalwood oil is obtained by distillation of the heartwood of 20-year-old trees, and this has caused, during recent years, a lowering of natural sources, not compensated by sufficient plant regeneration. This oil is widely used in aromatherapy and it is employed by industries as an ingredient of perfumes and cosmetics. Furthermore, several biological activities have been reported, including antidepressant, anti-inflammatory, antifungal, antiviral [2], anticarcinogenic [3] and antitumorous [4,5], ones.

The volatile composition of *Santalum album* (*S. album* L.) essential oil, contains >90% sesquiterpene alcohols. According to the International Standard Organization (ISO 2002), *S. album* L. essential oil must have a free alcohol content, expressed as santalols, not lower than 90%; especially, (*Z*)-α-santalol must fall within the 41–55% range, while (Z)-β-santalol within the 16–24% range [6]. These two compounds together are responsible for the chemo-protective effects and neuroleptic properties of the oil, as observed in *in vitro* and *in vivo* assays [7–9]. In addition to (*Z*)-α- and (*Z*)-β-santalol, the Australian regulation on Sandalwood oil also regulates the content of (*Z*)-α-trans bergamotol, epi-β-santalol, α-bisabolol, (*E,E*)-farnesol, (*Z*)-lanceol and (*Z*)-nuciferol [10]. Except for (*Z*)-α-santalol, (*Z*)-β-santalol and (*E,E*)-farnesol, the determination of these components of interest is hindered by the unavailability of commercial standards on the market. Although several synthetic procedures have been exploited for the production of aforementioned components, such ways are not cost-effective and, hence, sandalwood essential oil remains the only viable source of these sesquiterpene alcohols [11–16]. Commonly-used fractional distillation may be an fruitless procedure, since these components have the tendency to be distilled at the same temperature as a mixture [17]. In similar situations, prep-GC may be considered as a valid tool for the isolation of compounds of interest in a pure form, provided that a proper stationary phase is selected, to attain baseline separation of such components or, whenever this is not achievable, exploiting the coupling of more (different) stationary phases, in the heart-cut mode [18].

Recently, a new preparative system was developed for the collection of pure volatile components from complex samples, consisting of the hyphenation of three GC separation dimensions (GC–GC–GC). Such a system was successfully used for the collection of discrete amounts of components of interest [30], or unknown molecules for further identification [31], in a reduced collection time if compared with conventional prep-GC applications and with a high degree of

purity. In these applications, the collection yield was raised by injecting a higher-than-optimum volume of an undiluted sample (2–3 μL in splitless mode) onto the first GC widebore column. Overloading the column obviously led to a decrease in the separation efficiency (reduced by 40–50%) with respect to the optimal injection conditions; however, it allowed for mg amounts of the desired compounds to be collected. On the other hand, the separation and collection of sufficient quantities of very-low or trace-level components from a sample matrix is more challenging, since the required amounts to be loaded would overwhelm the injection capability of a split/splitless GC device. A viable option would be the use of a large-volume injection technique, however such approach could lead to column damage and/or contamination, following the introduction of non-volatile sample components as well as of high amounts of the more abundant volatile ones. In such situations, the use of either an additional front-end (micro)packed GC column [32], or an LC dimension can be exploited to attain an increased sample capacity, while at the same time affording a class-type separation of the sample components [33]. In this work, we demonstrate the feasibility of using a versatile multidimensional preparative system, for the multicollection of some of the most important sesquiterpene alcohols contained in sandalwood essential oil, namely: (*Z*)-α-santalol, (*Z*)-β-santalol, (*Z*)-α-trans bergamotol, epi-(*Z*)-β-santalol, α-bisabolol, (*Z*)-lanceol, and (*Z*)-nuciferol.

7.3.0 Experimental

73.1 Chemical and samples

Sandalwood essential oil (*S. album L.*, Indonesian), GC-grade *n*-hexane, LC-grade dichloromethane, *tert*-butyl methyl ether (MTBE), *n*-hexane and nootkatone were kindly provided by Sigma–Aldrich/Supelco (Bellefonte, USA).

A stock solution, containing 20 mg mL^{-1} of nootkatone was prepared in dichloromethane and used for recovery and calibration purposes. The essential oil was diluted 1:2 (*v/v*) in dichloromethane prior to injection.

7.3.2 LC pre-separation

The LC pre-separation of the sandalwood essential oil was performed on an LC system (Shimadzu, Kyoto, Japan) consisting of a CBM-20A communication bus module, two LC-20AD dual-plunger parallel-flow pumps, a DGU-20A online degasser, an SPD-20A UV detector, a CTO-20A column oven and a SIL-20AC autosampler. Twenty microliters of the sandalwood oil solution were injected onto a 250 mm × 4.6 mm ID × 5 μm *dp* amino column (SUPELCOSIL^{TM} LC-NH_2, Supelco, Milan, Italy). Mobile phases consisted of

(A) *n*-hexane and (B) methyl tert-butyl ether, under the following stepwise gradient conditions: 0–3 min, 0% B, 3–15 min, 3% B, 15–25 min, 10% B, 25–35 min, 30% B, 35–45 min, 100% B. Flow-rate was 1 mL/ min (reduced to 0.35 mL/min during the transfer steps). Data were acquired by the LCsolution software ver 1.25 (Shimadzu, Kyoto, Japan).

7.3.3 LC-GC inteface

The LC–GC interface was based on a dual side-port syringe, controlled by means of an AOC-5000 autosampler (Shimadzu). Chromatography band transfer was achieved, in the stop-flow mode, through a modified 25-µL syringe. The lower part of the syringe was connected, *via* two transfer lines, to the LC detector exit and to waste. A teflon plug was located at the end of the syringe plunger, the latter was characterized by an external diameter smaller than the barrel internal one, thus enabling the mobile phase to flow into the syringe. In the waste mode, the plunger plug was located below both lines and the effluent was directed to waste. In the cut position, the plunger plug was located between the upper and lower lines and the effluent flowed to a large volume injector (LVI) [34].

7.3.4 Multidimensional prep-GC analysis

The preparative MDGC instrument consisted of three GC 2010 systems (GC1, GC2, and GC3) connected by means of three Deans-switch transfer devices, namely TD1 (between GC1 and GC2), TD2 (between GC2 and GC3) and TD3 (between GC3 and the collection station). The Deans switch elements were connected to three advanced pressure control systems (APC1, APC2, and APC3), which supplied He as a carrier gas [30]. GC1 was equipped with a split/splitless injector, an Optic 3 large volume injector (ATAS GL International, Eindhoven, The Netherlands) and a flame ionization detector (FID1). The LVI temperature-program and flow-rate were optimized as described in our previous work [33]. During the transfer step (4 min) and for the first 0.50 min of the GC analysis run time, the split mode was used (flow rate was 332 mL/min at 35 ºC), followed by a 1 min run in the splitless mode. After this period, the split mode was again applied (at 126 mL/min) while heating the injector to 280ºC (at 15ºC/s). When a conventional split/splitless injector was used, the temperature was maintained at 280ºC.

The GC1 column was a Supelcowax-10 (100% polyethyleneglycol, PEG) 30 m × 0.53 mm ID × 2.0 µm d_f (Supelco, Bellefonte,USA), preceded by a 1-m

segment of uncoated pre-column of the same ID. For the preparative LC–GC–GC applications, the following pressure program was applied: 80 kPa for 0.50 min, then to 140 kPa at 400 kPa/min, maintained constant afterwards (initial gas linear velocity: ≈ 22 cm/s at 50ºC). Oven temperature program: 50ºC for 1.50 min, to 300ºC at 15ºC/min. APC1 pressure: 27.5 kPa for 0.50 min, then to 125 kPa at 400 kPa/min. When the system was operated in preparative GC–GC–GC mode, the carrier gas and the APC1 pressures were maintained constant at 140 and 125 kPa, respectively. Oven temperature program: 150°C (1 min) to 240ºC at 5ºC/min (30 min).The transfer line between GC1 and GC2 was maintained at 280ºC. FID1 (280ºC) was connected to TD1 *via* a 0.25 m × 0.18 mm ID stainless steel uncoated column. GC2 column (2D) was an Equity-5 [poly(5% diphenyl/95%dimethylsiloxane)] 30 m × 0.53 mm ID × 5 µm d_f (Supelco). Oven temperature program for all the applications: 50ºC to 150ºC (held until the end of the primary-column heart-cut window) at 4ºC/min, then to 300ºC at 5ºC/min (15 min). Initial gas linear velocity was 35 cm/s (150ºC). The APC2 pressure program, in the case of the preparative LC–GC–GC applications, was: 7.8 kPa for 0.50 min to 95 kPa at 400 kPa/min, while during the preparative GC–GC–GC experiments the APC2 pressure was maintained constant at 95 kPa. The transfer line between GC2 and GC3 was maintained at 240ºC. FID2 (280ºC) was connected to TD2 *via* a 0.37 m × 0.25 mm ID stainless steel uncoated column. The GC3 column (used in preparative GC–GC–GC experiments only) was either an SLB-IL 59 (custom-made ionic liquid) 30 m × 0.53 mm ID × 0.85 µm d_f (Supelco) or a MEGA-DEX DET-Beta (diethyl tertbutylsilyl- β-cyclodextrin) 20 m × 0.53 mm ID × 1 µm d_f (MEGA, Legnano, Italy). Oven temperature program when the MEGA-DEX DET-Beta column was installed: 50–150ºC (held until the end of the second-dimension heart-cut window) at 2.5ºC/min, then to 220ºC at 2ºC/min. For the SLB-IL-59 column the program was as follows: 50–150ºC (held until the end of the second-dimension heart-cut window) at 4ºC/min, then to 240ºC at 5ºC/min. Initial carrier gas linear velocity was 53 cm/s for the SLB-IL 59 capillary, and 44 cm/s for the MEGA-DEX DET-Beta column (150ºC). The APC3 pressures (used in preparative GC–GC–GC experiments only) were maintained constant: 50 kPa when the SLB-IL-59 column was installed, while 70 kPa was applied in the case of the MEGA-DEX DET-Beta column. FID3 (330ºC) was connected to TD3 via a 1 m × 0.32 mm ID stainless steel uncoated column. Detector gasses (for FID1, 2 and 3) were: H_2, 50.0 mL/min; air, 400 mL/min; make up (N_2), 40.0 mL/min; sampling rate, 5 Hz.

Data were collected by LC–GCsolution and MDGCsolution softwares (Shimadzu). Two different collection systems were used: in the preparative LC–GC–GC experiments, a lab-made device based on a modified injector was located into GC2 and connected to TD2 [30], to allow condensation of the

chemicals after the second GC separation. In the preparative GC–GC–GC configuration, a dedicated preparative station "Prep9000" (Brechbühler AG, Switzerland) was used after the GC3 column; the system was connected by means of a flexible heated transfer line to TD3 located in GC3 (280ºC), by means of a 1.4-m segment of uncoated 0.32 mm ID capillary. The system was equipped with a ten position carousel with empty tubes that allowed condensation of the chemicals to be collected at room temperature.

7.3.5 GC-FID and GC–MS analysis

A Shimadzu GC 2010 gas chromatograph equipped with an AOC-20i series autoinjector, and a GCMS-QP2010 Ultra system mass spectrometer were used to evaluate the recovery and degree of purity (Shimadzu). A 30 m × 0.25 mm ID × 0.25 µm d_f Supelcowax-10 column was used under the following conditions: oven temperature program, 100–300ºC at 5.0ºC/min; split/splitless injector (280ºC); injection mode, split 1:100 ratio; injection volume, 0.2 µL. GC-FID conditions were as follows: inlet pressure, 110 kPa; carrier gas, He; constant gas linear velocity, 30.0 cm/s. FID (310ºC) gases: H_2, 50.0 mL/min; air, 400 mL/min; make up (N_2), 40.0 mL/min; sampling rate, 10 Hz.

Data were acquired by the GCsolution software ver. 2.41 (Shimadzu). GC–MS conditions were as follows: inlet pressure, 30.6 kPa; carrier gas, He; constant gas linear velocity, 30.0 cm/s; source temperature, 200ºC; interface temperature, 250ºC; mass scan range, 40–400 *m/z*; scan frequency, 5 Hz. Data were acquired by the GCMS solution software ver. 2.71, while the FFNSC ver. 2.0 mass spectral database was used for database matching (Shimadzu).

7.3.6 LC–GC transfer recovery evaluation

The LC–GC transfer recovery was evaluated comparing the splitless injection of 1 µL of the 20 mg/mL nootkatone solution (20 µg) into GC1, with the peak area obtained by the LC–GC transfer of 10 µL of the same solution injected in LC (200 µg).

7.3.7 Evaluation of the collection recovery

A five-point calibration curve was constructed (n = 3), at 0.01, 0.1, 1, 5, and 10 µg μL^{-1} concentration levels, using nootkatone as a representative component

for the oxygenated sesquiterpene family (R^2 = 0.9996). The concentration levels were selected in order to cover a wide concentration range for the isolated components, diluted in ≈ 0.1 mL of *n*-hexane when flushed from the collection tube.

7.4 Results and discussion

This investigation was focused on the versatile use of a multidimensional preparative instrumentation in two different configurations, namely preparative GC–GC–GC and LC–GC–GC, for the collection of seven highly pure sesquiterpene alcohols from sandalwood essential oil. With regard to (*E,E*)-farnesol, it was intentionally excluded from evaluation, due to the known low abundance/absence in the *S. album* L. sample evaluated. A scheme of the instrumentation is reported in Fig. 7.0.

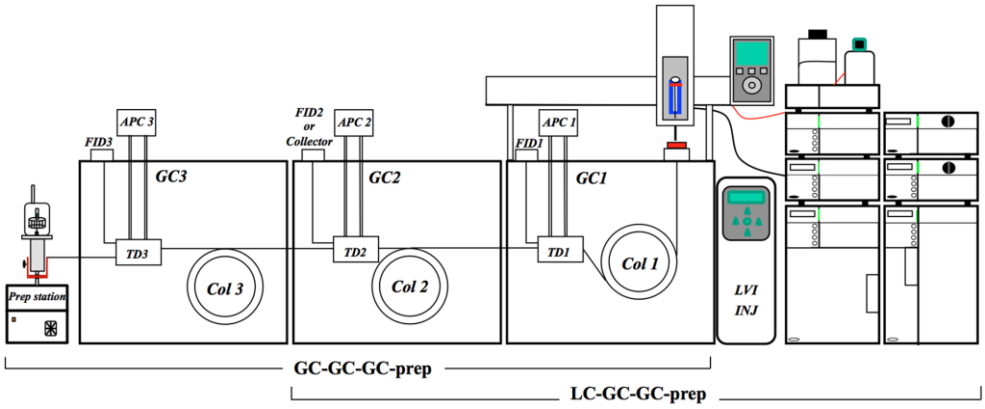

Figure 7.0. Scheme of the multidimensional preparative system. The two configurations used are marked.

In the preparative GC–GC–GC application, a wide-bore column (30 m × 0.53 mm ID) was employed in GC1, in consideration of its higher sample capacity allowed the injection of high sample amounts (1–2 µL), by means of a conventional split/splitless injector. Such a choice allowed the collection of milligrams of each alcohol in a reasonable analytical time, and namely those components whose relative concentrations in the sample were higher than about 5%: (*Z*)-α-santalol (44.6%), (*Z*)-α-trans bergamotol (5.9%), (*Z*)-epi-β-santalol (3.2%), and (*Z*)-β-santalol (19.2%). On the other hand, it is well known that such a column will deliver much lower efficiency with respect to a micro-bore

one (0.25 mm ID), especially when a high sample amount is injected. This is clear from a visual inspection of the chromatogram in Fig.7.1, where several co-elutions occur, between the alcohols to be collected themselves and/or other sample components.

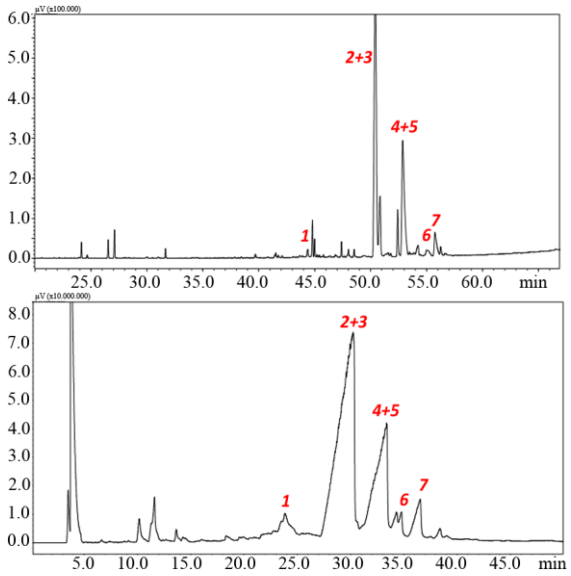

Figure 7.1. Sandalwood essential oil GC-FID chromatogram on (A) 30 m × 0.25 mmID × 0.25 µm d_f, (1 µL 1:10, split 100:1) and (B) 30 m × 0.53 mm ID × 2.0 µm d_f (1 µL neat in splitless mode) Supelcowax-10 column. For peak assignment see Table 7.0.

As an example, (*Z*)-α-trans bergamotol (peak 2) co-eluted totally with (Z)-α-santalol, the most abundant component of sandalwood oil (peak 3); (*Z*)-epi-β-santalol (peak 4) co-eluted with (*Z*)-β-santalol (peak 5), α-bisabolol (peak 1), (*Z*)-lanceol (peak 6) and (*Z*)-nuciferol (peak 7) co-eluted with other sample components. As previously reported [30,31,33], a multidimensional approach can be successfully used to increase the efficiency of the system, since the purity of the chemicals separated will be higher due to the coupling of stationary phases with somewhat different retention mechanisms, as depicted in Fig. 7.2. Considering the chemical composition of the essential oil, mainly consisting of oxygenated sesquiterpene components with similar boiling points and polarity, the first GC column was selected in order to provide the best chromatographic peak shape for santalols. Consequently, a medium-polarity stationary phase consisting of 100% polyethylene glycol was chosen, in accordance with the international regulations [6]. The second GC column, containing [poly(5% diphenyl/95% dimethylsiloxane)], was selected in order to

provide a very well known orthogonal separation mechanism with respect to the first dimension. Similarly, the different selectivity of a medium-polarity ionic-liquid based capillary column demonstrated to be effective for use in the third GC dimension, for the final purification step [35].

The first collection was devoted to (*Z*)-α-santalol (44.6%, fraction A). As predicted, in the stand-by chromatogram a high degree of co-elution occurred, mainly with (*Z*)-α-trans bergamotol, due to the high sample amount injected (≈1 mg), in the splitless mode. The entire 27.55–30.20 min fraction (upper chromatogram in Fig. 7.2) was transferred to the 5% diphenyl column; the co-elution between (*Z*)-α-santalol and (*Z*)-α-trans bergamotol still remained, for the reason that these compounds show very similar chromatographic behavior also on the apolar column (Fig. 7.2A-2D). However, the secondary separation allowed the purification of (*Z*)-α-santalol from minor co-eluting components. A second, reduced heart-cut window, namely 43.90–45.20 min, was thus selected to avoid the transfer of (*Z*)-α-trans bergamotol onto the third separation column. The resulting chromatogram (Fig. 7.2A-3D) shows a further purification of (*Z*)-α-santalol from other components (8%), which allowed the transfer of a pure fraction (cut: 50.49–52.00 min) to the collection system. Finally, the collection tube was flushed with *n*-hexane (100 μL), and the resulting solution was analyzed by using GC–MS and GC-FID for qualitative and quantitative purposes, respectively. Fig. 7.2A cap. shows a degree of purity of 91.1% of the collected fraction. In more detail, 0.85 mg of (*Z*)-α-santalol, the principal component of the oil, was collected in only two runs (total collection time: 2 h) with an overall recovery of 95.3%, as reported in Table 7.0. The same approach was then applied for the collection of (*Z*)-α-trans bergamotol (5.9%, fraction B): the collection was even more hindered by the complete co-elution of the target component with a much higher amount of (*Z*)-α-santalol. With the intent to transfer to the second dimension similar amounts of (*Z*)-α-santalol and (*Z*)-α-trans bergamotol, only a slice of the tail part of the first peak containing the co-elution was transferred onto the second column. In such a respect, a cut from 30.36 to 30.92 min was defined, so that most of the more abundant (*Z*)-α-santalol was left behind, together with other minor components, as shown in Fig. 7.2B-2D. With the objective to pinpoint the most effective GC column to achieve the complete separation on the third column, a selection was performed among different commercially available stationary phases. After, chromatographic resolution (R_S) obtained for the separation of the two compounds was evaluated.

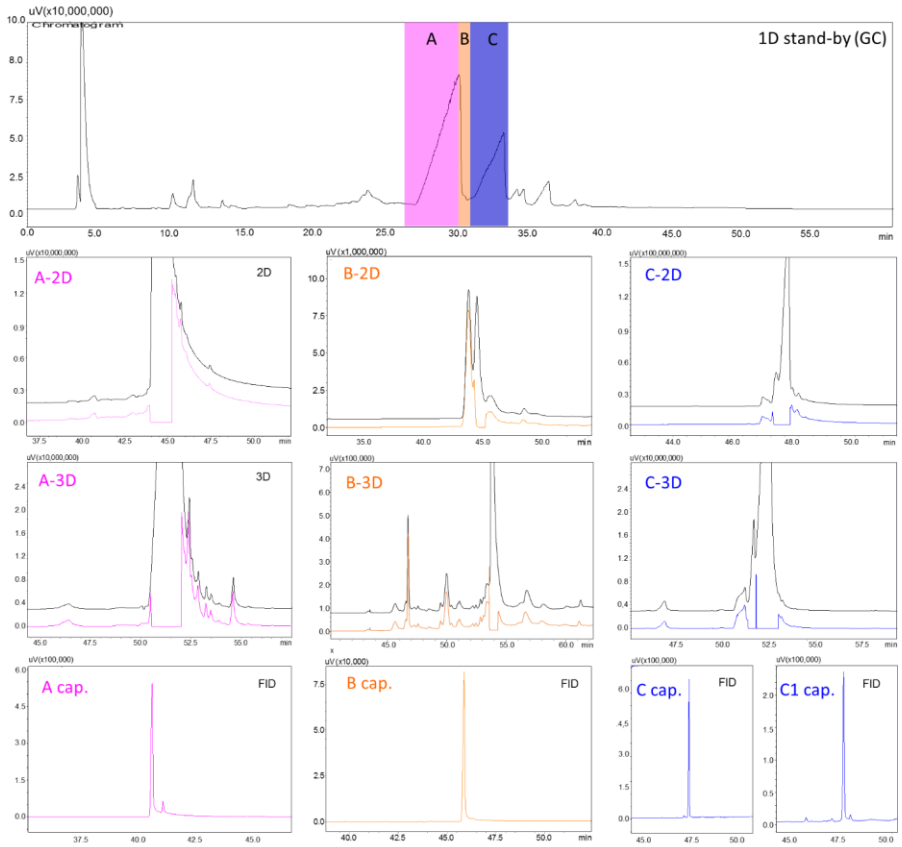

Figure 7.2. Preparative GC–GC–GC-collections of (*Z*)-α-santalol (A), (*Z*)-α-trans bergamotol (B), (*Z*)-epi-β-santalol (2.7%) and (*Z*)-β-santalol (C). Upper chromatogram: stand-by traced. A cap. columns. Abbreviations: 2D: second dimension, 3D: third dimension, Cap.: capillary GC-FID analysis.

Table 7.0. The amount of each collected compound, together with the instrument configuration applied. The purity and average recovery of each fraction collected are reported based on the amount injected per run and in total collected after a certain number of GC runs/hours.

ID	Compound	Abundance %	Prep approach	µg injected per run	mg collected	Runs/Collection time (hours)	Average Recovery %	Purity %
1	α-bisabolol[a]	0.7	LC-GC-GC	70.0	0.61	10 runs = 15 hours	87	99
2	α-santalol[b]	44.6	GC-GC-GC	446.0	0.85	2 runs = 2 hours	95	91
3	α-*trans* bergamotol[b]	5.9	GC-GC-GC	59.0	0.55	10 runs = 10 hours	93	97
4	*epi*-β-santalol[b]	3.2	GC-GC-GC	32.0	0.30	10 runs = 10 hours	90	93
5	(*Z*)-β-santalol[b]	19.2		192.0	1.73			98
6	(*Z*)-lanceol[b]	1.4	LC-GC-GC	14.2	0.65	5 runs = 7.5 hours	92	96
7	(*Z*)-nuciferol[c]	4.0		40.0	0.19		95	93

[a] Molecular weight = 222, [b] Molecular weight = 220, [c] Molecular weight = 218

A non-pure (*Z*)-α-santalol fraction, containing (*Z*)-α-trans bergamotol, was purposely obtained from the oil by monodimensional GC, and after analyzed under GC-FID conditions on the 100% polyethylene glycol, poly(5% diphenyl/95% dimethylsiloxane), ionic liquid and diethyl tertbutylsilyl-β-cyclodextrin chiral stationary phases. For such an experiment, a single Deans switch (TD1) was used, connected to the column and to the lab-made collection system. The highest R_S value of (4.7) was obtained by the chiral column, while R_S values equal to 2.7, 2.4, and 0.8 were obtained on the PEG, [poly(5% diphenyl/95% dimethylsiloxane)], and ionic liquid columns, respectively. As a consequence, the chiral column was chosen as the third GC dimension; a second heart-cut, in the 44.70–45.40 min retention-time window, was made, allowing the complete separation of (*Z*)-α-trans bergamotol from the residual amount of (*Z*)-α-santalol, as shown in Fig. 7.2B-3D. Finally, a third heart-cut from 53.66 to 54.39 min allowed the collection of (*Z*)-α-trans bergamotol with high purity (97%, Fig.7.2B cap.). About 0.5 mg were collected in 10 runs (total collection time 10 h), as reported in Table 7.0, with an overall recovery of 90.5%. The third collection process was devoted to epi-(*Z*)-β-santalol (3.2%) and (*Z*)-β-santalol (19.2%). Due to the complete co-elution of these compounds on the PEG column, both were transferred to the second column at the same time. In such a respect, a cut (fraction C) was performed between 31.10 and 33.25 min, thus enabling a purification from minor components (Fig. 7.2C-2D). After the transfer of the fraction to the ionic liquid column (47.50–48.10 min), an additional purification step was achieved, even if a complete separation of the two target components was not obtained: nevertheless, once transferred to the collection system in two consecutive heart-cuts (51.32–51.74 and 51.76–52.94 min) and flushed from the collection tubes, epi-(*Z*)-β-santalol and (*Z*)-β-santalol showed a degree of purity of 92.5% and 98%, respectively (Fig. 7.2C cap. and C1 cap.). In a total of 10 runs, 0.3 mg of epi-(*Z*)-β-santalol and 1.73 mg of (*Z*)-β-santalol were collected with an overall recovery of ∼90%.

The collection of the remaining components with a relative concentration lower than 5% in the sample was carried out by means of two preparative LC–GC–GC applications. The LC pre-separation step allowed a neat sample amount injection about 5–10 times higher than in conventional GC (10 µL *vs*. 1–2 µL). The transfer of selected LC fractions achieved an increased productivity for the collection of low-amount components. Furthermore, the pre-separation step allowed the transfer of simplified sub-samples, thus requiring less GC purification before the collection. In this concern, based on the complexity of the LC fractions, a different number of heart-cuts (GC dimensions) could be selected without any instrumental modification. Two GC dimensions were applied after the LC pre-separation, exploiting a lab-made collection system connected to the TD2 outlet [30].

In order to verify the LC–GC transfer recovery, 1 µL of a 20 mg mL^{-1} nootkatone solution (20 µg) was injected into GC1 in the splitless mode, and the peak area obtained compared with those achieved by the LC–GC transfer of 10 µL of the same solution (200 µg). The transfer recovery was calculated by transferring 1 mL of the LC eluent containing the nootkatone standard with a reduced flow of 350 µL/min, in both the LC conditions used for the transfer of the fractions from the real-world sample (100% *n*-hexane and 70% *n*-hexane/30% MTBE mobile phases). An overall recovery of 112% was achieved in 5 consecutive runs.

The first collection process was devoted to α-bisabolol (0.7%) (fraction D) while the second to the collection of (*Z*)-lanceol (1.4%) and (*Z*)-nuciferol (4.0%) (fraction E). The optimization of the LC–GC transfer process was made using a method previously optimized [33]. Fig. 7.3 summarizes the collection processes of the three components. Twenty µL of the sandalwood oil solution were injected onto the LC NH_2 column operated under stepwise gradient conditions. Fraction D of the LC effluent, containing α-bisabolol with a total volume of 1400 µL, eluted with 100% *n*-hexane, was directed to the GC from 19.10 to 23.10 min. As can be noticed, a highly simplified fraction was transferred to the first GC PEG column (Fig. 7.3D-1D), allowing the purification of the band of interest from a reduced number of matrix components. The following heart-cut, from 24.24 to 24.78 min, transferred the fraction to the [poly(5% diphenyl/95% dimethylsiloxane)] column (Fig. 7.3D-2D), affording a further purification from other components (accounting for about 9% of the fraction). After the transfer of the purified peak to the collection system (cut: 44.32–44.94 min), the GC-FID trace of the fraction flushed from the tube showed a degree of purity of 99.2% (D cap.): a total of ten collections provided 0.61 mg of highly pure α-bisabolol, with an average recovery of 87.1%.

The final application was devoted to the simultaneous collection of (*Z*)-lanceol and (*Z*)-nuciferol (fraction E): an LC fraction of 1400 µL, eluted with 30% of MTBE, was transferred (cut: 28.91 to 32.91 min) to GC1. The chromatogram relative to the 1D GC PEG column, reported in Fig. 7.3(E-1D), shows again a reduced complexity and a higher concentration of the components to be collected. Two heart-cut windows were selected from 35.35 to 37.00 min for (*Z*)-lanceol and from 37.48 to 39.12 min for (*Z*)-nuciferol. On the [poly(5% diphenyl/95%dimethylsiloxane)] second column an almost baseline separation was achieved for the two analytes, purified from *circa* 15% of co-eluents remaining after the PEG separation. The final heart-cuts, from 58.16 to 58.81 min and from 59.07 to 59.42 min, allowed the collection into separate tubes of highly pure components (Fig. 7.3E cap. and E1 cap.). In five consecutive

collections, 0.65 mg of (*Z*)-lanceol (E cap.) and 1.9 mg of (*Z*)-nuciferol (E1 cap.) were collected with an overall recovery of 91.5% and 95.0%, respectively.

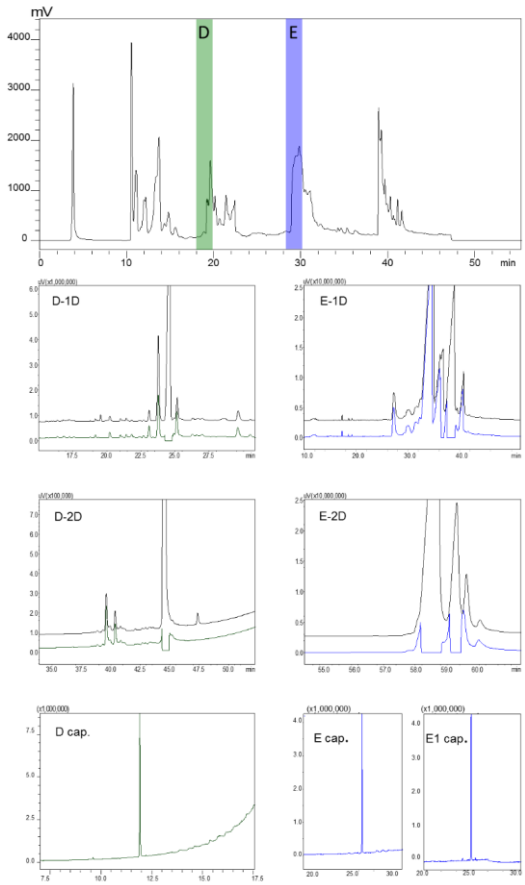

Figure 7.3. Scheme of the preparative LC–GC–GC process for the collection of (D) α-bisabolol and (E) (*Z*)-lanceol and (*Z*)-nuciferol. Upper chromatogram: LC stand-by injection of 10 µL of neat sandalwood oil.

Conclusions

In the present study, seven of the most important oxygenated sesquiterpene components were isolated from sandalwood essential oil in high amounts (190–1730 µg), in a short collection time (no sample preparation, about 1 hr *per* GC-GC-GC analysis, and about 90 min *per* LC–GC–GC analysis).

Depending on the components to be collected, the system was operated in two different configurations, in a very flexible manner, and without the need for any hardware or software modification.

References

[1] L.D. Kapoor, Handbook of Ayurvedic Medicinal Plants, CRC, Boca Raton, FL, 1990.

[2] F. Benecia, M.C. Courreges, Phytomedicine 6 (1999) 119.

[3] S. Banerjee, A. Ecavade, A.R. Rao, Cancer Lett. 68 (1993) 105.

[4] C. Dwivedi, A. Abu-Ghazaleh, Eur. J. Cancer Prev. 6 (1997) 399.

[5] C. Dwivedi, Y. Zang, Eur. J. Cancer Prev. 8 (1999) 449.

[6] Oil of Sandalwood (Santalum album L.), II ed., ISO 3518:2002(E), 2002-03-01,Geneva, Switzerland, 2002.

[7] T.H. Kim, H. Ito, T. Hatano, J. Takayasu, H. Tokuda, H. Nishino, T. Machiguchi,T. Yoshida, Tetrahedron 62 (2006) 6981.

[8] C. Dwivedi, H.B. Valluri, X.M. Guan, R. Agarwal, Carcinogenesis 27 (2006).

[9] S. Chilampalli, X.Y. Zhang, H. Fahmy, R.S. Kaushik, D. Zeman, M.B. Hildreth,C. Dwivedi, Anticancer Res. 30 (2010) 777.

[10] AS 2112—2003 Australian StandardTM, Oil of Sandalwood (Santalum spicatum(R. Br) A.DC.).

[11] C. Fehr, I. Magpantay, J. Arpagaus, X. Marquet, M. Vuagnoux, Angew. Chem. Int. Ed. 48 (2009) 7221.

[12] G. Buchbauer, I. Stappen, C. Pretterklieber, A. Wolschann, Eur. J. Med. Chem. 39 (2004) 1039.

[13] H. Monti, C. Corriol, M. Bertrand, Tetrahedron Lett. 23 (1982) 5539.

[14] K. Sato, O. Miyamoto, S. Inoue, K. Honda, Chem. Lett. 8 (1981) 1183.

[15] E.J. Corey, H.A. Kirst, J.A. Katzenel, J. Am. Chem. Soc. 92 (1970) 6314.

[16] D. Solas, J. Wolinsky, J. Org. Chem. 48 (1983)1988.

[17] P. Guha, S.C. Bhattacharya, J. Indian Chem. Soc. 21 (1944) 261.

[18] L. Mondello, M. Catalfamo, A.R. Proteggente, I. Bonaccorsi, G. Dugo, J. Agric. FoodChem. 46 (1998) 54.

[19] V. Schurig, M. Juza, B.S. Green, J. Horakh, A. Simon, Angew. Chem. Int. Ed.Engl. 35 (1996) 1680.

[20] P.G. Ruhle, J. Niere, P.D. Morrison, R. Jones, T. Caradoc-Davies, A.J. Canty, M.G.Gardiner, V.-A. Tolhurst, P.J. Marriott, Anal. Chem. 82 (2010) 4501.

[21] G.T. Eyres, S. Urban, P.D. Morrison, J.-P. Dufour, P.J. Marriott, Anal. Chem. 80 (2008) 6293.

[22] J. Ledauphin, J.-F. Saint-Clair, O. Lablanquie, H. Guichard, N. Founier, E.Guichard, D.J. Barillier, Agric. Food Chem. 52 (2004) 5124.

[23] G.T. Eyres, S. Urban, P.D. Morrison, P.J. Marriott, J. Chromatogr. A 1215 (2008) 168.

[24] C. Ruhle, G.T. Eyres, S. Urban, J.-P. Dufour, P.D. Morrison, P.J. Marriott, J. Chromatogr. A 1216 (2009) 5740.

[25] X. Feng, B.C. Benitez-Nelson, D.B. Montluc¸on, F.G. Prahl, A.P. McNichol, L. Xu, D.J.Repeta, T.I. Eglinton, Geochim. Cosmoschim. Acta 105 (2013)14.

[26] S. Nojima, D.J. Kiemle, F.X. Webster, C.S. Apperson, C. Schal, PLoSONE 6 (2011) 1.

[27] L. Kim, B. Mitrevski, K.L. Tuck, P.J. Marriott, J. Sep.Sci. 36 (2013) 1774.

[28] H.E. Park, S.-O. Yang, S.-H. Hyun, S.J. Park, H.-K. Choi, P.J. Marriott, J. Sep.Sci. 35 (2012) 416.

[29] G.I. Ball, L. Xu, A.P. McNichol, L.I. Aluwihare, J. Chromatogr. A 1220 (2012) 122.

[30] D. Sciarrone, S. Pantò, C. Ragonese, P.Q. Tranchida, P. Dugo, L. Mondello, Anal. Chem. 84(2012) 7092.

[31] D. Sciarrone, S. Pantò, A. Rotondo, L. Tedone, P.Q. Tranchida, P. Dugo, L.Mondello, Anal. Chim. Acta 785 (2013) 119.

[32] H. J. Cortes (Editor), Multidimensional chromatography, Techniques and Applications, Marcel Dekker, Inc., New York and Basel, 1990 pp. 75–144.

[33] D. Sciarrone, S. Pantò, P.Q. Tranchida, P. Dugo, L. Mondello, Anal. Chem. 86 (2014) 4295.

[34] G. Purcaro, M. Zoccali, P.Q. Tranchida, L. Barp, S. Moret, L. Conte, P. Dugo,L. Mondello, Anal. Bioanal. Chem. 405 (2013) 1077.

[35] C. Ragonese, D. Sciarrone, P.Q. Tranchida, P. Dugo, L. Mondello, J.Chromatogr. A 1255 (2012) 130.

Chapter 8

Research in the field of flow modulation comprehensive two-dimensional gas chromatography

8.1.0 Evaluation of a novel helium ionization detector within the context of (low-)flow modulation comprehensive two-dimensional gas chromatography

The present study is focused on the use and evaluation of a novel helium ionization detector, defined as barrier discharge ionization detector (BID), within the context of (low-)flow modulation comprehensive two-dimensional gas chromatography (FM GC×GC). The performance of the BID device was compared to that of a flame ionization detector (FID), under similar FM GC×GC conditions. Following development and optimization of the FM GC×GC method, the BID was subjected to fine tuning in relation to acquisition frequency and discharge flow. Moreover, the BID performance was measured and compared to that of the FID, in terms of extra-column band broadening, sensitivity and dynamic range. The comparative study was carried out by using standard compounds belonging to different chemical classes, along with a sample of diesel fuel. Advantages and disadvantages of the BID system, also within the context of FM GC×GC, are critically discussed.

8.1.1 Introduction

In comprehensive 2D GC, the widths of GC×GC peaks are related to a series of operational parameters, such as modulation conditions, gas linear velocity, stationary phase chemistry, column dimensions, *etc*. However, and in practically all instances, detectors used in the GC×GC field should be characterized by low dead volumes and a fast acquisition frequency, to limit extra-column band broadening and for reliable quantification, respectively. Together with mass spectrometry, the most popular detection system used in GC×GC has been the flame ionization detector [1,2]. FIDs are characterized by

a near universal response to organic compounds, good sensitivity, a low dead volume, a fast acquisition frequency (*e.g.*, 250 Hz) and a wide dynamic range. The detector can be considered as a carbon-selective one, with a near equal mass response of C in hydrocarbons. Such a feature enables: (I) the use of a single compound for calibration purposes; (II) the calculation of mass percent composition by considering analyte response relative to the sum of the FID responses for all observed peaks [3]. The discharge helium ionization detector (DHID) is a universal and sensitive detector, which can be used for the analysis of compounds with a poor or no response to the FID, and present in too low amounts for detection with a thermal conductivity detector. Compounds eluting from the capillary column are ionized in a secondary ionization region by high-energy photons generated in a nearby He discharge zone. The separation of the discharge chamber, from the secondary ionization zone, along with the use of a countercurrent He gas flow, guarantees that only pure He passes through the discharge chamber, limiting the possibility of contamination [3].

Only a single GC × GC-DHID research (using cryogenic modulation) has been described [4]. Specifically, Winniford *et al.* used a miniaturized pulsed discharge detector (acquisition frequency: 100 Hz) in photoionization modes for universal and selective detection. Mixtures of alkanes and aromatic compounds were used to evaluate the detector performance. The authors affirmed that extra-column band broadening was 20% ± 5% more compared to an FID, while sensitivity was similar.

The present investigation is based on the use, as detection system, of a recently-developed DHID in FM GC × GC experiments. The novel device is defined as barrier discharge ionization detector (BID), with such a definition from here onwards used [5]. The FM approach applied is based on that introduced by Seeley [6] (later corroborated by Amirav [7]), even though with reduced gas flow requirements [8]. The analytical results attained were directly compared with FID-derived ones, in terms of extra-column band broadening, sensitivity and dynamic range. Moreover, BID parameters such as acquisition frequency and discharge flow were finely tuned.

8.1.2.0 Experimental

8.1.2.1 Chemicals and samples

C_9-C_{10} *n*-alkanes, ethyl- and pentylbenzene, 2-phenylethanol and 1-nonanol, octanal and α-ionone, $C_{16:0}$ and $C_{18:1}$ fatty acid methyl esters (FAMEs) were supplied by Sigma-Aldrich/Supelco (Bellefonte, PA, USA). Solutions were

prepared in *n*-hexane. A diesel fuel sample was attained from a local petrochemical station, and was injected neat.

8.1.2.2 Instrumentation and software

All comprehensive two-dimensional GC-BID applications were carried out on a system consisting of a Shimadzu GC Tracera instrument (Kyoto, Japan), equipped also with an FID system. A description of the BID system is available [5]. A He purifier (VICI Valco Instruments, Houston, TX, USA) was used to reduce carrier gas impurities. Data were acquired by using the GCsolution software ver. 2.42 (Shimadzu). Bidimensional chromatograms were generated by using the ChromSquare software ver. 2.2 (Shimadzu).The GC was equipped with an AOC-20i auto-injector, and a split-splitless injector. The primary column was: SLB-5 ms [(silphenylene polymer, practically equivalent in polarity to poly(5% diphenyl/95%methylsiloxane)] 20 m × 0.18 mm ID × 0.18 μm d_f. The secondary column was: SPB-50 [poly(50% diphenyl/50% dimethyl siloxane)] 5 m × 0.32 mm ID × 0.20 μm d_f. Both columns were supplied by Sigma-Aldrich/Supelco. Flow modulation was performed following the model proposed by Seeley [6]. Briefly, the modulator was constructed by using two MXT Y-unions (Restek Corporation, Bellefonte, PA, USA) and a 2-way solenoid valve (located outside the GC), connected to an auxiliary pressure source. The output ports of the solenoid valve were connected to the unions by using two metallic branches. One of the Y-unions was linked to the primary-column outlet, while the other directed the flow to the second dimension. A stainless steel accumulation loop measuring 20 cm × 0.51 mm ID (SGE, Ringwood,Victoria, Australia) bridged the two Y-unions. Modulation period was 4,500 ms, with a 600 ms flushing period. Both detectors were maintained at a temperature of 310ºC. The injector in all applications was maintained at a temperature of 310ºC. BID and FID acquisition frequency was 250 Hz in all applications. Optimized BID discharge He flow: 70 mL/min. FID gas flows:H_2: 40 mL/min; make-up (He): 40 mL/min; air: 400 mL/min.

Temperature conditions, initial injector and auxiliary pressures (gauge), along with first and second dimension gas linear velocities and volumetric flows, in the isothermal (alkanes, alcohols, ketones, aldehydes, aromatics, FAMEs) and temperature-programmed (diesel fuel) GC×GC-BID/FID experiments are listed in Table 8.1.0.

Table 8.1.0. FM GC×GC-BID/FID conditions of: temperature (Temp.), injector (Inject.) and auxiliary (Aux.) pressures (gauge), first and second dimension (D1 and D2) gas flows and average linear velocities, loop average linear velocity during accumulation (ALV_{acc}) and re-injection (ALV_{inj}).

Parameters	**GC×GC-BID**			**GC×GC-FID**		
Temp.	120°C (standards)	200°C (FAMEs)	40-310°C (8°C/min)	120°C (standards)	200°C (FAMEs)	40-310°C (8°C/min)
Initial Inject. (kPa)	156.8	192.3	123.7	144.1	180.4	108.6
Final Inject.	-	-	187.1	-	-	175.2
Initial Aux. (kPa)	73.4	89.7	58.3	54.3	70.8	43.2
Final Aux.	-	-	113.7	-	-	101.6
Initial D1 (cm/s - mL/min)	17.5 - 0.44	18.8 -0.44	16.1 - 0.45	18.8 - 0.44	20.0 - 0.44	16.1 - 0.41
Final D1	-	-	11.6 - 0.23	-	-	11.6 - 0.22
Initial D2 (cm/s - mL/min)	144 - 7.8	163 - 7.8	121.8 - 7.8	144 - 6.8	163 - 6.8	134.4 - 7.58
Final D2	-	-	184.4 - 7.75	-	-	196.4 - 7.56
Initial ALV_{acc} (cm/s - mL/min)	2.7 - 0.44	3.0 - 0.44	2.4 - 0.45	3.1 - 0.44	3.3 - 0.44	2.5 - 0.41
Final ALV_{acc}	-	-	1.8 - 0.23	-	-	1.8 - 0.22
Initial ALV_{inj} (cm/s - mL/min)	48.5 - 7.8	53.2 - 7.8	42.4 - 7.8	47.5 - 6.8	52.1 - 6.8	45.5 - 7.58
Final ALV_{inj}	-	-	58.3 - 7.75	-	-	60.2 - 7.56

8.1.3.0 Results and discussion

8.1.3.1 Optimized FM GC×GC operational conditions

Considering FM method optimization, a major difference between the FID and BID systems must be considered, namely the different intra-detector pressure conditions. Specifically, the BID device is operated at a pressure higher than atmospheric. Obviously, the same capillary columns and FM accumulation loop

(20 cm × 0.51 mm ID; volume = 40.9 μL) were used in the FID and BID experiments. In general, first and second dimension gas linear velocities, as well as FM and BID conditions, were evaluated in isothermal applications on C_{9-10} *n*-alkanes (120ºC) and $C_{16:0}/C_{18:1}$FAMEs (200ºC). Once optimized, the FM (accumulation and re-injection periods) and BID operational conditions were maintained constant in all applications. With regard to gas linear velocities and flows, the isothermal applications provided a good experimental basis for the temperature-programmed experiment (on diesel fuel). For the alkanes application (120ºC), the applied GC×GC-BID inlet pressure was 156.8 kPa, while the auxiliary pressure was 73.4 kPa. The secondary-column outlet pressure (or BID operational pressure) was 19.3 kPa, corresponding to a discharge flow of 70 mL/min. During the accumulation period (3,900 ms), such pressures generated a primary column + loop flow of approx. 0.44 mL/min, corresponding to average linear velocities of approx. 17.5 and 2.7 cm/s, in the column and loop, respectively. At the end of the accumulation period, an isolated first-dimension effluent band would occupy a loop length of *ca*. 11 cm. During the re-injection step (600 ms), the loop + second-dimension flow was approx. 7.8 mL/min, corresponding to a loop linear velocity of approx. 48.5 cm/s, and a second-dimension one of about 140 cm/s (Table 8.1.0). The duration of the re-injection step was sufficient to push the effluent band for a loop length of about 29 cm, enabling 100% transfer onto the second column. With regard to the optimized GC×GC-FID operational conditions, the detector gas flows were those normally applied for GC×GC applications. The GC×GC-FID inlet pressure was 144.1 kPa, while the auxiliary pressure was 54.3 kPa. During the accumulation period, the primary column + loop flow corresponded to approx. 0.44 mL/min, corresponding to average linear velocities of approx. 19 and 3.1 cm/s, in the column and loop, respectively. An isolated first-dimension effluent band would occupy a loop length of *ca*. 12 cm, at the end of the accumulation step. During the re-injection process, the loop + second-dimension flow was approx. 6.8 mL/min, corresponding to a loop linear velocity of approx. 48 cm/s, and a second-dimension one of about 140 cm/s (Table 8.1.0). It is noteworthy that the secondary-column gas velocities were practically the same in the BID and FID applications. Again, the length of the re-injection step enabled 100% transfer of the effluent band from the loop onto the second column. Peak widths (4σ) in both application types were very similar (430–480 ms range) as can be seen from the data listed in Table 8.1.1 (n = 3).

Table 8.1.1. Peak widths (4σ) of alkanes (C_{9-10}) and FAMEs ($C_{16:0-18:1}$) in GC×GC-BID (at different discharge flows) and GC×GC-FID applications (n = 3). Peak widths are expressed in ms.

	GC×GC-BID		**GC×GC-FID**
	55 mL/min	**70 mL/min**	
C_9	550	480	460
C_{10}	470	430	450
$C_{16:0}$	700	660	650
$C_{18:1}$	1210	1170	1150

To confirm the initial satisfactory results, further isothermal applications were performed on $C_{16:0}$ and $C_{18:1}$FAMEs (200ºC), at a solution concentration of 100 mg/L. The gas linear velocities/flows were similar to those generated in the alkane applications and are reported in Table 8.1.0. As can be seen in the chromatogram expansions illustrated in Figure. 8.1.0, modulation of the $C_{16:0}$ FAME was satisfactory in both the BID and FID analyses, with peak widths (4 σ) again very similar as can be seen from the information reported in Table 8.1.1 (n = 3). In the BID experiments, the split ratio used was 3.3 times higher making a direct comparison between the two traces easier. A noteworthy issue is that leaks become immediately apparent when using the BID device, in FM GC×GC experiments, because the detector responds to the modulated air constituents. To avoid the presence of air within the GC×GC system all connections were carefully inspected, while a high purity (99.9999%) He cylinder was connected directly to a He purifier, the latter being linked to the GC×GC instrument. Even though such precautions were taken, the presence of interfering peaks (≈ 75,000 μV) was observed in the BID trace (signals marked by an asterisk in Figure. 8.1.0).

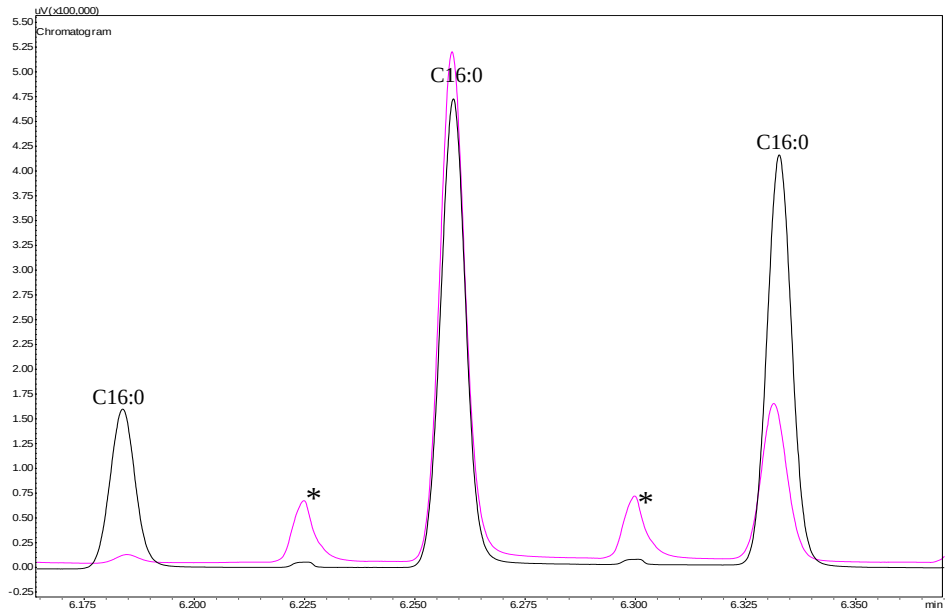

Figure. 8.1.0. GC×GC-BID (upper trace) and GC×GC-FID expansions relative to modulated $C_{16:0}$ FAME (the asterisks indicate an interference), at a concentration of 100 mg/L.The traces have been slightly moved from their original positions.

The same interferences, even though at a much lower intensity (≈ 5000 µV), were also present in the FID chromatogram (Figure. 8.1.0). Both, primary-column bleed (silphenylene polymer) and the injection solvent certainly contributed in a non-quantified manner to the formation of such peaks. The possible influence of gas contaminants or modulation flow fluctuations will be discussed in relation to the diesel fuel experiments.

8.1.3.2 Optimized BID operational conditions and analytical performance

The performance of the BID was evaluated at different acquisition frequencies (50, 125, 250 Hz) in FM GC×GC applications on $C_{9–10}$ *n*-alkanes, with negligible differences observed in terms of peak characteristics (height and width). The highest acquisition rate was selected for all applications, it being sufficient in general to reliably reconstruct practically any type of modulated peak. The performance of the BID was also evaluated at different discharge gas flows, again in FM GC×GC applications on $C_{9–10}$ *n*-alkanes and $C_{16:0–18:1}$

FAMEs. It is noteworthy that while the FID is mass-sensitive, the BID is concentration-sensitive and, therefore, with a response related to gas flows. With regard to the discharge flow, the manufacturer suggests the use of 50 mL/min, for a column flow up to 10 mL/min (higher than those generated in the present research). However, it was found that the FM GC×GC-BID peak widths practically matched those of the FM GC×GC-FID system at a discharge flow of 70 mL/min. Lower discharge flows (*e.g.*, 55 mL/min) generated broadened peaks compared to the FM GC×GC-FID result, presumably due to less efficient sweeping of the column effluent toward the BID collector electrode. A direct comparison between modulated GC×GC-BID results for C_{10} alkane, performed using a discharge flow of 55 and 70 mL/min, is reported in Figure. 8.1.1.

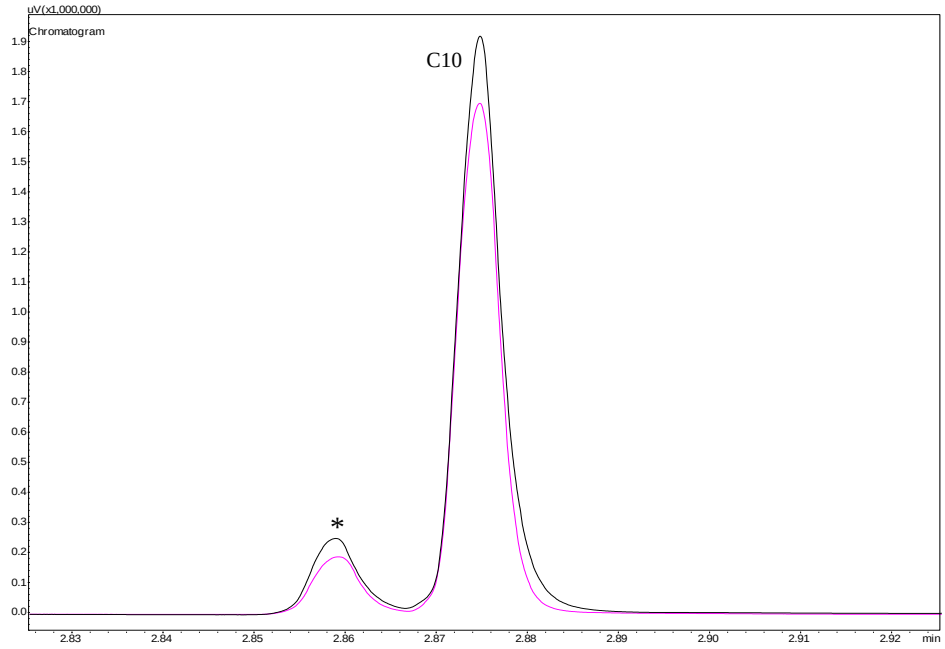

Figure. 8.1.1. GC×GC-BID expansions relative to the modulated C_{10} alkane, using discharge flows of 55 and 70 mL/min (the asterisk indicates an interference). The trace with the narrower C_{10} alkane peak was carried using a discharge flow of 70 mL/min.

Again, the interfering peak is visible but with at a much higher intensity compared to Figure. 8.1.0, due to the more abundant presence of the injection solvent (C_{10} alkane eluted just after the main solvent peak). On the basis of the initial GC×GC experimental results, it can be concluded that the BID can

provide a performance altogether comparable to that of the FID, considering the contribution to extra-column band broadening.

Sensitivity is a fundamental detection aspect and was investigated using a variety of standard compounds belonging to different chemical classes (C_9-C_{10} alkanes, ethyl- and pentylbenzene, 2-phenylethanol and 1-nonanol, octanal, α-ionone, $C1_{6:0}$-$C_{18:1}$ (FAMEs), each at a concentration of 100 mg/L (injected volume: 0.5 µl; split ratio: 1:70). Measurements were made through isothermal modulated GC×GC-BID and GC×GC-FID experiments at 120ºC, apart from the FAMEs (analysed at 200ºC); the tallest modulated peak was considered for the signal-to-noise (*s/n*) measurements. In all cases, BID signals were found to higher by factors of (n = 2): 1.4 for the alkanes (average of the two compounds), 4.1 for the benzenes (average of the two compounds), 5.9 for the alcohols (average of the two compounds), 6.8 for octanal, 5.2 for α-ionone, 2.5 for the FAMEs (average of the two compounds). Considering all ten compounds, BID signals were higher by a factor of 4.1, compared to the FID. Unmodulated experiments were also performed to eliminate the possible dependence of sensitivity on the modulation phase. The observed unmodulated results basically confirmed the modulation ones. Though in general six chemical classes represent a minority of the possible chemical classes, the results obtained do provide a good indication on detection response.

The dynamic ranges of the BID and FID systems were also evaluated. Solutions of ethyl- and pentylbenzene were prepared at seven concentration levels (0.5, 1, 10, 100, 1000, 10,000, 100,000 mg/L; injected volume: 0.5 µL, split ratio: 1:70), with each level subjected to isothermal FM GC×GC-BID and GC×GC-FID applications. The lowest calibration level can be considered as approx. the GC × GC-BID LoQ (limit of quantification) for both benzenes, considering a *s/n* value of 10 (the tallest modulated peak was considered). It is noteworthy that any BID LoQ value is tightly related to the specific column flow conditions (in this case second column), it being a concentration-sensitive detector. On the other hand, because FID systems are mass sensitive, peak areas do not change with gas flow, even though peak widths and heights do. GC×GC-BID response factors were calculated at each concentration level (n = 2), and plotted against mg/L values in a graph. The graph for ethylbenzene is illustrated in Figure. 8.1.2: as can be seen, detector linearity was maintained up to a concentration of 1000 mg/L, while BID saturation occurred at higher concentrations. A very similar dynamic range performance was observed for pentylbenzene.

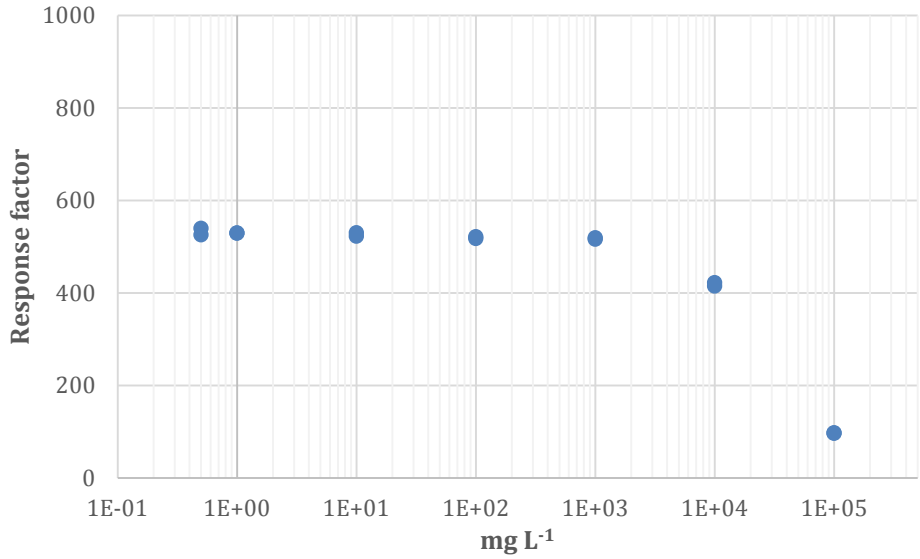

Figure. 8.1.2. Graph reporting the BID dynamic range for ethylbenzene.

With regard to the GC × GC-FID dynamic range, as expected it was linear over the entire range of concentrations for both benzenes; in such a respect, the performance of the BID was inferior. However, the lower sensitivity of the FID was confirmed by the fact that the lowest calibration level for both benzenes corresponded approximately to the limit of detection (considering a *s/n* value of 3). At this point, a sample of diesel fuel was subjected to temperature-programmed BID and FID analysis, maintaining as far as possible equivalent gas velocity conditions, and considering the isothermal experiments. Obviously, injection conditions were the same (injected volume: 0.4 µL; split ratio: 1:50). The initial GC×GC-BID inlet pressure was 123.7 kPa, while the auxiliary pressure was 58.3 kPa (40ºC); at the end of the analysis (310ºC), the inlet pressure reached 187.1 kPa, while the auxiliary pressure was 113.7 kPa. In the first dimension, the applied pressure conditions enabled a gradual decrease of the gas linear velocity (16.1 → 11.6 cm/s) and flow (0.45 → 0.23 mL/min) throughout the duration of the temperature program. Such a choice produced a general increase in D1 analyte elution temperatures (compared to constant velocity conditions), thus reducing the degree of wraparound and enabling the entire fan of diesel peaks to fit within the 2D plane. With regard to the FM conditions, even though the accumulation and re-injection gas linear velocity (and flow) values varied throughout the analysis (Table 8.1.0), modulation was satisfactory from the beginning to the end of the analysis. Considering the D2

conditions, the gas flow (7.8 ml/min) was maintained constant, causing an increase of gas velocity throughout the run (Table 8.1.0), again reducing the degree of wraparound. Very similar gas linear velocity and flow conditions were generated in the temperature-programmed GC×GC-FID analysis. The FM GC×GC-BID and GC×GC-FID chromatograms are shown in Figure. 8.3a and b, respectively.

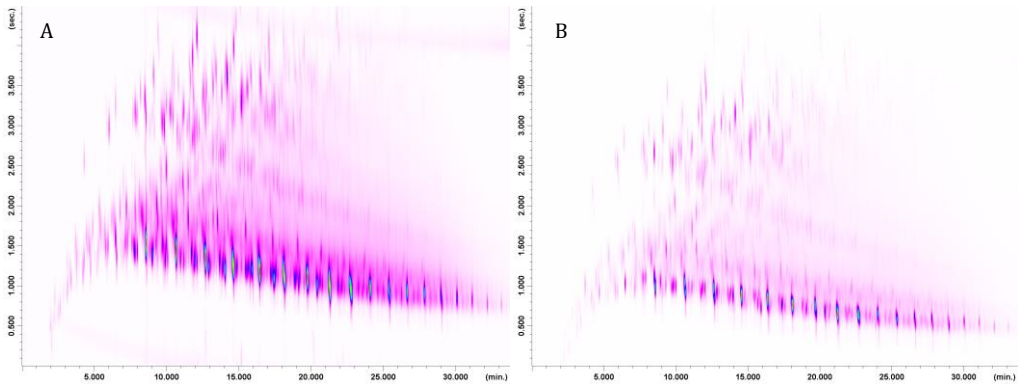

Figure. 8.1.3(a, b). FM GC×GC-BID and FM GC×GC-FID chromatograms of a diesel fuel sample.

The chromatograms were generated at the same intensity level [the signal range (from the baseline to the highest modulated peak) was 40,000–18,500,000 µV and 0–13,000,000 µV for the BID and FID trace, respectively]. Both chromatograms were wraparound corrected using a specific software function. As can be seen, the elution pattern is altogether comparable in both dimensions. In both experiments, an improved evaluation of the interfering peaks was attained considering that the diesel fuel was not diluted prior to analysis, and that the initial oven temperature was rather low (40ºC). At the beginning of the GC×GC-BID experiment, the intensity of the modulated interference was ≈18,000 µV, while it was completely absent in the GC×GC-FID application. Because the interference tracks the increase in linear velocity throughout the analysis (Figure. 8.3a), it can be presumed that it is related to the presence of contaminants in the gas carrier (N_2, O_2, H_2O, column bleed), rather than to modulation flow fluctuations. The intensity of the interfering streak located in the upper part of the GC×GC-BID chromatogram increases with temperature. In general, the overall higher sensitivity of the BID detector is clearly visible, in this case for (mainly) saturated and aromatic hydrocarbons. Two expansions

derived from the chromatograms illustrated in Figure. 8.3a and b are reported in Figure. 8.4a and b; in the latter, four peaks are indicated by the letters A (a linear hydrocarbon), B (a cyclic hydrocarbon), C (an aromatic), and D (an aromatic). GC×GC-BID total area values were increased by factors of 3.9 (A), 5.2 (B), 3.0 (C), and 6.5 (D), respectively, compared to the GC × GC-FID application.

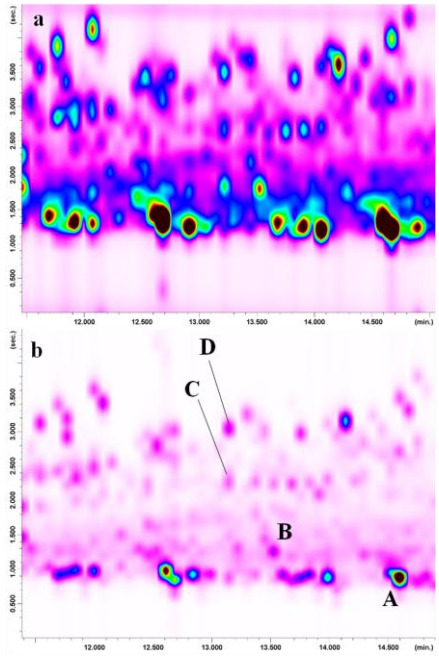

Figure. 8.1.4(a, b). Two expansions derived from the chromatograms illustrated in Figure. 8.3a and b. Chemical classes of peaks indicated by letters are reported in the text.

Conclusions

The BID, within the context of FM GC×GC, provided an overall satisfactory analytical performance. The main advantage of the novel detector, compared to the FID, was certainly a higher sensitivity observed for all the classes of compounds subjected to analyses. After fine tuning of BID parameters, detector derived band broadening was comparable to that of the FID. The main BID disadvantages were the reduced dynamic range, and the high sensitivity toward flow fluctuations.

References

[1] P.J. Marriott, Adahchour, S-T. Chin, B. Maikhunthod, H-G. Schmarr, S. Bieri, Trends Anal. Chem. 34 (2012) 1.

[2] H.J. Cortes, B. Winniford, J.C. Luong, M. Pursch, J. Sep. Sci. 32 (2009) 883.

[3] C.J. Poole, J. Chromatogr. A doi: 10.1016/j.chroma.2015.02.061.

[4] B.L. Winniford, K. Sun, J.F. Griffith, J.C. Luong, J. Sep. Sci. 29 (2006) 2664.

[5] K. Shinada, S. Horike, S. Uchiyama, R. Takechi, T. Nishimoto, Shimadzu Review SR13_001E

[6] J.V. Seeley, N.J. Micyus, J.D. McCurry, S.K. Seeley, Am. Lab. 38 (2006) 24.

[7] M. Poliak, M. Kochman, A. Amirav, J. Chromatogr. A 1186 (2008) 189.

[8] P.Q. Tranchida, F.A. Franchina, P. Dugo, L. Mondello, J. Chromatogr. A 1359 (2014) 271.

8.2.0 Four-stage (low-)flow modulation comprehensive gas chromatography-quadrupole mass spectrometry for the determination of recently-highlighted cosmetic allergens

The present research is based on the development and use of a flow-modulation comprehensive two-dimensional gas chromatography-quadrupole mass spectrometry (FM GC×GC-qMS) method for the determination of recently-highlighted (by the Scientific Committee on Consumer Safety) fragrance allergens (54) in cosmetics. FM GC×GC-qMS conditions were finely tuned to generate flow conditions (≈ 7 mL min^{-1}) compatible with the qMS system used. Six-point calibration curves, over the range 1, 5, 10, 20, 50, 100 mg L^{-1}, were constructed for the 54 target allergens, with satisfactory linearity observed in all cases. Absolute quantification was performed by using extracted ions; target analyte identification was performed through measurement of ion ratios (qualifier/quantifier), full-scan MS database matching and the use of linear retention indices. Additional analytical figures of merit subjected to measurement were intra-day repeatability, accuracy at the 25 and 5 mg L^{-1} levels, and limits of detection and quantification. The number of data points per peak, along with mass spectral skewing, were also subjected to evaluation.

8.2.1 Introduction

The determination of fragrance allergens (skin sensitizers) has been subjected to considerable attention in Europe: in 1999, the Scientific Committee on Cosmetic Products and Non-Food Products (SCCNFP) identified a set of 24 fragrance contact allergens, for which label information should be provided to consumers in relation to their presence in cosmetics [1]. The 24 allergens (plus two extracts) are regulated by the European Directive 2003/15/EC setting a maximum residue limit for "leave-on" and "rinse-off" products of 0.001% (10 ppm) and 0.01% (100 ppm), respectively.

In 2012, the Scientific Committee on Consumer Safety (SCCS) not only confirmed the previously-regulated allergens, but extended the attention to additional substances which have been shown to be skin sensitizers [2]. Specifically, 82 compounds were classified as contact allergens, of which 54 were single chemicals and 28 were natural extracts. The SCCS also indicated that a general level of exposure of up to 0.8 μg cm^{-2} (0.01% in cosmetic products) may be tolerated by the majority of consumers.

The determination of contact allergens is not new to the field of multidimensional GC: for example, the 24 compounds indicated by the SCCNFP were subjected to cryogenic GC×GC-qMS analysis by Debonneville and Chaintreau [3], while in a recent research, classical MDGC-qMS was used for the analysis of the 54 compounds reported by the SCCS [4]. In the latter work, several heart-cuts were performed to cover the retention time windows of all the 54 target analytes.

The FM GC×GC-qMS method herein proposed is directed to the determination of the 54 compounds highlighted by the SCCS.

8.2.2.0 Experimental

8.2.2.1 Chemicals and samples

Fifty-three allergen standards were used (Table 8.2.0). A standard was not commercially-available (mixture of α- and β-santalol), thus it was isolated from sandalwood oil using a lab-constructed preparative MDGC system described in Chapter 7. Two internal standards (IS), namely benzene-2-bromoethenyl (IS1) and 4,4'-dibromobiphenyl (IS2), were used at a concentration of 20 mg L^{-1}. Quantification was performed by using extracted ions (Table 8.2.0). Methanol (purity > 99 %) was used to form the calibration solutions (1, 5, 10, 20, 50, 100 mg L-1). All standards and the solvent were supplied by Sigma-Aldrich/Supelco (Bellefonte, PA, USA). The five commercial perfumes (P1-P5) were purchased in a local store.

8.2.2.2 Instrumentation and software

All FM GC×GC-qMS applications were performed on a system consisting of two independent GC2010 gas chromatographs (GC1 and GC2), and a QP-2010 Ultra qMS (Shimadzu, Kyoto, Japan). The two GC ovens were linked through a heated transfer line (310°C). The primary GC was equipped with an AOC-20i auto-injector and a split-splitless injector (310°C).

The primary column (situated in GC1), an SLB-5ms [silphenylene polymer virtually equivalent in polarity to poly(5% diphenyl/95% methyl siloxane)] 20 m × 0.18 mm ID × 0.18 μm d_f (Sigma-Aldrich/Supelco), was connected to the modulator, after passing through the heated transfer line. An SLB-35 [equivalent in polarity to poly(35% diphenyl/65% methyl siloxane)] 5 m × 0.25

mm ID × 0.25 μm d_f capillary (Sigma-Aldrich/Supelco), was used as second analytical column.

GC conditions: inj. vol.: 1 μL; split ratio: 10:1; GC1 temp. program: 45°C-228°C at 3°C min^{-1}; GC2 temp. program: 50°C-233°C at 3°C min^{-1}; initial and final inlet pressures (He): 130.8 and 216.2 kPa; initial and final auxiliary pressures (He): 65.2 and 143.2 kPa.

Flow modulation was performed following the model proposed by Seeley [5]. Briefly, the modulator was constructed by using two MXT Y-unions (Restek Corporation, Bellefonte, PA, USA) and a 2-way solenoid valve (located outside the GC), connected to an auxiliary pressure source. The output ports of the solenoid valve were connected to the unions by using two metallic branches. One of the Y-unions was linked to the primary-column outlet, while the other directed the flow to the second dimension. A fused silica accumulation loop measuring 40 cm × 0.53 mm ID (Sigma-Aldrich/Supelco) bridged the two Y-unions. Modulation period was 5,400 ms, with a 500 ms flushing pulse.

Quadrupole MS conditions: ionization mode: electron ionization (70 eV). Interface and ion source temperatures: 250° and 200°C, respectively. Mass range: 40-360 *m/z*; scan frequency: 25 Hz. Mass spectral matching was carried out by using the FFNSC 3.0 database (Shimadzu).

Table 8.2.0. Allergen peak identification, quantifier/qualifier ions and ratio (q/Q), q/Q values at three different peak points (I, II, III) along with CV% values, IS-analyte combination, LoDs/LoQs, R^2 values, accuracy (A%) expressed as percentage errors at the 25 and 5 mg L^{-1} levels, and intra-day precision measured at the100 and 1 mg L^{-1} levels.

Peak	Allergen	Quantifier	Qualifier	q/Q	q/QI	q/Q II	q/Q III	CV%	IS	LoD (mg L^{-1})	LoQ (mg L^{-1})	R^2	A% (25 mg L^{-1})	A% (5 mg L^{-1})	CV% (100 mg L^{-1})	CV% (1 mg L^{-1})
1	α-Pinene	93	77	0.26	0.28	0.26	0.25	5.3	IS1	0.05	0.16	0.9989	1.1	9.4	2.3	2.0
2	Benzaldehyde	106	77	0.96					IS1	0.17	0.55	0.9984	2.9	3.7	0.4	1.6
3	β-Pinene	93	69	0.31					IS1	0.06	0.20	0.9992	2.0	8.6	1.5	1.8
4	Limonene*	68	93	0.72	0.73	0.72	0.67	4.2	IS1	0.05	0.16	0.9990	4.6	13.2	1.4	2.8
5	Benzylalcohol*	108	79	1.10	1.02	1.10	1.20	8.2	IS1	0.25	0.83	0.9974	6.7	2.4	1.9	9.8
6	Salicylaldehyde	122	93	0.20					IS1	0.14	0.45	0.9971	13.3	10.2	1.8	11.0
7	Terpinolene	121	136	1.14					IS1	0.06	0.21	0.9993	3.4	12.1	1.0	3.6
8	Linalool*	71	93	0.77	0.83	0.77	0.76	4.7	IS1	0.21	0.71	0.9991	7.6	14.4	1.0	14.5
9	Camphor	95	81	0.75					IS1	0.09	0.30	0.9990	7.9	14.8	1.4	5.7
10	Menthol	81	95	0.78					IS1	0.09	0.31	0.9992	5.1	14.6	1.0	4.4
11	Methylsalicylate	152	120	0.53					IS1	0.07	0.24	0.9985	13.5	6.8	2.1	1.9
12	α-Terpineol	59	93	0.71					IS1	0.10	0.33	0.9975	11.5	5.4	2.8	3.1
13	Methyl 2-octynoate*	95	79	0.70					IS1	0.18	0.61	0.9986	2.4	1.3	2.6	5.5
IS1	2-Bromostyrene	103	182	0.60												
14	Citronellol*	69	81	0.51	0.54	0.51	0.46	8.6	IS1	0.29	0.97	0.9949	11.1	3.2	4.3	3.9
15a	Neral (Citral isomer I)*	69	109	0.12					IS1	0.19	0.62	0.9960	2.7	5.7	1.7	5.7
15b	Geranial (Citral isomer II)*	69	84	0.27					IS1	0.17	0.57	0.9975	3.6	13.3	2.6	2.7
16	Carvone	82	108	0.36					IS1	0.06	0.21	0.9994	8.0	12.8	1.1	6.5
17	Linalyl acetate	93	80	0.45					IS1	0.11	0.35	0.9930	10.6	7.9	1.6	9.8

18	Geraniol*	69	84	0.09	0.08	0.09	0.08	5.1	IS1	0.27	0.89	0.9987	8.4	6.4	1.8	5.4
19	(E)-Cinnamicaldehyde*	131	103	0.51					IS1	0.21	0.70	0.9968	3.8	14.5	2.8	9.9
20	Anisylalcohol*	138	109	0.08	0.08	0.08	0.09	8.0	IS1	0.27	0.89	0.9980	11.5	14.0	2.6	10.8
21	(E)-Anethol	148	59	0.56					IS1	0.09	0.29	0.9987	11.8	13.6	2.2	3.3
22	Hydroxycitronellal*	59	71	0.44					IS1	0.10	0.34	0.9989	12.7	9.1	1.8	10.8
23	(E)-Cinnamylalcohol*	133	91	0.80					IS1	0.21	0.69	0.9978	4.8	14.5	2.1	0.6
24	α,α-Dimethylphenethylacetate	132	91	0.76					IS1	0.07	0.18	0.9983	2.9	11.2	2.3	9.6
25a	(Z)-α-Damascone	69	123	0.18					IS1	0.12	0.37	0.9983	1.3	8.1	2.8	5.7
25b	(E)-α-Damascone	69	123	0.18					IS1	-	-	-	-	-	-	-
26	Eugenol*	164	149	0.31	0.32	0.31	0.30	4.0	IS1	0.12	0.39	0.9995	6.8	8.3	2.5	4.5
27a	(Z)-β-Damascenone	69	123	0.42					IS1	0.09	0.31	0.9984	6.7	9.9	2.8	7.4
27b	(E)-β-Damascenone	69	121	0.68					IS1	0.20	0.66	0.9982	12.5	2.3	2.0	7.4
28	δ-Damascone	69	81	0.17					IS1	0.16	0.54	0.9983	1.9	9.9	2.8	3.4
29a	(Z)-β-Damascone	177	123	0.42					IS1	0.09	0.31	0.9984	6.7	9.9	4.4	5.7
29b	(E)-β-Damascone	177	123	0.42					IS1	-	-	-	-	-	-	-
30	Vanillin	152	109	0.17	0.17	0.17	0.18	5.0	IS1	0.20	0.65	0.9980	9.4	12.4	2.8	13.4
31	Majantol	106	91	0.41					IS1	0.07	0.22	0.9992	5.0	14.3	1.5	6.9
32a	Ebanol (isomer I)	121	107	0.95	0.86	0.95	0.93	5.2	IS1	0.21	0.69	0.9988	4.6	9.8	2.0	9.8
32b	Ebanol (isomer II)	121	107	0.95					IS1	-	-	-	-	-	-	-
33	Coumarin*	118	146	0.94					IS1	0.07	0.24	0.9979	2.2	10.8	1.5	14.7
34	Isoeugenol*	164	149	0.30					IS1	0.11	0.35	0.9978	11.5	3.7	1.3	7.8
35	3-Methyl, α-ionone*	135	150	0.67					IS1	0.06	0.21	0.9993	4.3	14.5	1.2	6.7
36	Lilial*	189	147	0.44	0.41	0.44	0.44	3.9	IS1	0.05	0.18	0.9991	6.4	8.6	1.5	6.4
37	6-Methylcoumarin	160	132	0.64					IS1	0.29	0.97	0.9933	2.3	2.0	3.8	8.0

38	Amylsalicylate	120	138	0.33					IS1	0.09	0.29	0.9992	9.4	3.4	1.5	2.3
39	3-Propylidenephthalide	159	174	0.52	0.51	0.52	0.50	2.4	IS1	0.11	0.37	0.9987	10.3	4.7	1.4	8.9
40	Caryophylleneoxide	93	107	0.73					IS1	0.30	1.00	0.9981	1.6	8.1	2.3	4.4
41	α-Amylcinnammaldehyde*	129	117	0.78					IS2	0.07	0.23	0.9948	8.6	14.7	1.9	5.9
42a	Lyral (isomer I)*	136	79	0.78	0.69	0.78	0.87	11.5	IS2	0.10	0.33	0.9968	1.7	10.0	1.6	5.0
42b	Lyral (isomer II)*	136	79	0.75					IS2	-	-	-	-	-	-	-
43a	Iso E super (isomer I)	191	121	0.58					IS2	0.06	0.20	0.9957	4.8	13.5	1.5	1.8
43b	Iso E super (isomer II)	191	121	0.58					IS2	-	-	-	-	-	-	-
43c	Iso E Super (isomer III)	191	121	0.51					IS2	0.28	0.92	0.9980	8.5	10.9	1.8	4.8
44	α-Amylcinnamylalcohol*	133	91	0.69					IS2	0.17	0.58	0.9940	9.0	5.4	4.1	3.0
45a	(2Z,6Z)-Farnesol (isomer I)*	69	81	0.30					IS2	0.30	1.00	0.9981	10.4	23.5	4.2	12.3
45b	(2E,6E)-Farnesol (isomer II)*	69	81	0.30					IS2	-	-	-	-	-	-	-
46	α-Hexylcinnamaldehyde*	129	117	0.75	0.69	0.75	0.71	4.4	IS2	0.15	0.50	0.9949	7.4	22.6	2.1	7.1
47	Methylcedrylketone	161	119	0.53					IS2	0.12	0.39	0.9966	3.6	23.4	1.8	2.0
48	Benzylbenzoate*	105	91	0.44					IS2	0.07	0.23	0.9968	2.3	9.9	1.7	3.2
49	Galaxolide (Hexamethyl-Indanopyran)	243	213	0.36					IS2	0.09	0.31	0.9953	4.6	14.9	2.3	4.0
50	Benzylsalicylate*	91	65	0.13	0.12	0.13	0.13	4.7	IS2	0.04	0.14	0.9975	3.7	5.3	1.1	4.6
51	16-Hexadecanolide	55	69	0.60					IS2	0.11	0.37	0.9955	2.7	14.4	0.7	5.7
IS2	4 4"-Dibromobiphenyl	152	76	0.42												
52	Benzylcinnamate*	131	91	0.92					IS2	0.22	0.73	0.9989	3.5	7.7	1.5	5.0
53	Sclareol	177	109	0.76					IS2	0.26	0.88	0.9975	7.4	11.1	3.5	12.8
54a	α-Santalol	94	122	0.28					IS2	0.17	0.58	0.9910	8.0	10.8	10.0	12.0
54b	β-Santalol	94	122	0.29					IS2	-	-	-	-	-	-	-

Allergens introduced by the European Directive 2003/15/EC

Table 8.2.1. Initial-final FM GC×GC gas flow and ALV conditions. Abbreviations: accum.: accumulation; re-inj.: re-injection.

	D1	D2	FM accum.	FM re-inj.
Gas flows (mL min^{-1})	0.46-0.33	7.0-7.0	0.46-0.33	7.0-7.0
ALV conditions (cm s^{-1})	16-13	235-250	2.2-1.7	35-37

8.2.3.0 Results and discussion

8.2.3.1 Optimized FM GC×GC-qMS operational conditions

FM GC×GC method optimization can be a rather complicated task, and is here described treating the first and second column, along with the FM, in an independent manner. G1 temperature program was 45°C-228°C at 3°C/min, while a small positive offset of 5°C was used in GC2. The different oven temperatures slightly reduced retention of many polar allergens on D2, reducing wrap-around. General information on gas flows and average linear velocities (ALVs) are summarized in Table 8.2.1.

The initial and final FM re-injection ALVs were approx. 34.8 cm s^{-1} (7.0 mL min^{-1}) and 37.1 cm s^{-1} (7.0 mL min^{-1}), respectively. Again, considering such ALV values and the duration of the re-injection step (500 ms), the intra-loop chromatography band should be pushed ≈ 17.5 and 18.5 cm, at the beginning and end of the analysis, respectively. The use of a long loop enables a four-stage FM process [6]: at the beginning of the analysis (50°C), and after the first accumulation process, the analyte band would reach an intra-loop distance of approx. 11 cm; the first re-injection step would push the band another 17.5 cm, with the front end reaching a distance of about 28.5 cm; after the second accumulation step, the band should reach a distance within the loop of about 39.5 cm, and then be entirely released from the loop with the second re-injection step. Efficient four-stage modulation was observed at the end of the analysis, as can be derived by considering the data reported in Table 8.2.1 and by performing the same simple calculations.

The FM GC×GC-qMS method was applied to the analysis of a standard solution at the 50 mg L^{-1} level, and is shown in Figure 8.2.0. As can be seen, the allergens are nicely spread out across the 2D plane, while the overall quality of the chromatographic separation is satisfactory. Peak assignment is reported in Table 8.2.0, with the total number of target analytes exceeded fifty-four because some specific allergens consist in the sum of isomers (*e.g.*, peaks 25 a-

b correspond to (*Z*)-α-damascone and (*Z*)-β-damascone, respectively). The qMS system was operated at a mass spectral generation frequency of 25 Hz, it being sufficient for adequate peak reconstruction.

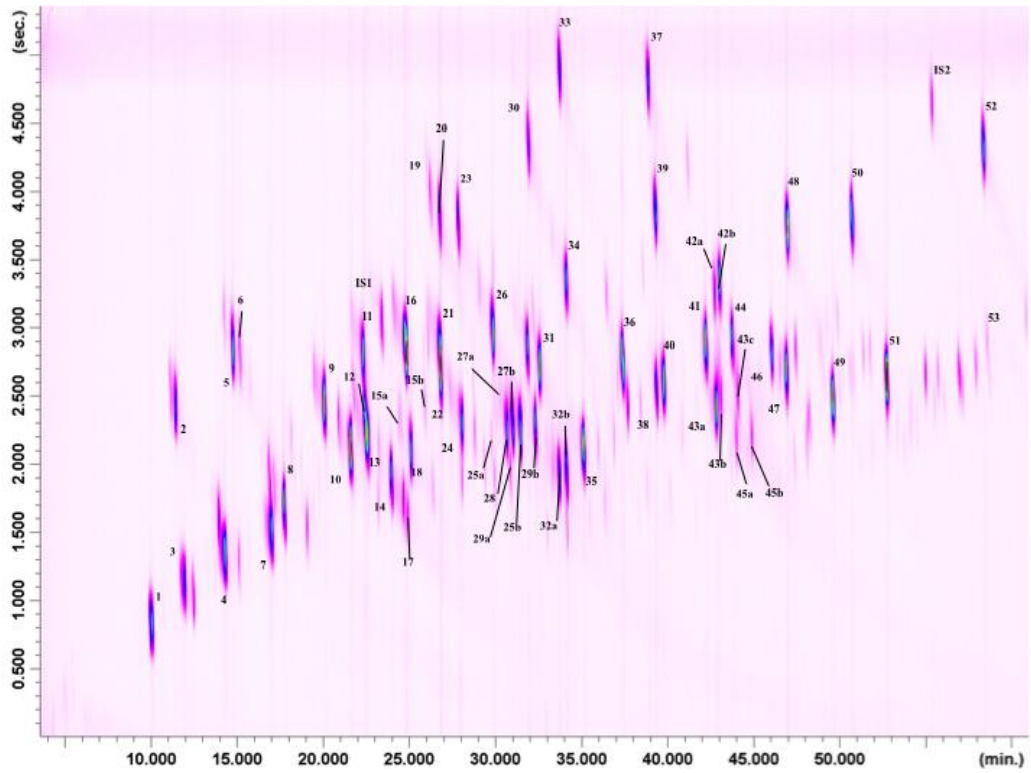

Fig. 8.2.0. FM GC×GC–qMS chromatogram of the allergen solution at the 50 mg L^{-1}level. For peak identification refer to Table 8.2.0.

For example, considering three analytes with a low, intermediate and high D2 retention time, namely peaks 1 (α-pinene), 33 (coumarin), and 51 (16-hexadecanolide), these were re-constructed with 15, 16, and 14 data points, respectively. Considering an average of fifteen data points per peak, this corresponds to a peak width of approx. 600 ms. Each second-dimension separation is confined by a 5,400 ms time space in which nine 600-ms peaks can fit. The FM GC×GC-qMS elution window time was 3,420 s (4-61 min), corresponding to about 633 modulations, and to a peak capacity of *circa* 5,700. Such a peak capacity can only be considered as an indication, it being higher than the real value.

8.2.3.2 Figures of merit and perfume applications

Six-point calibration curves (1, 5, 10, 20, 50, 100 mg L^{-1}; n = 3 at each level) were constructed by using two ISs (benzene-2-bromoethenyl and 4,4'-dibromobiphenyl), each related to specific target analytes on the basis of their MW values (Table 8.2.0). Peak areas were derived by using a significant ion (quantifier) for each allergen, while an additional ion was used for qualitative purposes (the ion ratio was considered). For seven sets of isomers [(*Z*,*E*)-α-damascone, (*Z*,*E*)-β-damascone, ebanol (I,II), lyral (I,II), Iso E super (I,II), farnesol (I,II), (α,β)-santalol], a single isomer was used for calibration and, hence, was representative of each compound class; for neral and geranial (Citral isomers), the two β-damascenone isomers (*Z*,*E*), and the third Iso E super isomer, a calibration function was derived for each isomer, because of the different responses of the quantifier ion. The general extrapolated qualifier/quantifier ion ratios are listed in Table 8.2.0. The reported ion ratios are average values, derived from all the calibration applications and from the *m/z* intensity at the peak apex.

Coefficients of regression were in the range 0.9995 (eugenol)-0.9910 (α-santalol); linearity was confirmed by using Mandel's fitting test [7]. Intra-day precision for the lowest and highest calibration point, expressed as coefficient of variation (CV%), was in the range 0.6 % [(*E*)-cinnamylalcohol] and 14.7 % (coumarin) at the 1 mg L^{-1} level, and 0.4 % (benzaldehyde) and 10.0 % (α-santalol) at the 100 mg L^{-1} level (Table 8.2.0).

Accuracy was measured through the analysis of a standard solution at a concentration level of 25 mg L^{-1} (a concentration not used for the construction of the calibration curve), and another at the 5 mg L^{-1} level. The range of percentage errors (n = 3), in absolute values, went from 1.1 % (α-pinene) to 13.5 % (methylsalicylate), at a concentration of 25 mg L^{-1}, and from 1.3 % (methyl 2-octynoate) to 23.5 % [(2Z,6Z)-farnesol], at a concentration of 5 mg L^{-1} (Table 8.2.0).

The instrumental limit of detection (LoD) and quantification (LoQ) values were calculated by measuring the average intensity of noise near the peak relative to the standard compound of interest (the most intense modulated peak was considered), at the 1 mg L^{-1} level. The signal-to-noise ratio (s/n) of each allergen, at a concentration of 1 mg L^{-1}, was then derived; LoDs and LoQs were then extrapolated by considering a s/n value of 3 and 10, respectively. The calculated LoDs and LoQs were in the ranges 0.04 (methylsalicylate) - 0.30 (caryophylleneoxide, two farnesol isomers) mg L^{-1}, and 0.14 (methylsalicylate) - 1.00 (caryophylleneoxide, two farnesol isomers) mg L^{-1}, respectively (Table 8.2.0). The method LoD and LoQ values were 10 times higher because perfume

sample dilution, prior to GC×GC analysis, must be accounted for during quantification. Consequently, the LoQ value for caryophylleneoxide (the highest of the entire group of target compounds) in perfume is 10.00 mg L^{-1}.

MS skewing occurs in particular for rapidly-eluting compounds in scanning MS instrumentation, and is related to the fast variation of analyte concentration in the ion source during the scanning process. The main consequence of MS skewing is the generation of inconsistent spectral profiles. Skewing was evaluated for 15 allergens (at the 50 mg L^{-1} level) by deriving ion ratios at 20% peak height (left- and right-hand), and at the apex, and by calculating coefficient of variation (CV%) values. Ion-ratio profiles were quite consistent (Table 8.2.0), with a CV% value exceeding 10% only in one case (11.5%), specifically for lyral (isomer I).

Five commercial perfumes (P1-P5) were subjected to FM GC×GC-qMS analysis, each three times consecutively. Apart from evaluation of the ion ratios, allergen identification was performed by: I) comparison of linear retention index values with those of the standard compounds; II) MS database matching. The full-scan FM GC×GC-qMS chromatogram, relative to sample P4, is shown in Figure 8.2.1. Overall, 20 allergens were subjected to identification and quantification in P4 (Table 8.2.2); as can been observed from the data reported in the table, seven allergens were present in excess of 1000. mg L^{-1} in the undiluted sample, and hence outside the range of the calibration solutions. Quantification information derived for the other four perfumes is also listed in Table 8.2.2. Twenty-four allergens were quantified in P1, with eleven in excess of 1000 mg L^{-1} and one below the method LoQ (methylsalicylate); twenty-one allergens were found in P2, with five at a concentration higher than 1000 mg L^{-1} and two at a concentration lower than the method LoQ (3-propylidenephthalide, α-hexylcinnamaldehyde); P3 contained the highest number of allergens, namely twenty-seven, with seven in excess of 1000 mg L^{-1} and two below the method LoQ (3-propylidenephthalide, 16-hexadecanolide); finally, twenty-three allergens were quantified in P5, with five in exceeding the 1000 mg L^{-1} level and two below the method LoQ (coumarin, 6-methylcoumarin).

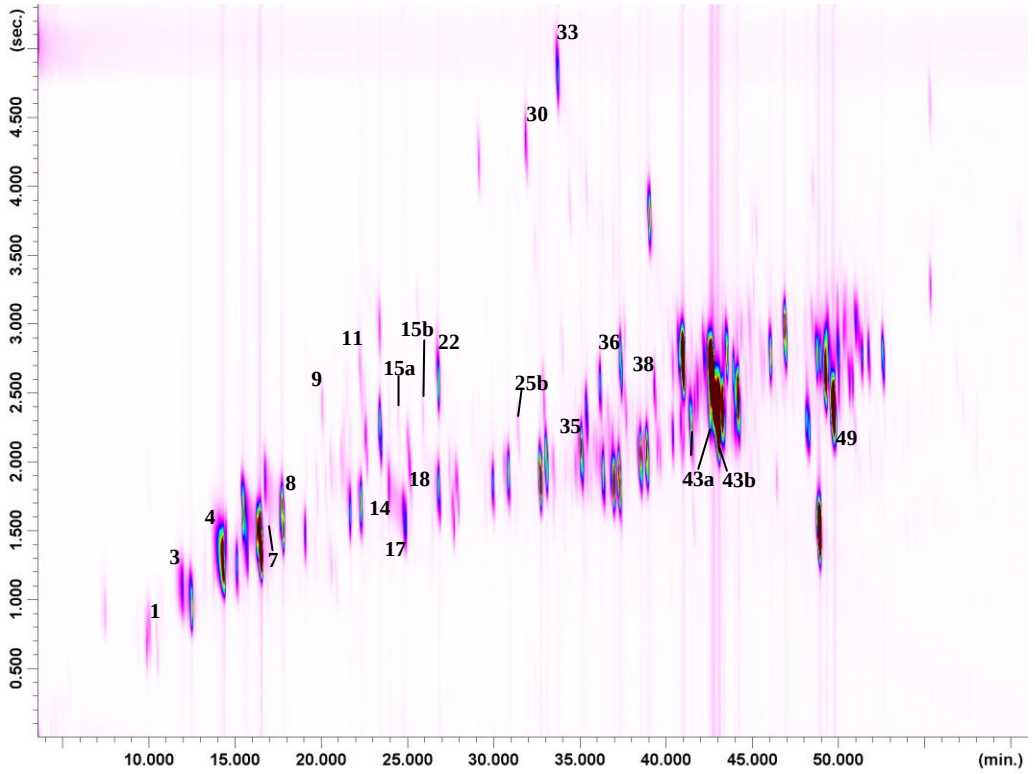

Fig. 8.2.1. FM GC×GC–qMS chromatogram of sample P4. For peak identification refer to Table 8.2.0.

Table 8.2.2. Quantitative data (mg L^{-1}) relative to the commercial perfume samples (P1-P5).

Peak	Allergen	P1	P2	P3	P4	P5
1	α-Pinene	177.4	141.8	822.1	112.3	108.5
3	β-Pinene	> 1000	> 1000	> 1000	827.2	376.6
4	Limonene*	> 1000	> 1000	> 1000	> 1000	> 1000
5	Benzylalcohol*	-	-	-	-	747.1
7	Terpinolene	43.6	-	30.5	55.4	-
8	Linalool*	> 1000	> 1000	> 1000	> 1000	228.2
9	Camphor	-	18.9	178.4	82.6	-
10	Menthol	-	-	80.4	-	38.1
11	Methylsalicylate	< LoQ	-	5.1	20.8	542.8
12	α-Terpineol	34.3	60.5	59.6	-	-

13	Methyl 2-octynoate*	10.9	-	22.6	-	-
14	Citronellol*	117.4	193.1	522.4	307.0	853.9
15a	Neral (Citral isomer I)*	-	> 1000	320.0	559.1	-
15b	Geranial (Citral isomer II)*	-	> 1000	683.2	435.3	-
16	Carvone	-	86.4	-	-	-
17	Linalyl acetate	> 1000	-	> 1000	> 1000	-
18	Geraniol*	-	104.0	270.3	207.0	432.8
19	(E)-Cinnamicaldehyde*	342.2	-	-	-	-
22	Hydroxycitronellal*	274.2	18.0	164.9	836.5	159.7
23	(E)-Cinnamylalcohol*	-	44.6	-	-	-
25b	(E)-α-Damascone	-	557.9	-	74.4	-
26	Eugenol*	55.1	294.0	-	-	-
27b	(E)-β-Damascenone	-	-	244.5	-	-
28	δ-Damascone	-	581.3	-	-	-
30	Vanillin	> 1000	-	-	502.3	79.5
31	Majantol	3.2	-	-	-	-
32a	Ebanol (isomer I)	152.2	-	-	-	-
33	Coumarin*	> 1000	114.0	-	938.6	< LoQ
34	Isoeugenol*	11.9	-	-	-	5.9
35	3-Methyl, α-ionone	> 1000	475.6	75.4	> 1000	63.5
36	Lilial*	-	-	-	416.0	> 1000
37	6-Methylcoumarin	-	-	-	-	< LoQ
38	Amylsalicylate	-	-	84.0	452.4	-
39	3-Propylidenephthalide	-	< LoQ	< LoQ	-	-
40	Caryophylleneoxide	-	28.2	-	-	-
42a	Lyral (isomer I)	> 1000	-	211.3	-	-
43a	Iso E super (isomer I)	> 1000	-	> 1000	> 1000	-
43b	Iso E super (isomer II)	-	-	485.8	> 1000	-
44	α-Amylcinnamylalcohol*	-	-	33.1	-	401.3
45a	(2Z,6Z)-Farnesol (isomer I)*	-	-	-	-	113.2
46	α-Hexylcinnamaldehyde*	11.5	< LoQ	-	-	11.7
47	Methylcedrylketone	> 1000	-	> 1000	-	-
49	Galaxolide (Hexamethyl-Indanopyran)	> 1000	-	> 1000	> 1000	> 1000
50	Benzylsalicylate*	-	-	-	-	> 1000
51	16-Hexadecanolide	-	-	< LoQ	-	> 1000
52	Benzylcinnamate*	-	-	-	-	263.0

*Allergens introduced by the European Directive 2003/15/EC

Conclusions

An FM GC×GC-qMS method for the determination of recently-highlighted contact allergens in perfume has been herein described. If the European Directive 2003/15/EC maximum concentration value for "rinse-off" products (10 ppm) is set as concentration limit, then the FM GC×GC-qMS method is sufficiently sensitive for all the 54 allergens considered. Moreover, and if required, the high-resolution untargeted analysis of perfume constituents can be performed.

The FM model proposed is a low-costing and effective alternative to cryogenic modulation; in fact, both the hardware and operational costs are rather limited, with many of the well-known benefits of GC×GC maintained. Future research will be devoted to the use of FM GC×GC, combined with mass spectrometry, in other significant applicational areas.

References

[1] Fragrance allergy in consumers, SCCNFP/0017/98, December 1999.

[2] Opinion on fragrance allergens in cosmetic products, SCCS/1459/11, June 2012.

[3] C. Debonneville, A. Chaintreau, J. Chromatogr. A 1027 (2004) 109.

[4] A. Rey, E. Corbi, C. Pérès, N. David, J. Chromatogr. A doi: 10.1016/j.chroma.2015.05.045.

[5] J.V. Seeley, N.J. Micyus, J.D. McCurry, S.K. Seeley, Am. Lab. 38 (2006) 24.

[6] P.Q. Tranchida, F.A. Franchina, P. Dugo, L. Mondello, J. Chromatogr. A 1372 (2014) 236.

[7] N.R. Draper, H. Smith, Applied Regression Analysis, second ed., Wiley, New York, 1981.

8.3.0 Flow modulation comprehensive two-dimensional gas chromatography-mass spectrometry using ≈ 4 ml min^{-1} gas flows

The main objective of the herein described research was focused on performing satisfactory flow modul, in comprehensive two-dimensional gas chromatography-mass spectrometry experiments, using an MS-compatible second-dimension gas flow of approx. 4 mL min^{-1}. The FM model used was based on that initially proposed by Seeley and co-workers (Am. Lab. 2006, 38, 24-26). The use of limited gas flows was enabled through fine tuning of the FM parameters, in particular the duration of the re-injection (or flushing) process. Specifically, the application of a long re-injection period (i.e., 700 ms) enabled efficient accumulation-loop flushing with gas flows of about 4 mL min^{-1}. It was possible to apply such extended re-injection periods by using different restrictor lengths in the connections linking the modulator to the auxiliary pressure source. FM GC×GC-MS applications were performed on a mixture containing $C_{9\text{-}10}$ alkanes, and on a sample of essential oil. GC×GC-MS sensitivity was compared with that attained by using conventional GC-MS analysis, in essential oil applications. It was observed that signal intensities were, in general, considerably higher in the FM GC×GC-MS experiments.

8.3.1 Introduction

The FM process proposed by Seeley *et al.* in 2006 was characterized by an accumulation step, and a shorter re-injection one [1]. For example, in that research the accumulation and re-injection durations were 1.4 s and 0.1 s, respectively. A gas flow of 20 mL min^{-1} was used for efficient loop flushing. During the latter process, the first-dimension flow is interrupted. Even though the generation of such a high gas flow can be considered as a main disadvantage (especially for mass spectrometric detection), it has been widely accepted that high gas flows are required to efficiently re-inject the content of the accumulation loop onto the second column [2-4].

In the present research, it will be shown that by using the information reported in refs. [1] and [5], with additional modification to the FM configuration, it is possible to perform FM GC×GC, combined with mass spectrometry (MS), using gas flows of ≈ 4 mL min^{-1}, and thus extending the applicability of such an FM approach to practically any commercial MS system.

8.3.2.0 Experimental

8.3.2.1 Chemicals and samples

C_9 and C_{10} alkanes were supplied by Sigma-Aldrich/Supelco (Bellefonte, PA, USA), and diluted in *n*-hexane to an approximate concentration of 10 μg mL^{-1} prior to injection. A sample of Artemisia essential oil was obtained from hydrodistillation of the aerial parts of Artemisia arborescens. The essential oil was diluted approx. 1:20 in *n*-hexane prior to analysis.

8.3.2.2 Instrumentation and software

All FM GC×GC-MS applications were performed on a system consisting of two independent Shimadzu (Kyoto, Japan) GC2010 gas chromatographs (GC1 and GC2), and a Shimadzu QP-2010 Ultra quadrupole mass spectrometer (qMS). The two GC ovens were linked through a heated transfer line. The primary GC was equipped with an AOC-20i auto-injector and a split-splitless injector (350°C).

The primary column (situated in GC1), an SLB-5ms 30 m × 0.25 mm ID × 0.25 μm d_f [silphenylene polymer virtually equivalent in polarity to poly(5% diphenyl/95% methylsiloxane)], was passed through the heated transfer line. An SLB-35ms 5 m × 0.25 mm ID × 0.25 μm d_f capillary [poly(35% diphenyl/65% dimethylsiloxane)] was used as second analytical column. Flow modulation was performed following the model proposed by Seeley [1]. Briefly, the modulator was constructed by using two MXT Y-unions (Restek Corporation, Bellefonte, PA, USA) and a 2-way solenoid valve (located outside GC1), connected to an auxiliary pressure source (advanced pressure control - APC). A scheme of the FM is shown in Figure 8.3.0. The output ports of the solenoid valve were linked to two metal branches, the latter being connected to the two Y-unions by using two restrictors (two segments of uncoated column). One of the Y-unions was linked to the primary-column outlet (here defined upstream union), while the other (here defined downstream union) directed the flow to the second-dimension (^{2}D).

In the so-called “symmetrical configuration” (SC), two uncoated columns each measuring 10 cm × 0.25 mm ID were used to connect the metal branches to the unions. Differently, in the “asymmetrical configuration” (AC) a 10 cm × 0.25 mm ID uncoated column was connected to the up-stream union, while a 19 cm × 0.18 mm ID uncoated column (plus the 10 cm × 0.25 mm ID uncoated

capillary) was linked to the downstream one. All capillaries were supplied by Sigma-Aldrich/Supelco.

A stainless steel accumulation loop measuring 20 cm, with a 0.51 mm ID (SGE, Ringwood, Victoria, Australia), bridged the two Y-unions. The flow modulator was located in GC1.

GC×GC parameters for the alkane experiments: inj. vol.: 0.4 µL; split ratio: 10:1; isothermal temperature in both ovens was 120°C. For injector/auxiliary pressure and modulation conditions see the Section 8.3.3.

GC×GC parameters for the Artemisia essential oil application: inj. vol.: 0.4 µL; split ratio: 10:1; the following temperature program was used in both ovens: from 70° C to 310° C at 1.5° C/min. Initial inlet pressure: 68.7 kPa; initial auxiliary pressure: 43.7 kPa (the flow was maintained constant). Modulation period: 5.2 s (accumulation period 4.5 s/injection period 0.7 s).

qMS parameters: mass range was *m/z* 40-350; spectral acquisition frequency: 25 Hz (20 Hz in the essential oil application); ionization mode: electron ionization (70 eV); interface and ion source were maintained at 250°C and 200°C, respectively. Mass spectral matching was carried out by using the FFNSC 3.0 database (Shimadzu). Data were acquired by using the GCMSsolution software (Shimadzu). Two-dimensional chromatograms were generated by using the ChromSquare software v. 2.2 (Shimadzu).

GC-MS applications were performed using the same GC×GC-MS instrumentation as above described, but with a direct connection of the primary column to the ion source. When not specified, the experimental conditions were the same as in the GC×GC-MS essential oil analysis. Initial inlet pressures were 2.5 and 29.4 kPa, in the 0.4 and 0.65 mL min^{-1} experiments (flows were maintained constant), respectively. Mass spectral acquisition frequency was 1 Hz.

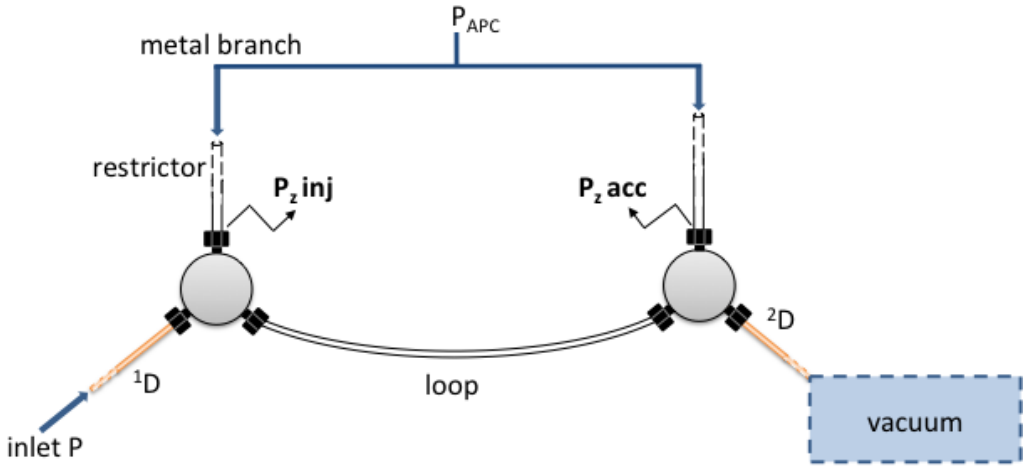

Fig. 8.3.0. Scheme of the FM (in the asymmetrical configuration). Abbreviations: P = pressure; P_{APC}= auxiliary pressure; P_z acc = pressure at the downstream point of the union during accumulation; P_z inj = pressure at the upstream point of the union during re-injection.

8.3.3 Results and discussion

In previous research, it was found that efficient FM could be performed by using a re-injection step of 500 ms and a second-dimension gas flow of about 6 mL min^{-1} (C_9 alkane; 120°C) [5]. Even though efficient FM was performed under such conditions, it is obvious that such a gas flow can still be considered rather high for MS analysis, with a further reduction desirable. On the basis of the information reported in ref. [5], one could conclude that a further decrease of the ^{2}D gas flow could be achieved simply by increasing even more the duration of the re-injection period. However, if the re-injection step is too long, then the period of ^{1}D stop-flow will terminate before the end of the re-injection stage. For example, if a re-injection step of 800 ms is applied (*e.g.*, at 6 mL min^{-1}), with a hypothetical stop-flow period of 600 ms, then first-dimension effluent will enter the FM loop for the remaining 200 ms (for convenience defined as "200-ms band"). During the following accumulation step (e.g., 4,000 ms at 0.5 mL min^{-1}), one or both of two factors will occur and are here reported: I) because the 200-ms band enters the loop at a 6 mL min^{-1} flow, while the following accumulation step is performed at 0.5 mL min^{-1}, the front end of the entire band (formed by the 200-ms band + 4,000-ms accumulation band) will be more diluted than the rear part; II) breakthrough of part of the leading edge of the 200-ms band during accumulation. Factor I will practically always take place, while the occurrence of factor II is dependent on the specific

FM conditions. Both factors will cause a baseline rise prior to the modulated peak. Such theoretical considerations were, at this point, evaluated experimentally: C_9 and C_{10} alkanes were subjected to FM GC×GC-qMS analyses under isothermal conditions (120°C), and using a loop of dimensions 20 cm × 0.51 mm ID. This is a standard procedure used to optimize, as rapidly as possible, the modulation conditions. Obviously, the two alkanes have similar boiling points and elute within an acceptable time-frame at 120°C. The choice of a shorter accumulation loop (and a single accumulation/re-injection step) was also made to simplify the FM optimization process. It is noteworthy that, initially, two restrictors of the same dimensions (10 cm × 0.25 mm ID) were used to link each metal branch (deriving from the solenoid valve) to the FM (SC). The slight pressure drops created by using the two restrictions are here considered for calculation of the gas flow/linear velocity conditions (Table 8.3.0). Inlet/APC pressures, along with modulation conditions, are also listed in Table 8.3.0. Even though very helpful for FM method optimization, the gas flow and average linear velocity conditions herein reported (calculated with the support of the HP FlowCalc 2.0 software) and discussed are to be considered only as approximations.

Table 8.3.0. FM GC×GC operational conditions in the isothermal applications, using the symmetrical (SC) and asymmetrical (AC) configurations. Abbreviations: Accum. = accumulation period; Re-inject. = re-injection period.

	SC 5 mL min^{-1}	**AC 4 mL min^{-1}**
Inlet P (kPa)	89.5	89.5
^{1}D ALV (cm s^{-1})	8	11
^{1}D flow (mL min^{-}	0.3	0.4
APC (kPa)	61.4	61.4
P_z acc	59.8	49.8
P_z inj	59.8	59.8
^{2}D ALV	198	186
^{2}D flow	5	4
ALV_{acc} (ALV_{inj})	2.2 (32)	3 (32)
Accum. (ms)	4,500	4,500
Re-inject. (ms)	700	700

An SC experiment was performed at a ^{2}D He flow of ≈ 5 mL min^{-1}, thus a further gas flow reduction compared to previous research [3]. The pressures applied generated an ALV_{acc} (average linear velocity during accumulation) of 2.2 cm s^{-1}; at the end of the 4,500-ms accumulation period, the analyte band should occupy a loop length of nearly 10 cm. The ALV_{inj} (average linear velocity during re-injection) increased to 32 cm s^{-1} during the 700-ms re-injection period. The latter condition enabled the complete expulsion of the analyte band from the loop. As can be seen in the chromatogram expansion shown in Figure 8.3.1A there is a baseline rise prior to the modulated peaks, due to the excessively long re-injection step and, consequently, to an interruption of the stop-flow period. The w_h value for the most intense modulated peak was about 205 ms.

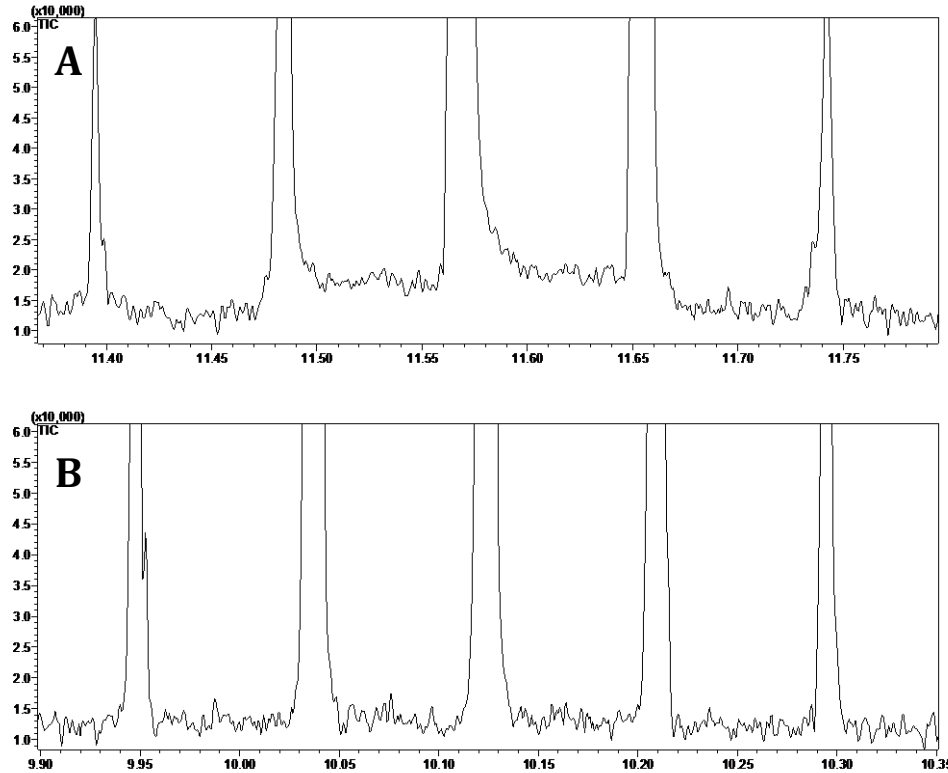

Figure 8.3.1. Raw chromatogram expansions showing the modulation of C_9 alkane at ^{2}D flows of ≈ 5 mL min^{-1}(Fig. 8.3.1.A—SC) and ≈ 4 mL min−1(Fig. 8.3.1.B—AC).

The possibility to extend the stop-flow period was investigated by using two different uncoated columns (restrictors) to connect the solenoid valve metal branches to the FM (asymmetrical configuration – Figure 8.3.0). Specifically, a 10 cm × 0.25 mm ID uncoated column was connected to the upstream union (^{1}D connection), while a 19 cm × 0.18 mm ID uncoated column was connected to the 10 cm × 0.25 mm ID uncoated capillary, which in turn was linked to the down-stream union. In terms of flow resistance, a 19 cm × 0.18 mm ID + 10 cm × 0.25 mm ID column combination is equivalent to an 80 cm × 0.25 mm ID capillary. It is noteworthy that such a solution (the use of different restrictors) was proposed in the initial work of Seeley *et al.* [1]. The lower flow resistance at the upstream union will generate a pressure pulse (during re-injection), thus extending the stop-flow period and causing backflush. The extent to which backflush occurred was not herein investigated. In this respect, other authors have investigated the occurrence of FM backflushing using an asymmetrical configuration [6].

The AC application was performed using the same pressure conditions as with the symmetrical configuration, with a calculated ^{1}D He flow of 0.4 mL min^{-1}. The second-dimension He flow, during the accumulation period (about 87% of the modulation period), was calculated to be approx. ≈ 4 mL min^{-1}, and increased to approx. ≈ 5 mL min^{-1}, during re-injection.

The conditions of gas flow generated an ALV_{acc} of 3.0 cm s^{-1}; at the end of the accumulation period (4,500 ms), the analyte band should occupy a loop length of 13.5 cm. The ALV_{inj} intra-loop average linear velocity increased to 32 cm s^{-1} during the 700-ms re-injection period. Most importantly, the modulation process this time was satisfactory as can be seen in the expansion illustrated in Figure 8.3.1 B. It is noteworthy that the two chromatogram expansions, shown in Figures 8.3.1 A-B, are characterized by the practically same y-axis signal intensity. The w_h value for the most intense modulated peak was about 290 ms.

At this point of the research, a temperature-programmed FM GC×GC-qMS experiment was performed on a real-world sample, namely Artemisia essential oil. The injector and auxiliary pressure gradients used, enabled constant flow conditions throughout the analysis: ^{1}D and ^{2}D flows were approx. 0.4 and 4 mL min^{-1}, respectively. The modulation period was 5,200 ms, with a 700-ms re-injection period. The full-scan chromatogram for this essential oil application is shown in Figure 8.3.2 A. The zone confined by a rectangle is illustrated in Figure 8.3.2 B with the aim of highlighting the satisfactory chromatography performance.

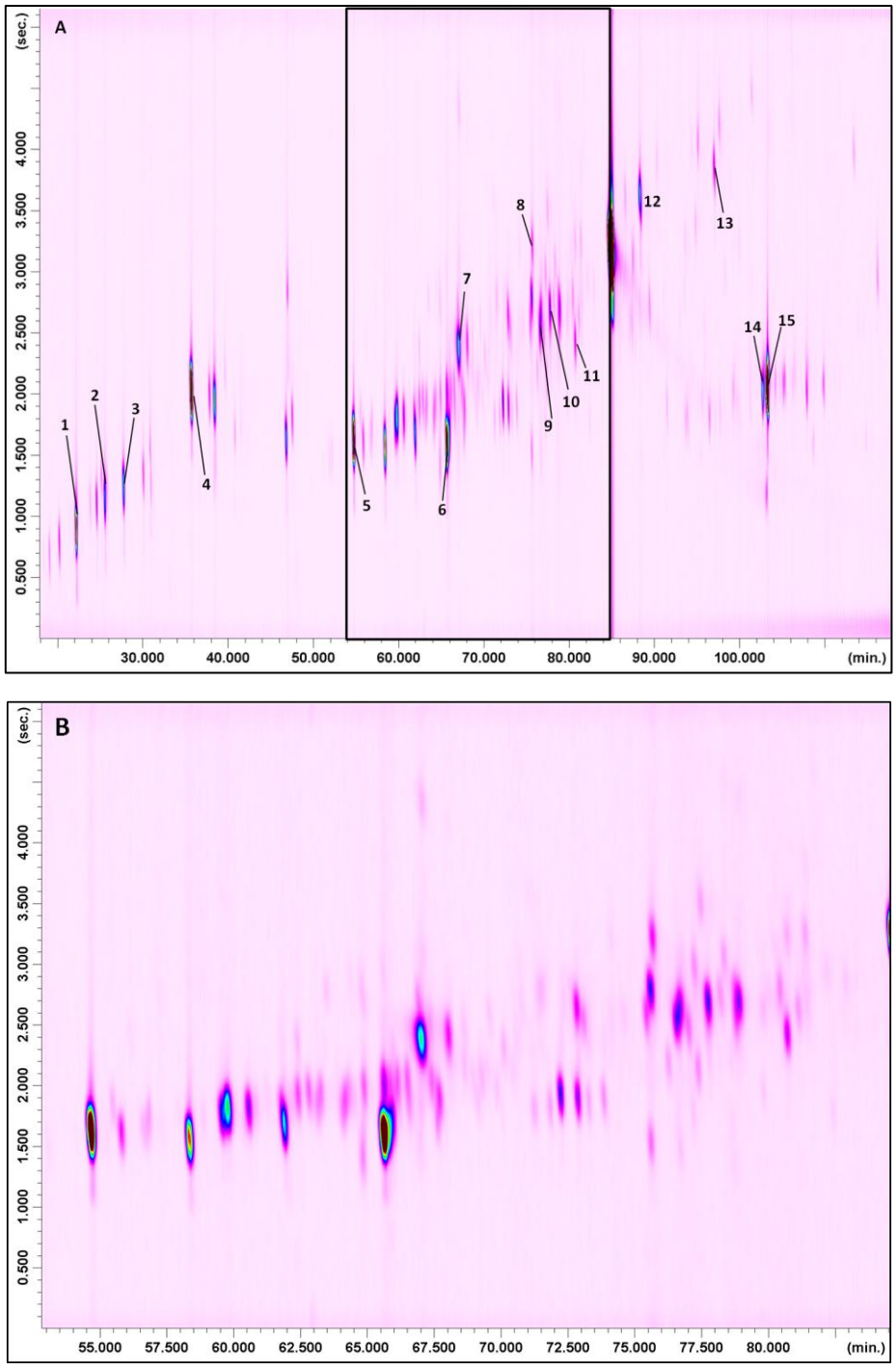

Figure 8.3.2. (A) 2D chromatogram relative to the analysis of Artemisia essential oil. ***(B)*** The central zone confined by a rectangle in Fig. 8.3.2 A.

As previously emphasized, the main objective of the present investigation was to demonstrate that it is possible to perform FM, in a satisfactory manner, using a ^{2}D gas flow of ≈ 4 mL min^{-1}. Such an aim was made possible by using the aforedescribed asymmetrical configuration. Another highly important issue is represented by sensitivity, in relation to straightforward GC-qMS. Such a comparison was carried out by connecting the primary column directly to the mass spectrometer. Two GC-qMS essential oil applications were carried out, namely at 0.4 and 0.65 mL min^{-1}. The former gas flow was selected because it was practically equivalent to that generated in the first GC×GC dimension in the essential oil experiment; the other constant He flow was used because it is a value commonly used for a 30 m × 0.25 mm ID column (≈ 30 cm s^{-1}).

The MS spectral acquisition frequency was adjusted (1 Hz), so that the attained number of data-points-per-peak was similar in both GC and GC×GC experiments. Signal-to-noise ratios (*s/n*) were calculated (n = 2) by considering the width of the noise at the side of each peak and the signal intensity, for the 15 compounds numbered in Figure 8.3.2 A. GC×GC *s/n* values refer to the most intense modulated peak (Table 8.3.1).

Table 8.3.1. Tentative peak identification for the compounds indicated in Figure 3A; *s/n* values in the GC×GC and GC (0.4 and 0.65 mL min^{-1}) experiments; ratios of GC×GC and GC (at both 0.4 and 0.65 mL min^{-1}) *s/n* values.

n°	Compound	*s/n* GC×GC	*s/n* GC 0.4	*s/n* GC 0.65	*s/n* GC×GC/GC 0.4	*s/n* GC×GC/GC 0.65
1	Myrcene	310	103	134	3	2.3
2	Limonene	108	33	46	3.2	2.3
3	γ-terpinene	120	40	58	3	2.1
4	Camphor	806	169	245	4.8	3.3
5	Lavandulyl isovalerate	548	115	160	4.8	3.4
6	Lavandulyl<2-methyl> butyrate	547	104	144	5.3	3.8
7	α-dehydro-himachalene	92	28	39	3.3	2.4
8	γ-dehydro-himachalene	31	28	38	1.1	0.8
9	Junenol	52	10	12	5.3	4.2
10	Spirambrene	55	13	18	4.3	3
11	Epi-β-bisabolol	20	13	17	1.5	1.2
12	Guaiazulene	113	33	47	3.4	2.4
13	Callitrisin	31	11	16	2.7	2
14	12-ol-γ-curcumene	13	25	37	5.2	3.4
15	Z-lanceol acetate	1034	220	299	4.7	3.5

The selected analytes were characterized by both different chemistries (tentative MS database identification was performed) and ^{2}D retention times. Considering the GC-qMS application, performed at 0.4 mL min^{-1}, FM GC×GC-qMS *s/n* values were always higher (increases were in the 1.1-5.3 range). On average, the *s/n* GC×GC-qMS/GC-qMS (0.4 mL min^{-1}) enhancement was calculated to be 3.7. Proceeding onto the GC-qMS application, carried out at 0.65 mL min^{-1}, as expected the general *s/n* GC×GC-qMS/GC-qMS enhancement was more limited (Table 8.3.1). FM GC×GC-qMS *s/n* values were always higher (increases were in the 1.2-3.8 range) except for peak 8 (γ-dehydro-himachalene). On average, the *s/n* GC×GC-qMS/GC-qMS (0.65 mL min^{-1}) increase was found to be 2.5.

Even though signal intensity in GC×GC is related to a series of variables (i.e., modulation phase and ratio, ^{2}D column dimensions, chemistry of the ^{2}D stationary phase, ^{2}D gas flow), the values herein provided do give an indication on sensitivity enhancement, and are certainly to be considered as a positive aspect (even though far from the sensitivity increases attained in cryogenic GC×GC).

Conclusions

The herein described research represents further progress with respect to recent FM research [5]. In fact, the possibility to perform satisfactory flow modulation at gas flows of ≈ 4 mL min^{-1} does widen the field to practically any commercial MS device.

Further research, probably, will not be devoted to a further reduction of gas flows (^{2}D separations would be too slow). The main final objective is the proposal of an FM GC×GC-MS system, capable of providing the best separation performance, under the conditions herein reported of ^{1}D and ^{2}D gas flows.

References

[1] J.V. Seeley, N.J. Micyus, J.D. McCurry, S.K. Seeley, Am. Lab. 38 (2006) 24.

[2] M. Poliak, M. Kochman, A. Amirav, J. Chromatogr. A 1186 (2008) 189.

[3] P.Q. Tranchida, F.A. Franchina, P. Dugo, L. Mondello, J. Chromatogr. A 1255 (2012) 171.

[4] J.V. Seeley, S.K. Seeley, E.K. Libby, Z.S. Breitbach, D.W. Armstrong, Anal. Bioanal. Chem. 390 (2008) 323.

[5] P.Q. Tranchida, F.A. Franchina, P. Dugo, L. Mondello, J. Chromatogr. A 1359 (2014) 271.

[6] P.McA. Harvey, R.A. Shellie, P.R. Haddad, J. Chromatogr. Sci. 48 (2010) 245.

Page intentionally left blank

Chapter 9

Research in the field of sensomic analysis

9.1 Aroma-active compounds in the traditional Armenian soup seasoning herb Heracleum transcaucasicum

The volatile fraction isolated from dried shoots of *Heracleum transcaucasicum* Manden (syn. *Heracleum pastinacifolium* C. Koch), by solvent extraction and solvent-assisted flavour evaporation (SAFE), was screened for odour-active compounds by application of an aroma extract dilution analysis (AEDA). In the flavour dilution (FD) factor range of 1 to 2048, 51 odorants were detected, among which soup seasoning-like smelling sotolon (3-hydroxy-4,5-dimethyl-2(5*H*)-furanone) showed the highest FD factor (2048). Its characteristic odour, which closely matched the overall aroma of the dried shoots, in combination with its high FD factor and the absence of any further odour-active compound exhibiting a similar smell, suggested that sotolon constitutes the character impact compound in the aroma of *H. transcaucasicum*. Stable isotope dilution quantitation using ($^{13}C_2$)sotolon as internal standard revealed a concentration of ~ 12 mg/kg sotolon in dried *H. transcaucasicum* shoots, which is several orders of magnitude higher than its odour detection threshold. Further quantitation experiments revealed that during traditional culinary use, sotolon is transferred from *H. transcaucasicum* shoots in aroma-active amounts to Armenian karshm soup.

9.2 Introduction

The Transcaucasian hogweed *Heracleum transcaucasicum* Manden, also known as *Heracleum pastinacifolium* C. Koch is a perennial herb in the Apiaceae family. The species was first described from Armenia, but is also native to Azerbaijan, Iran, and the eastern Anatolia region of Turkey [1-6]. *H. transcaucasicum* plants may reach a height of 25–100 cm. Each spring, from the subterranean parts a striated, hollow stem grows with pinnate, hairy and serrated leaves, divided into 3–4 lobed segments. Later, white flowers with 5 petals develop, arranged in umbels with 3–5 rays. Fruits are two-parted schizocarps, 8–10 mm in length and 5–6 mm in diameter.

Like other *Heracleum* species, *H. transcaucasicum* may contain potentially toxic furocoumarins [3,4]. Nevertheless, it has been locally used in folk medicine and also as a culinary herb. Traditionally, *H. transcaucasicum* has been applied to treat various kinds of gastrointestinal problems. It was reported to possess antifungal properties [6], and its essential oil showed moderate antitumoral properties [2]. In the region around the Armenian city of Vayk (Vayots Dzor province), *H. transcaucasicum* is used to flavour karshm soup, a unique speciality served as traditional starter. Young *H. transcaucasicum* shoots are collected in the meadows of the Lesser Caucasus Mountains in late spring before flowering and dried in bunches (Figure 9.1).

Figure 9.1 Dried *H. transcaucasicum* shoots.

For karshm soup, the dried shoots are cooked in an excess of water to remove the strong bitterness. After cooling, the cooking water is discarded and the softened plant material is crushed into small pieces. Water, lentils, crushed walnuts, and some wheat flour are added and the mixture is cooked. Finally, the soup is seasoned to taste with salt and red pepper powder and served with a topping of freshly chopped garlic and some traditional Armenian flatbread (lavash).

Fresh and dried *H. transcaucasicum* shoots exhibit an intense odour that is reminiscent of lovage leaves, fenugreek seeds, or liquid protein hydrolysate based seasonings. The molecular background of this characteristic odour in *H. transcaucasicum* has yet been unclear. Phytochemical research conducted on *H. transcaucasicum* constituents so far was mainly focused on furocoumarins in roots and fruits [3,4], while only two studies on volatiles present in the aerial parts have been published so far [2,5]. In both cases, not the genuine plant constituents were analysed, but the constituents of a hydrodistilled oil. Firuzi *et al.* [2], reported elemicin as dominating compound in the essential oil, whereas

Torbati *et al.* found myristicin with the highest percentage [5]. However, no attempt was made to clarify the odour contribution of the individual constituents and, in particular, none of the compounds reported could plausibly explain the characteristic soup seasoning-like odour.

To fill such a gap, the primary aim of the present study was to apply an aroma extract dilution analysis [7], to the volatiles gently isolated from dried shoots of *H. transcaucasicum* by solvent extraction and solvent-assisted flavour evaporation [8], and assign the structures of the detected odorants.

9.3.0 Experimental

9.3.1 Plant material and chemicals

Shoots of *H. transcaucasicum* were collected in the Lesser Caucasus Mountains near Vayk, in May 2016, tied into bunches, and dried at ambient temperature. The dried material was shipped to Germany by air. Dry matter content was 89% as determined by means of an MA35 Moisture Analyzer (Sartorius, Göttingen, Germany).

Reference odorants 1−6, 9, 11−22, 24, 25, 27−33, 35−42, 44, 45, 48, 49, and 51 were purchased from Sigma-Aldrich (Taufkirchen, Germany). Odorant 7 was from Alfa Aesar (Karlsruhe, Germany), 26 from Acros Organics (Schwerte, Germany), 43 and 50 from Merck (Darmstadt, Germany), and 46 and 47 from Lancaster (Mühlheim am Main, Germany). The following reference odorants were synthesised according to literature procedures: 8 [9], 10 [10], 23 [11], 34 [12]. For identification refer to Table 9.0.

($^{13}C_2$)sotolon was synthesized as detailed in [13]. *n*-Alkanes, C_6−C_{28}, were obtained from Sigma-Aldrich. Dichloromethane, diethyl ether, and pentane were freshly distilled before use. Purified silica gel was prepared from silica gel 60 (0.040−0.063 mm) purchased from VWR (Darmstadt, Germany) as detailed recently [14].

9.3.2 Isolation of volatiles

Shoots of *H. transcaucasicum* were ground at the temperature of liquid nitrogen, by means of a Cryomill (Retsch, Haan, Germany). The powder (5 g) and anhydrous sodium sulfate (5 g) were added to dichloromethane (50 mL) and stirred for 3 h at ambient temperature. After filtration, non-volatiles were removed by SAFE at 40°C and ~10 mPa. The distillate was concentrated to a final volume of 1 mL, first using a Vigreux column (50 × 1 cm) and subsequently a Bemelmans microdistillation device [15].

9.3.3 Gas chromatography–olfactometry - GC–O

A Trace GC Ultra gas chromatograph (Thermo Scientific, Dreieich, Germany) was equipped with a cold-on-column injector, an FID, a tailor-made sniffing port [10], and one of the following columns: DB-FFAP, 30 m × 0.32 mm ID, 0.25 µm film thickness or DB-5, 30 m × 0.32 mm ID, 0.25 µm film thickness (both Agilent Technologies, Waldbronn, Germany). A deactivated fused silica capillary, 5 m × 0.32 mm ID, was used as pre-column. The carrier gas was helium at a constant flow of 2 mL/min. The oven start temperature was 40 °C (2 min), while the following gradient was 6 °C/min; final temperatures were 230 °C (FFAP) and 240 °C (DB-5), while the final holding time was 5 min. The column effluent was split 1:1 using a deactivated Y-shaped glass device and two deactivated fused silica capillaries (50 cm × 0.25 mm ID) connecting the splitter outlets to the FID and the sniffing port, respectively. The sniffing port, was heated to 230°C and the FID was operated at 250°C. During GC–O analysis, the panellists sniffed the column effluent, marked the retention time of each odorant detected in the FID chromatogram and added an odour description. GC–O results of three trained panellists were combined. Linear retention indices (RI) of the odour-active compounds were calculated from their retention times and the retention times of adjacent *n*-alkanes by linear interpolation.

9.3.4 AEDA

The *H. transcaucasicum* volatile concentrate (1 mL) was successively diluted 1:2 with dichloromethane and each diluted sample representing dilutions of 1:2, 1:4, 1:8, 1:16, etc. of the initial solution was analysed by GC–O (FFAP column). For each aroma-active compound, the highest dilution in which the respective odorant was detected by any of three trained panellists defined its FD factor.

9.3.5 Structure assignment of odorants

Preliminary structure assignment was achieved by comparing RI and odour quality of the *H. transcaucasicum* odorants as obtained from GC–O analysis to compiled data of reference odorants. Assignments were then confirmed by analysing the respective reference compounds by GC–O and gas chromatography–mass spectrometry (GC–MS) in parallel, *i.e.*, same instrument and same day, to the *H. transcaucasicum* volatiles isolate. This was performed using two columns of different polarity (DB-5 and FFAP).

To avoid coelution problems, the *H. transcaucasicum* volatiles isolate was fractionated before GC–MS analysis. For such a purpose, a SAFE distillate obtained from dried *H. transcaucasicum* shoots, as detailed above, was extracted with aqueous sodium carbonate (0.5 mol/L; 1 × 100 mL, 2 × 50 mL). The combined aqueous extracts were washed with dichloromethane (50 mL), acidified (pH 2) with hydrochloric acid (16%), and re-extracted with dichloromethane (1 × 100 mL, 2 × 50 mL). The organic re-extracts were combined, dried over anhydrous sodium sulfate and concentrated (0.5 mL) to obtain the acidic volatiles fraction (AF). The acid-free SAFE distillate representing the neutral and basic volatiles fraction (NBF) was dried over anhydrous sodium sulfate, concentrated (1 mL), and further fractionated by column chromatography (1 cm ID) using purified silica gel (8 g) and the following pentane/diethyl ether mixtures (v+v; 50 mL each) as eluents: 100+0, 90+10, 70+30, 50+50, and 0+100. The eluate was collected in five 50 mL portions and each portion was concentrated (0.5 mL) to obtain fractions NBF1 to NBF5. Fractions AF and NBF1 to NBF5 were then analysed by GC–O, to localise the odorants that had been detected during AEDA, before they were subjected to GC–MS analysis.

Mass spectra in the EI mode were recorded from *m/z* 35–300 at 70 eV using either a sector field system consisting of a HP 5890 gas chromatograph (Hewlett-Packard, Heilbronn, Germany) connected to a MAT 95 S mass spectrometer (Finnigan, Bremen, Germany) or a Pegasus III GC×GC–TOFMS system (Leco, Mönchengladbach, Germany) detailed recently [14]. Mass spectra in the CI mode were obtained using the MAT 95 S system at 115 eV and isobutane as the reagent gas.

9.3.6 Quantitation of sotolon

The volatiles from 0.5 g powdered *H. transacaucasicum* shoots were basically isolated as detailed before, but at the beginning of the 3-h extraction procedure, ($^{13}C_2$)sotolon (2 µg) in dichloromethane (1 mL) was added. The SAFE distillate was fractionated as described above and the AF containing the sotolon isopologues was concentrated to 5 mL.

An aliquot of the concentrate (1 µL) was analysed by heart-cut two-dimensional gas chromatography–mass spectrometry (GC–GC–MS). The system consisted of a CombiPal autosampler (CTC Analytics, Zwingen, Switzerland), a Trace Ultra GC (Thermo), a GC 3800 gas chromatograph (Varian, Darmstadt, Germany) and a Saturn 2200 ion trap mass spectrometer (Varian). The Trace Ultra GC was equipped with a cold-on-column injector, a

30 m × 0.32 mm ID, 0.25 μm film thickness DB-FFAP column, a moving column stream switching (MCSS) device, an FID, and a tailor-made sniffing port [10]. The FID and the sniffing port were connected to the monitor outlet of the MCSS device via uncoated fused silica capillaries (0.25 mm ID) and a Y-shaped glass splitter. The transfer outlet of the MCSS device was connected by an uncoated fused silica capillary (0.32 mm ID) *via* a heating hose (250°C) to a 30 m × 0.25 mm ID, 0.25 μm film DB-1701 column (Agilent), in the GC 3800 gas chromatograph. The end of this column was connected to the inlet of the mass spectrometer.

The temperature program for the oven in first dimension was 40°C (2 min), then 6°C/min to 230°C. At the elution time of sotolon (25.8 min), the effluent of the first column was conveyed during 1.2 min by the time programmed MCSS device to the second oven. Transferred volatiles were refocused inside the second oven by a jet of cold nitrogen gas directed at a point close to the end of the uncoated capillary. After a waiting time of 1.5 min, the cooling gas was turned off and the second oven temperature program was started. The previously trapped volatiles were re-chromatographed in the second dimension using a start temperature of 40°C (2 min), a gradient of 6°C/min, and an end temperature of 240°C. The mass spectrometer was run in the CI mode with methanol as reagent gas and recorded a mass range of *m*/*z* 60 to 250.

The area counts corresponding to the isotopically unmodified analyte and the internal standard ($^{13}C_2$)sotolon were obtained by integration of the sotolon peak in the extracted ion chromatograms using the molecular ions *m*/*z* 129 and 131, respectively. Sotolon concentration was calculated from these area counts, the amount of *H. transcaucasicum* shoots used, the amount of standard added, and a calibration line equation previously determined from the analysis of defined sotolon/($^{13}C_2$)sotolon mixtures using the approach detailed recently [16].

9.3.7 Model experiments

The following traditional recipe for karshm soup was used as base for the model experiments: dried shoots of *H. transcaucasicum* (100 g) are gently cooked in tap water (4 L) for 30 min. After cooling, the water is discarded and the cooked shoots are crushed into small pieces. A fresh portion of tap water (4 L), crushed walnuts (175 g), lentils (150 g), and wheat flour (80 g) are added and the mixture is cooked for 90 min.

According to the proportions of the ingredients used in the above recipe, model experiments were conducted with 0.5 g of dried *H. transcaucasicum* shoots and

20 mL of water. The mixture was heated to 100°C in a thick-walled borosilicate glass tube with closed lid and PTFE seal for 30 min. After cooling down, the cooked shoots were separated from the cooking water. The shoots were homogenized with a glass rod. Dichloromethane (50 mL), anhydrous sodium sulfate (5 g), and ($^{13}C_2$)sotolon (2 µg) were added, the mixture was stirred for 3 h and then filtered. The cooking water was transferred to a separatory funnel, dichloromethane (50 mL) and ($^{13}C_2$)sotolon (2 µg) were added and the mixture was vigorously shaken for 10 min. The organic phase was separated and the water phase was extracted a second time with dichloromethane (50 mL). The combined organic phases were dried over anhydrous sodium sulfate. In a second experiment, the separated pre-cooked shoots were crushed with a mortar and pestle and further cooked in a fresh portion of water (20 mL) for 90 min. The double-cooked shoots and the second cooking water were extracted with dichloromethane as detailed above. Further workup of the organic phases obtained from the cooked shoots and the cooking water samples, including SAFE, isolation of AF, and concentration, as well as GC–GC–MS measurements were done as detailed before.

9.4.0 Results and discussion

9.4.1 Odour-active compounds in H. transcaucasicum shoots

The volatiles of young, dried *H. transcaucasicum* shoots were isolated by solvent extraction and SAFE distillation [8], and subjected to odorant screening by AEDA [7]. The results revealed 51 odorants in the FD factor range of 1 to 2048 (Table 9.0). The highest FD factor (2048) was found for sotolon (42), a compound exhibiting the same soup seasoning-like odour that dominated the overall sensory impression of the *H. transcaucasicum* shoots. High FD factors were also determined for vanilla-like smelling vanillin (50, FD 512), beeswax-like smelling 3-phenylpropanoic acid (51, FD 512), violet-like smelling *β*-ionone (31, FD 256), caramel-like smelling 4-hydroxy-2,5-dimethyl-3(2*H*)-furanone (36, FD 256), nutmeg-like smelling myristicin (45, FD 256), and beeswax-like smelling phenylacetic acid (49, FD 256) (Figure 9.1). Further odour-active compounds included acetic acid (13, FD 64), 2,3-diethyl-5-methylpyrazine (14, FD 64), 2,3-butanedione (1, FD 32), 2-acetyl-1-pyrroline (8, FD 32), 2-methoxy-3-isopropylpyrazine (12, FD 32), methyl 3-(methylthio)propanoate (15, FD 32), citronellol (25, FD 32), and dodecanoic acid (48, FD 32).

Table 9.0. Aroma-active compounds in the SAFE distillate obtained from dried *H. transcaucasicum* shoots.

n°	Odorant	Odour	RI		FD factor
			FFAP	DB-5	
1	2,3-Butanedione	Buttery	1000	593	32
2	Hexanal	Green, grassy	1078	800	2
3	1-Butanol	Malty, solvent-like	1142	675	2
4	Heptanal	Citrusy, fatty	1193	904	1
5	3-Hydroxy-2-butanone	Buttery	1279	800	2
6	Octanal	Citrusy, soapy	1280	1003	16
7	1-Octen-3-one	Mushroom-like	1293	979	8
8	2-Acetyl-1-pyrroline	Popcorn-like	1332	922	32
9	1-Hexanol	Green, grassy	1350	872	1
10	(*Z*)-1,5-Octadien-3-one	geranium leaf-like	1376	983	16
11	Nonanal	Citrusy, soapy	1389	1103	16
12	2-Methoxy-3-isopropylpyrazine	Bell pepper-like	1427	1094	32
13	Acetic acid	Vinegar-like	1443	612	64
14	2,3-Diethyl-5-methylpyrazine	Earthy	1480	1158	64
15	Methyl 3-(methylthio)propanoate	Cabbage-like	1515	1034	32
16	(*E*)-2-Nonenal	Fatty	1533	1160	2
17	Linalool	Citrusy, flowery	1535	1100	4
18	Propanoic acid	Sour, sweaty	1538	836	2
19	Methylpropanoic acid	Sweaty, cheesy	1559	789	2
20	Butanoic acid	Sweaty, cheesy	1619	821	8
21	2- and 3-Methylbutanoic acid	Sweaty, cheesy	1660	872	8
22	Estragol	Aniseed-like	1666	1202	1
23	3-Methyl-2,4-nonanedione	Hay-like	1708	1251	16
24	Pentanoic acid	Sweaty, cheesy	1726	914	4
25	Citronellol	Flowery, rose-like	1757	1230	32
26	*trans*-Anethol	Aniseed-like	1803	1283	16
27	Geraniol	Flowery, rose-like	1823	1256	2
28	Hexanoic acid	Sweaty, cheesy	1836	1018	4
29	2-Phenylethanol	Honey-like	1888	1116	8
30	γ-Octalactone	Coconut-like	1906	1263	2
31	β-Ionone	Flowery, violet-like	1928	1492	256
32	Heptanoic acid	Sweaty, cheesy	1933	1083	2
33	Maltol	Caramel-like	1974	1110	1
34	*trans*-4,5-Epoxy-(*E*)-2-decenal	Metallic	2003	1382	4
35	γ-Nonalactone	Coconut-like	2029	1360	16
36	4-Hydroxy-2,5-dimethyl-3(2*H*)-furanone	Caramel-like	2030	1071	256
37	Octanoic acid	Musty, cheesy	2060	1279	4
38	γ-Decalactone	Peach-like	2140	1471	8
39	Eugenol	Clove-like	2164	1359	16
40	3-Ethylphenol	Leathery	2180	1169	8
41	Nonanoic acid	Musty, soapy	2185	1280	2
42	Sotolon	Soup seasoning-like	2190	1108	2048
43	Thymol	Thyme-like	2190	1294	8
44	2-Aminoacetophenone	Foxy	2210	1300	1
45	Myristicin	Nutmeg-like	2259	1531	256
46	Decanoic acid	Musty, soapy	2266	1373	2
47	4-Vinylphenol	Phenolic, earthy	2396	1237	4
48	Dodecanoic acid	Waxy, soapy	2455	2169	32
49	Phenylacetic acid	Beeswax-like	2544	1261	256
50	Vanillin	Vanilla-like	2569	1406	512
51	3-Phenylpropanoic acid	Beeswax-like	2801	1435	512

The characteristic soup seasoning-like odour in combination with its high FD factor and the absence of any further odour-active compound exhibiting this kind of odour quality suggested that sotolon constitutes the character impact compound in the aroma of *H. transcaucasicum* shoots.

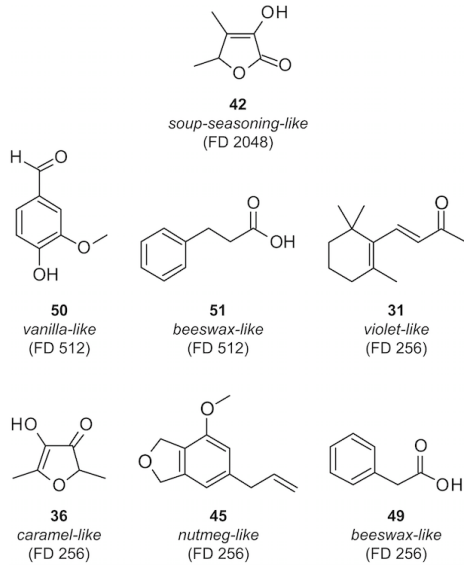

Figure 9.2. Most potent odorants (FD factor ≥ 256) in the SAFE distillate obtained from dried *H. transcaucasicum* shoots.

The compound was already known as a synthetic odorant [17], when it was first reported in food, namely in aged sake, by Takahashi *et al.* in 1976 [18]. Shortly after, Tokitomo *et al.* reported its presence in raw cane sugar and suggested its meanwhile common trivial name [19], which was derived from the Japanese word for raw cane sugar, soto. Sotolon is the aroma impact compound of fenugreek seeds [20,21], lovage leaves [22,13], and a key aroma compound in sherry [23], port wine [24], and buckwheat honey [25]. Sotolon furthermore contributes to the aroma of many other kinds of foods such as coffee [26], green tea [27], blackberries [28], durian [29], rice [30], soy sauce [31], miso [32], and gravy [33], and has been classified a generalist among the key food odorants in the human diet [34].

To support the suggested role of sotolon as character impact compound in *H. transcaucasicum* shoots, the compound was quantified by a stable isotope dilution assay (SIDA) using the isotopologue ($^{13}C_2$)sotolon as internal standard. This approach resulted in a concentration of 11.5±0.6 mg/Kg. Considering the odour threshold of sotolon, which is as low as 1.7 µg/L in water [35], a concentration of 11.5 mg/kg is able to sufficiently explain the dominating role

of sotolon for the overall aroma impression of the *H. transcaucasicum* shoots. Sotolon concentrations in the same order of magnitude (3.3–25 mg/Kg) have been reported in fenugreek seeds [21], whereas the sotolon concentrations reported in dried lovage [13], and soy sauce [31], namely ~0.5–1 mg/Kg, were lower (Table 9.1). In the future, *H. transcaucasicum* might therefore be an interesting source of natural sotolon as food flavouring.

Table 9.1. Concentration of sotolon in dried *H. transcaucasicum* shoots in comparison to other sotolon-rich herbs, spices, and condiments.

Herb/spice/condiment	Sotolon (mg/Kg)	Data source
Dried *H. transcaucasicum* shoots	11.5[a]	this study
Dried lovage (*Levisticum officinale* W. D. J. Koch) leaves	0.84	[13]
Fenugreek (*Trigonella foenum-graecum* L.) seeds	3.3–25	[21]
Soy sauce	0.47	[13]
Soy sauce	1.1	[31]

[a] Mean of sextuplicate analysis, standard deviation was 0.6 (5%)

9.4.2 Behaviour of sotolon during traditional culinary use of H. transcaucasicum

As detailed in the Introduction, the preparation of karshm soup includes double cooking of *H. transcaucasicum* shoots. To clarify the fate of sotolon during this traditional use, the process was simulated in model experiments. The ratio of *H. transcaucasicum* shoots to water and the cooking times were adopted from the traditional recipe, but absolute amounts were reduced and residual ingredients (lentils, walnuts, etc.) were omitted. *H. transcaucasicum* shoots were first cooked for 30 min to simulate the traditional de-bittering. Cooked shoots and cooking water were isolated and separately analysed for sotolon by SIDA. In a second experiment, the de-bittered *H. transcaucasicum* shoots were crushed, suspended in a new portion of water, and once again cooked, this time for 90 min. Again, cooked plant material and cooking water were separately used for sotolon quantitation by SIDA.

Results (Table 9.2) showed that during the first cooking, the total amount of sotolon increased to 140%. An increase of sotolon had also been observed during boiling of fenugreek and lovage [13].

Table 9.2. Changes in sotolon during simulated preparation of karshm soup.

Material	Sotolon (µg)	Recovery[a] (%)
Dried *H. transcaucasicum* shoots (0.5 g)	5.74±0.28[b]	100
H. transcaucasicum shoots after first cooking (de-bittering)	2.10±0.05[c]	37

Water phase (20 mL) after first cooking	5.89±1.08[c]	103
H. transcaucasicum shoots after crushing and second cooking (simulated karshm soup preparation)	0.58±0.03[c]	10
Water phase (20 mL) after second cooking (karshm soup model)	1.46±0.13[c]	25

[a]Calculated from the amount of sotolon in the respective material divided by the amount of sotolon in the initial dried *H. transcaucasicum* shoots

[b]Mean ± standard deviation of sextuplicate analysis

[c]Mean ± standard deviation of duplicate model experiments

After the first cooking, ~ ¾ of sotolon was lost with the cooking water, whereas ¼, corresponding to 37% of the initial amount in the dried material remained in the shoots. After crushing and second cooking, the total amount of sotolon was unchanged (0.58 µg + 1.46 µg = 2.04 µg ≈ 2.10 µg), indicating that any precursors had already been used up during the first cooking process. Again, the major part of sotolon (1.46 µg; ~70 %) was transferred from the shoots into the aqueous phase. This resulted in an overall transfer rate from the dried shoots to the karshm soup model of 25%. The sotolon concentration in the final soup model was 1.46 µg/20 mL = 73 µg/L, thus more than 40 times above its odour detection threshold value in water (1.7 µg/L), indicating a vital contribution of sotolon to the flavour of karshm soup.

Conclusions

In summary, the results suggest that soup seasoning-like smelling sotolon is the character impact compound of dried *H. transcaucasicum* shoots. During traditional culinary use, sotolon is transferred from *H. transcaucasicum* shoots in aroma-active amounts to Armenian karshm soup.

References

[1] G.F. Akhundov (1954-2001) *Heracleum* L. In: Takhtajan AL (ed), vol 1-10. Armenian Academy of Sciences, Yerevan, pp 411−417 (in Russian).

[2] O. Firuzi, M. Asadollahi, M. Gholami, K. Javidnia, Food. Chem. 122 (2010) 117. doi:10.1016/j.foodchem.2010.02.026.

[3] G.K. Kasumova, S.V. Serkerov, Chem. Nat. Compd. 47 (2011) 358.

[4] F.K. Kurbanova, S. V. Serkerov, Chem. Nat. Compd. 48 (2012) 374.

[5] M. Torbati, H. Nazemiyeh, F. Lotfipour, S. Asnaashari, M. Nemati, F. Fathiazad, Adv. Pharm. Bull. 3 (2013) 415.

[6] M. Razzaghi-Abyaneh, M. Shams-Ghahfarokhi, M. Rai (2013) In: Razzaghi-Abyaneh M, Rai M (eds) Antifungal metabolites from plants. Springer, Berlin, pp 27.

[7] P. Schieberle, W. Grosch, Z. Lebensm. Unters. Forsch. 185 (1987) 111.

[8] W. Engel, W. Bahr, P. Schieberle, Eur. Food Res. Technol. 209 (1999) 237.

[9] R. G. Buttery, L. C. Ling, B. O. Juliano, J. G. Turnbaugh, J. Agr. Food Chem. 31 (1983) 823.

[10] M. Steinhaus, D. Sinuco, J. Polster, C. Osorio, P. Schieberle, J. Agric. Food Chem. 56 (2008) 4120.

[11] H. Guth, W. Grosch, Fett. Wiss. Technol. 91 (1989) 225.

[12] P. Schieberle, W. Grosch, Z. Lebensm. Unters. Forsch. 192 (1991) 130.

[13] I. Blank, P. Schieberle, W. Grosc. In: Schreier P, Winterhalter P (eds) Allured Publishing, Carol Stream, IL, pp 103.

[14] A. C. Lindhorst, M. Steinhaus, Eur. Food. Res. Technol. 242 (2016) 967.

[15] J. M. H. Bemelmans (1979), In: Land GG, Nursten HE (eds). Applied Science, London, pp 79.

[16] J-X. Li, P. Schieberle, M. Steinhaus, Eur. Food Res. Technol. (2016).

[17] H. Sulser, W. Buchi, M. Habegger, Z. Lebensm. Unters. Forsch. 418 (1972) 215.

[18] K. Takahashi, M. Tadenuma, S. Sato, Agr. Biol. Chem. Tokyo 40 (1976) 325.

[19] Y. Tokitomo, A. Kobayashi, T. Yamanishi, S. Muraki, Proc. Jpn. Acad. Ser. B 56 (1980) 457.

[20] P. Girardon, Y. Sauvaire, J. C. Baccou, J. M. Bessiere, Lebensm. Wiss. Technol. 19 (1986) 44.

[21] I. Blank, J. M. Lin, S. Devaud, R. Fumeaux, L. B. Fay, Acs. Sym. Ser. 660 (1997) 12.

[22] I. Blank, P. Schieberle, Flavour. Fragrance J. 8 (1993) 191.

[23] B. Martin, P. X. Etievant, J. L. Lequere, P. Schlich, J. Agr. Food Chem. 40 (1992) 475.

[24] A. C. S. Ferreira, J. C. Barbe, A. Bertrand, J. Agr. Food Chem. 51 (2003) 4356.

[25] Q. X. Zhou, C. L. Wintersteen, K. R. Cadwallader KR, J. Agr. Food Chem. 50 (2002) 2016.

[26] P. Semmelroch, G. Laskawy, I. Blank, W. Grosch , Flavour Fragrance J. 10 (1995) 1.

[27] R. Baba, K. Kumazaw, J. Agr. Food Chem. 62 (2014) 8308.

[28] K. Klesk, M. Qian, J. Agr. Food Chem. 51 (2003) 3436.

[29] J-X. Li, P. Schieberle, M. Steinhaus, J. Agr. Food Chem. 60 (2012) 11253.

[30] M. Jezussek, B. O. Juliano, P. Schieberle, J. Agr. Food Chem. 50 (2002) 1101.

[31] P. Steinhaus, P. Schieberle,. J. Agric. Food Chem. 55 (2007) 6262.

[32] K. Kumazawa, S. Kaneko, O. Nishimura, J. Agric. Food Chem. 61 (2013) 11968.

[33] M. Christlbauer, P. Schieberle, J. Agric. Food Chem. 59 (2011) 13122.

[34] A. Dunkel, M. Steinhaus, M. Kotthoff, B. Nowak, D. Krautwurst, P. Schieberle, T. Hofmann, Angew. Chem. Int. Ed. 53 (2014) 7124.

[35] German Research Center for Food Chemistry. In-house database of aroma compound thresholds. Determined according to American Society of Testing and Materials (2005) Standard E679-04. Standard practice for determination of odor and taste thresholds by a forced-choice ascending concentration series method of limits. In: ASTM Book of Standards, vol 15.08. American Society of Testing and Materials, West Conshohocken, PA, pp 38–44.

List of pubblications:

- "*The penetration of green sample-preparation techniques in comprehensive two-dimensional gas chromatography*"
Peter Q. Tranchida, **Mariarosa Maimone**, Giorgia Purcaro, Paola Dugo, Luigi Mondello
Trends in Analytical Chemistry, 71, (2015) 74–84.

- "*Impact of comprehensive two-dimensional gas chromatography with mass spectrometry on food analysis*"
Peter Q. Tranchida, Giorgia Purcaro, **Mariarosa Maimone** , Luigi Mondello
Journal of Separation Science, 39, (2016) 149-161.

- "*Evaluation of a Novel Helium Ionization Detector within the Context of (Low-)flow Modulation Comprehensive Two-dimensional Gas Chromatography*"
Flavio Antonio Franchina**, Mariarosa Maimone**, Danilo Sciarrone, Giorgia Purcaro, Peter Quinto Tranchida, Luigi Mondello.
Journal of Chromatography A, 1402, (2015) 102–109.

- "*Performance Evaluation of a Versatile Multidimensional Chromatographic Preparative System*"
Sebastiano Pantò, Danilo Sciarrone, **Mariarosa Maimone**, Carla Ragonese, Salvatore Giofrè, Paola Donato, Sara Farnetti, Luigi Mondello
Journal of Chromatography A, 1417, (2015) 96-103.

- "*Four-stage (low-)flow modulation comprehensive gas chromatography-quadrupole mass spectrometry for the determination of recently-highlighted cosmetic allergens*"
Peter Q. Tranchida, **Mariarosa Maimone**, Flavio A. Franchina, Thiago Rodrigues Bjerk, Giorgia Purcaro, Luigi Mondello
Journal of Chromatography A, 1439, (2016) , 144–151.

- "*Flow modulation comprehensive two-dimensional gas chromatography-mass spectrometry using ≈ 4 ml min^{-1} gas flows*"
Flavio A. Franchina, **Mariarosa Maimone**, Peter Q. Tranchida, Luigi Mondello
Journal of Chromatography A,1441, (2016) 134-139.

- "*Recent evolution of flow-modulation comprehensive gas chromatography within the context of mass spectrometry hyphenation*"

Flavio A. Franchina, Giorgia Purcaro, **Mariarosa Maimone**, Peter Q. Tranchida, Luigi Mondello
Chemistry Today 34, (2016), 6-10.

- "*Odour Active Compounds in the Traditional Armenian Soup Seasoning Herb Heracleum transcaucasicum*"

Mariarosa Maimone, Artur Manukyan, Peter Q. Tranchida, Martin Steinhaus
European Food Research and Technology, (2016), DOI: 10.1007/s00217-016-2815-9.

"*Green sample-preparation techniques in comprehensive two-dimensional chromatography*" in Green Extraction Techniques: Principles, Advances and Applications volume 76, Chapter 19 (Elsevier, B.V., Amsterdam, The Netherlands), In press.
Francesco Cacciola, **Mariarosa Maimone**, Paola Dugo, Luigi Mondello.